Assessing the ecotoxicity of NiO nanomaterial and acetaminophen to barley and the beneficial effects of SiO_2 nanomaterial co-application

Cristiano Fortuna Soares
Mestrado em Biologia Celular e Molecular
Departamento de Biologia
2016

Orientador
Fernanda Fidalgo, Prof. Auxiliar, Faculdade de Ciências da Universidade do Porto

Coorientador
Ruth Pereira, Prof. Auxiliar, Faculdade de Ciências da Universidade do Porto

U.PORTO

FACULDADE DE CIÊNCIAS
UNIVERSIDADE DO PORTO

Todas as correções determinadas pelo júri, e só essas, foram efetuadas.

O Presidente do Júri,

Porto, _____/_____/_____

For the elaboration of this master thesis, data present in the following scientific article and communications was used:

- Soares, C., Branco-Neves, S., de Sousa, A., Pereira, R., Fidalgo, F., 2016. Ecotoxicological relevance of nano-NiO and acetaminophen to *Hordeum vulgare* L.: combining standardized procedures and physiological endpoints. Chemosphere 165, 442-452 (DOI: 10.1016/j.chemosphere.2016.09.053) – see Annex;

- Soares, C., Branco-Neves, S., Pereira, R., Fidalgo, F., 2016. Phytotoxic effects of nano-NiO on the growth and oxidative status of barley plants. EMBO Young Scientists' Forum, Lisbon, Portugal;

- Soares, C., Branco-Neves, S., Pereira, R., Fidalgo, F., 2016. Beneficial effects of nano-silicon on the tolerance of barley exposed to high levels of NiO nanoparticles and acetaminophen. IJUP 16 - Encontro de Jovens Investigadores da Universidade do Porto, Portugal.

Acknowledgments

Após um ano de trabalho, recheado de altos e baixos, é agora altura de agradecer o envolvimento de diversas pessoas que, comigo, foram acompanhando tão de perto esta aventura.

Como não poderia deixar de ser, as primeiras palavras têm de ser dirigidas à Professora Fernanda. Antes de mais, OBRIGADO! Desde há já três anos que a professora acompanha, passo a passo, a minha vida académica e laboratorial. Agradeço-lhe toda a disponibilidade, entrega e dedicação. Agradeço-lhe a partilha de conhecimentos, o incentivo pelo rigor científico e os inúmeros conselhos e sugestões. Graças à professora, sei que hoje posso confiar no meu trabalho e nos resultados que aqui publico. Obrigado por todas as conversas, desabafos e risadas. Obrigado por ser mais que uma orientadora. Não existem palavras capazes de descrever o carinho que tenho por si, professora Fernanda. Gosto mesmo muito de si!

À professora Ruth: muito, muito obrigado! Foi um prazer enorme poder partilhar este trabalho consigo. Agradeço-lhe a disponibilidade incansável e as grandes lições de estatística e tratamento de dados. Sem dúvida que a sua co-orientação foi fundamental para a realização desta dissertação e, por isso, expresso o meu profundo reconhecimento. Obrigado pela forma como me acolheu e por toda a simpatia que tem mostrado para comigo. Espero, sinceramente, que possamos continuar a colaborar no futuro e a tentar relacionar a fisiologia vegetal e a ecotoxicologia em estudos posteriores.

À professora Ana Cunha, agradeço a simpatia que para comigo demonstrou nas idas a Braga, bem como a completa disponibilidade para me receber no seu laboratório. Obrigado pelas suas sugestões e, acima de tudo, pelo interesse demonstrado pelo trabalho. Agradeço ao Professor Manuel Azenha, pela ajuda quantificação do nano-NiO e pela disponibilidade e simpatia com que me acolheu.

Aos meus pais, Lia Fortuna Soares e Fernando Soares, por sempre acreditarem em mim e por fazerem tudo para que consiga realizar os meus sonhos. Desde pequeno me incentivaram a lutar por aquilo em que acreditava. Pois bem, aqui está o resultado… Não existem palavras capazes de descrever o quanto vos amo. Obrigado por sermos a melhor família do mundo: nós e a simba, como é claro.

Obrigado aos meus avós e restante família por me aceitarem como sou e acreditarem no meu valor enquanto pessoa. O vosso apoio tem sido fundamental e, muitas vezes, ajuda-me a ultrapassar as fases menos boas.

Simão, apenas te posso agradecer tudo o que fizeste, fazes e farás por mim. Perdoa-me, mas faltam-me palavras para descrever todo o apreço e gratidão que tenho para contigo. És mais que um amigo, és parte fundamental da minha vida e serás sempre. Sem ti, grande parte deste trabalho não teria sido possível. Obrigado pelos desabafos, pelos incentivos, pelos risos, pelos momentos, pela ajuda… Obrigado por tudo.

Catarina, agradeço-te a tua amizade diária e o teu grande acompanhamento nos últimos tempos. Tens sido incansável e nunca me esquecerei de todo o apoio que me tens dado. Gosto verdadeiramente de ti e estarei sempre aqui para o que precisares. Inês, minha colega de curso, minha eterna amiga bióloga… Já viste, começámos este percurso juntos e, agora, já quase o estamos a terminar. Obrigado por todos estes anos de amizade, carinho e partilha.

Joana, Ângela, Mariana e Raquel: OBRIGADO por estarem comigo há mais de 6 anos e por nunca a nossa amizade se ter desvanecido com a distância. Obrigado por acreditarem em mim. Sou um sortudo por ter alguém como vocês!

O meu obrigado à Alexandra, por todos os bons momentos que fomos passando ao longo destes três anos, bem como por toda a ajuda prestada no laboratório. Sem ti, isto não teria tanta piada.

A todos os que contribuíram para o sucesso desta dissertação, o meu reconhecido OBRIGADO.

Resumo

Dada a crescente industrialização, fármacos e nanomateriais estão a tornar-se importantes contaminantes, representando um potencial risco para as plantas. Neste contexto, um dos objetivos deste estudo consistiu na avaliação da relevância ecotoxicológica de óxido de níquel de tamanho nanométrico (nano-NiO) e acetaminofeno (AC), um dos mais utilizados fármacos, em *Hordeum vulgare* L. (cevada). Assim, integrando protocolos padronizados e diversas determinações bioquímicas, foi obtida uma perspetiva abrangente dos efeitos biológicos destes dois contaminantes. Após 14 dias de crescimento, a exposição de cevada a concentrações crescentes (0; 87,8; 131,7; 197,5; 296,5; 444,4; 666,7; 1000 mg kg $^{-1}$) de cada um dos contaminantes resultou num decréscimo no crescimento vegetal, acompanhado por um aumento significativo da peroxidação lipídica (PL), da concentração do anião superóxido ($O_2^{\cdot-}$) e de morte celular. De uma forma geral, o nano-NiO apresentou maior fitotoxicidade do que o AC e a avaliação de marcadores de *stress* oxidativo permitiu aumentar a sensibilidade da avaliação ecotoxicológica destes contaminantes.

Diversos estudos reportam que a aplicação de sílica é capaz de aumentar a tolerância das plantas a diversos tipos de stress abiótico. Assim, com o objetivo de avaliar o efeito protetor do dióxido de sílica na forma nanométrica (nano-SiO_2) contra a fitotoxicidade de nano-NiO e AC, plantas de cevada foram cultivadas na presença de nano-NiO (120 mg kg^{-1}) ou AC (400 mg kg^{-1}) ambos misturados com nano-SiO_2 (3 mg kg^{-1}). O tratamento das plantas com nano-NiO e AC culminou numa diminuição significativa do seu crescimento, ainda que não se tenham observado grandes efeitos nefastos nas enzimas envolvidas na assimilação do azoto. Em resposta ao tratamento com nano-SiO_2 observou-se uma menor inibição do crescimento das plantas tratadas com nano-NiO. Contudo, na exposição a AC não se registou o mesmo padrão de respostas. O nano-NiO induziu, significativamente, uma resposta negativa no aparelho fotossintético que, mais uma vez, foi revertida pelo co-tratamento com nano-SiO_2. Com base no conteúdo de $O_2^{\cdot-}$ e na PL, pode afirmar-se que nano-NiO induziu a ocorrência de stress oxidativo, mas a mistura com nano-SiO_2 mostrou-se bastante eficiente na mitigação do dano oxidativo, baixando os níveis de PL e estimulando a rede redox de tióis. Em oposição, o AC não provocou danos oxidativos severos, independentemente da presença ou ausência da nano-SiO_2. A avaliação dos componentes do sistema antioxidante (AOX) revelou que o nano-NiO induziu a acumulação de prolina e a redução do conteúdo de ascorbato nas folhas. Para além disso, a atividade da superóxido dismutase (SOD) foi significativamente aumentada e a catalase (CAT) e a peroxidase do ascorbato (APX) desempenharam um papel relevante na eliminação do H_2O_2. A estimulação do sistema AOX foi ainda mais notória na presença de nano-SiO_2, corroborando o seu efeito protetor contra a fitotoxicidade de nano-NiO. Relativamente à exposição a AC, registou-se um aumento de prolina nas folhas e detetaram-se diferenças significativas nas atividades de SOD, CAT e APX; todavia, a co-aplicação de nano-SiO_2 não alterou, de forma significativa, esta resposta.

Em suma, os resultados obtidos sugerem o potencial da nano-SiO_2 na mitigação dos efeitos fitotóxicos dos dois contaminantes, tendo contudo demonstrado mais eficácia quando co-aplicada com o nanomaterial metálico.

Abstract

Given the rising industrialization, nano-based products and pharmaceuticals are becoming relevant environmental contaminants, with potential risks to ecosystems and its primary producers. In this context, this study aimed to assess the phytotoxicity of nickel oxide nanomaterial (nano-NiO) and acetaminophen (AC), one of the most used pharmaceuticals all over the world, to *Hordeum vulgare* L. (barley). Combining standard procedures and biochemical parameters, a holistic approach was used to assess the biological effects of these two contaminants. The exposure of barley to increased concentrations (0, 87.8, 131.7, 197.5, 296.5, 444.4, 666.7, 1000 mg kg $^{-1}$) of both contaminants, during 14 days, resulted in a significant decrease in biomass and biometric parameters, followed by lipid peroxidation (LP), superoxide anion ($O_2^{\cdot-}$) increase and cell death. Overall, nano-NiO was more toxic than AC and the evaluation of oxidative stress markers increased the sensitivity of the phytotoxic evaluation of these two contaminants for barley plants.

Several studies report that silicon application is able to increase plant tolerance to different types of stress. Thus, the other main goal of this work was to assess the potential role of silicon dioxide nanomaterial (nano-SiO_2) in enhancing the tolerance of barley to both contaminants. For this purpose, plants were grown for 14 days under both nano-NiO (120 mg kg^{-1}) or AC (400 mg kg^{-1}) exposure mixed with nano-SiO_2 (3 mg kg^{-1}). The exposure of barley to nano-NiO and AC caused a significant decrease in growth-related parameters, without compromising nitrogen assimilation enzymes. Upon nano-SiO_2 co-exposure, the inhibitory effects of nano-NiO were partially reduced, though the same was not observed for plants under AC stress. Nano-NiO induced a negative response on the photosynthetic apparatus that was reverted by nano-SiO_2 co-application. Plants growing under nano-NiO stress exhibited an overproduction of $O_2^{\cdot-}$, which favored the occurrence of oxidative stress, but the co-treatment with nano-SiO_2 reverted this tendency, generally lowering or maintaining the levels of LP and stimulating the anti-redox pathway of thiols. In opposition, AC did not caused significant oxidative damage, regardless of the presence of nano-SiO_2. The evaluation of components of the plant antioxidant (AOX) system revealed that nano-NiO induced the accumulation of proline, along with a decrease in ascorbate, in leaves. Furthermore, SOD activity was significantly enhanced and catalase (CAT) and ascorbate peroxidase (APX) seemed to have a pivotal role in H_2O_2 detoxification in leaves and roots, respectively. The response of the AOX system was even more notorious upon nano-SiO_2 co-exposure, reinforcing the protective role of this nanomaterial. Regarding AC, proline content was positively affected in leaves and some significant changes were tracked in SOD, CAT and APX activities; however, the co-application with nano-SiO_2 did not majorly alter this pattern.

Overall, the obtained results suggest the potential of nano-SiO_2 in mitigating the phytotoxicity of both contaminants, although this protective role was more notorious upon nano-NiO co-exposure.

Keywords

Ecotoxicology, oxidative stress, antioxidant system, soil contamination, reactive oxygen species, photosynthesis, nano-based products, pharmaceuticals.

Table of Contents

List of Figures

List of Tables

Abbreviations and Acronyms

$^1O_2$ – oxygen singlet;
AC – acetaminophen;
ADP – adenosine diphosphate;
Ag – silver;
AOX – antioxidant;
APX – ascorbate peroxidase;
AsA – ascorbate;
AsA-GSH – ascorbate-glutathione;
BIP – α- α'-bipyridl;
BSA – bovine serum albumin;
Ca – calcium;
Car – carotenoid;
CAT – catalase;
Cd – cadmium;
Chla – chlorophyll a;
Chlb – chlorophyll b;
Cu – copper;
CYP - cytochrome P450;
DHAR - dehydroascorbate reductase;
DTNB – 5,5′-dithiobis(2-nitrobenzoic acid);
DTT – 1,4-dithiothreitol;
EC – emerging contaminants;
ECx - effective concentration causing x% of the effect.
EF1G – elongation factor 1 gamma;
ENM – engineered nanomaterial;
ETC – electron transport chain;
FAD - Flavin adenine dinucleotide;
F'_m – maximum Chl fluorescence in the light adapted state;
F_m – maximum Chl fluorescence in the dark adapted state;
F_0 - minimum Chl fluorescence in the dark adapted state;
F_v/F_m – maximum quantum yield;
GR – glutathione reductase;
GS – glutamine synthetase;
GSH – glutathione;
GSSG – oxidized glutathione;
GST – glutathione S-transferase;
H_2O_2 – hydrogen peroxide;
HS – Hoagland solution;
K – potassium;
LP – lipid peroxidation;
MDA – malondialdehyde;
MDHA – monodehydroascorbate;
MDHAR - monodehydroascorbate reductase;
Mg – magnesium;
MT – metallothionein;
N – nitrogen;
NA – nicotinamide;
Nano-NiO – nickel oxide nanomaterial;
Nano-SiO_2 – silicon dioxide nanomaterial;
NAPQUI - N-acetyl-p-benzoquinone;
NBT – nitroblue tetrazolium;
NEM – N-ethylmaleimide;
Ni – nickel;
NR – nitrate reductase;
$O_2^{\cdot -}$ - superoxide anion;
$OH^{\cdot}$ – hydroxyl radical;
P – phosphate;
P5C – Δ'-pyrroline-5-carboxylate;
P5CR - Δ'-pyrroline-5-carboxylate reductase;
P5CS – Δ'-pyrroline-5-carboxylate synthetase;
PAR – photosynthetically active radiation;
PCD – programmed cell death;
PK – potassium phosphate;
PMSF – phenylmethylsulfonyl fluoride;
Pro – proline;
PSII - photosystem II;
PVPP – polyvinylpolypyrrolidone;
ROS – reactive oxygen species;
RT – room temperature;
S – sulphur;
SDS – sodium dodecyl sulfate;
Si – silicon;
SN – supernatant;
SOD – superoxide dismutase;
STDEV – standard error of mean;
TBA – thiobarbituric acid;
TCA – trichloroacetic acid;
TCHQD – tetrachlorohydroquinone dehalogenase;
TEM – transmission electron microscopy;
Tm – melting temperature;
WHCmax – maximum water hold capacity;
Zn – zinc;
γ-ECS - γ-glutamylcysteine synthetase

1. INTRODUCTION

Over the recent years, the rapid growth of population in the world has been accompanied by a strong development of different industries and technologies. Consequently, and due to the anthropogenic action, the amount of produced waste is increasing, aggravating the anthropic pressure at numerous environmental matrices, such as water resources, oceans and rivers, atmosphere and soil. Therefore, a growing deterioration of ecosystems is occurring and the marked changes in their dynamics can ultimately affect ecosystem's services and functions (van der Perk, 2013).

Although there is some regulation to minimize the effects of pollution, derived from both natural and anthropogenic causes, laws and rules did not cover all the wastes and contaminants, are not always enforced and their application is not correctly supervised in many cases (van der Perk, 2013). In fact, different kinds of emerging contaminants (EC), originated from diverse sources and processes, like mining, pharmaceutical and technology industries, can attain the soil, posing a serious threat to its functions and associated biodiversity (Panagos et al., 2013).

A few decades ago, the problem about soil contamination, and its possible harmful consequences on human health, have started to gain a global recognition (Gómez-Sagasti et al., 2016). Nevertheless, several centuries ago, Hippocrates already pointed out the importance of soil to life defending the term of "health of the soil" as an important characteristic for human health and well-being (Krupenikov et al., 2011). According to Doran and Zeis (2000), this concept refers to the ability of soil to support life and maintain its biological productivity, while promoting environmental quality along with animal and plant health.

For all the stated reasons, it becomes increasingly important to unravel the effects of several classes of EC on different trophic levels in terrestrial ecosystems. Indeed, at the present, it is already recognized that is not possible to predict EC-associated risks only based on their concentrations in the environment (Ludwig and Iannuzzi, 2005); these kind of approaches merely allow the detection of contamination (occurrence of substances at higher concentrations than natural background or where they are not normally found) and do not estimate the occurrence of pollution with negative biological effects on the environment (Chapman, 2007).

According to the European Parliament, the environmental risk assessment of EC should include a comprehensive set of studies, focused on chemical, toxicological and ecological levels. Thus, different biomarkers are currently contemplated in OECD and

ISO guidelines to evaluate the risk of a certain EC (European Parliament and the Council, 2006).

Although the effects of different EC on many animal species are relatively well described (Crane et al., 2006; Hao and Chen, 2012; McGill et al., 2012; Patlolla et al., 2014; Nogueira et al., 2015), their toxicological and physiological relevance for plants is poorly studied and remains unclear. Plants play a central role in biosphere dynamics, being the main producers of ecosystems and the basis of human and animal feeding. As sessile organisms, plants are not able to move and have to directly deal with different types of adverse circumstances, such as soil degradation and contamination. In this way, the assessment of the potential risks of emerging contaminants on different plant species, including food crops, as well as the development of eco-friendly strategies to minimize their bioaccumulation and toxicity in plants should be adequately addressed.

1.1. Nanotechnology and metal-based nanomaterials

Nanotechnology is a new field of the technological sciences, dealing with materials at the nanometer scale (Whatmore, 2006). In this area, a particle is defined as a tiny object acting as an entire unit, in what regards its transport and properties (Arruda et al., 2015). The designation of nanomaterial has been changing throughout the years, being currently defined as "a natural, incidental or manufactured material containing particles, in an unbound state or as an aggregate or as an agglomerate and where, for 50% or more of the particles in the number size distribution, one or more external dimensions is in the size range 1 nm – 100 nm" (Rauscher et al., 2014). Although nano-based products are found in the nature, nanotechnology only started to emerge as a promising science since the final years of the 20th century, as a tool to face the massive dependence of properties (electronic, magnetic, optical, mechanical, etc.) on particle size and shape (Alkilany and Murphy, 2010).

Nowadays, nanotechnology occupies a pivotal place among the scientific community, given the global desire to produce materials with improved skills, which can be applied to different areas of knowledge, such as physical, chemical, biological and health sciences (Arruda et al., 2015).

Indeed, the current decade is already stated as the *Nano-era*, where thousands of engineered nano-materials (ENM) are applied on several consumer and cosmetic products (Hansen et al., 2008). Actually, the application of nano-based products is also positively affecting different economy sectors, from pharmaceuticals and cosmetics, to energy and agriculture businesses (Roco, 2003; Nowack and Bucheli, 2007). Based on estimations, in the year of 2013, there were more than 1600 available products

containing ENMs and it is predicted that this number will grow even more (Kurwadkar et al., 2014). Additionally, a previous reference suggested that nanotechnology market is expected to reach $30 billion in 2020, with an annual production of nano-based products of 58,000 tons (Gubbins et al., 2011); however, more recent findings propose that the global market of nanoscience reached the $1 trillion mark in the past year. With effect, USA is listed as the largest producer of nano-based products, but several European countries, like Germany, UK and Switzerland are also present in this survey (Kurwadkar et al., 2014).

The fast-growing increased application of nanomaterials will inevitably lead to their accumulation across the major environmental matrices. Thereby, it is not surprising that, paired with the development of this innovative science, serious concerns about the possible fate and accumulation of ENM in the environment have also become a reality among scientists. In fact, great controversy surrounding this issue has been generated, debating on the risks and benefits of ENM's wide application (Agency, 2007). It is now considered that risk assessment of ENM should be performed as brief as possible, in attempts to minimize their potential hazards.

The accumulation of ENM in the environment is already a present reality. The contamination of ecosystems by these nanomaterials can occur at different stages of their life-cycle, from their production until their recycle, with short or long emissions. Once into the environment, ENM can remain unchanged, but can also experience some modifications, changing their form, aggregation, chemical composition and possible biological consequences. Accordingly, studies conducted at 2010 found out that the geometry of gold-containing ENM mediates its interactions with biological systems (Albanese et al., 2010; Hutter et al., 2010). Given the widespread application of ENM all over the world, different studies have already detected their presence in different environments, like water and soil (Gottschalk and Nowack, 2011; Nowack et al., 2012; Sun et al., 2014), though not much is known about their fate and biological effects, especially regarding their interaction with living organisms, at the molecular and cellular levels (Barrena et al., 2009; Khot et al., 2012). Thus, aiming to clearly understand the mode-of-action of several ENMs, as well as their potential toxic effects on ecosystems and human health, new research efforts are necessary and urgent.

The introduction of nanomaterials in the environment can occur by different ways and as a result of unintentional practices, such as atmospheric emissions and the runoff of different industrial wastes (Helland et al., 2008; Klaine et al., 2008; Bhatt and Tripathi, 2011) (Figure 1). However, the intentional delivery of ENMs on the environment could also become a reality. Actually, several remediation programs announce the direct application of different ENM on the environment, for treating contaminated soils and

waters. For instance, remediation of contaminated groundwater can be performed by nanoparticle treatment (Tratnyek and Johnson, 2006; Klaine et al., 2008) and the treatment of polluted soils with nanomaterials is already a reality (Thomé et al., 2015). Also, nanotechnology is currently used to the detection of toxins in water and air (Dionysiou, 2004). In this sense, soil is one of the main matrices affected by this problem and ENM can attain the soil by multiple ways. One of them is closely linked to the direct deposition of airborne ENM, through pluviometric precipitation transport. Furthermore, according to Mueller and Nowack (2008), the application of bio-solids in agricultural lands represents another main source of soil contamination by ENM. Indeed, the presence of ENM has already been confirmed in sludge, which is commonly applied in agriculture practices. Regarding this matter, data from a recent study reported that almost 30% of the total amount of ENM released to the environment reached the soil trough sludge application in Europe (Sun et al., 2014) and other significant part attained by irrigation water.

Taking into account this scenario, there is an increased demand for quantifying ENM levels in soil, along with the responsible evaluation of their ecotoxicity significance. At the moment, most of the available data regarding this issue is based on mathematical predictive estimations (Sun et al., 2014). Thus, although these reports provide valuable scientific information, their accuracy cannot be entirely assumed. In this way, improved procedures for quantification of ENM in the environment should be investigated and properly implemented (Handy et al., 2008; Bour et al., 2015).

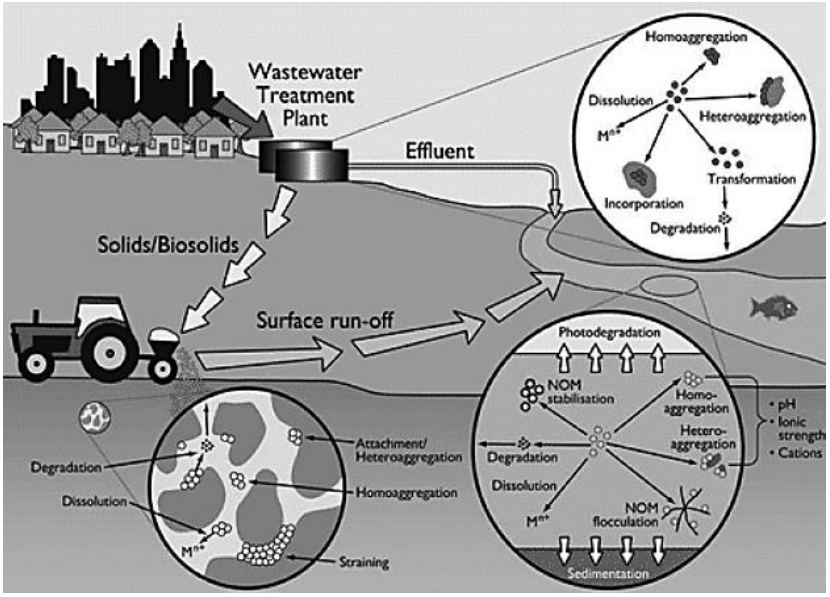

Figure 1. *Possible pathways of ENM introduction in several environmental matrices, such as effluents, soil and water resources.* Extracted from Batley et al. (2012).

Main classes of ENMs

ENM, or manufactured nanomaterials, are one of the main classes of nanoparticles, with particular physicochemical properties, since these nanomaterials are specifically designed to for a certain application. ENM can be subdivided in five classes: carbonaceous nanomaterial, metal oxide-based nanomaterial, semiconductors, metal-based nanomaterial and nanopolymers (Handy et al., 2008; Monica and Cremonini, 2009; Ma et al., 2010; Bhatt and Tripathi, 2011), all of them with great applications in the global market. Indeed, different society sectors, including engineering, public health and food industry, take advantage of these new technologies, applying them in a wide range of products, such as electronic gadgets, textiles, medical devices, cosmetics and food packages (Biswas and Wu, 2005; Monica and Cremonini, 2009; Kurwadkar et al., 2014; Arruda et al., 2015).

Among the different groups of ENM, the metal-based materials were classified as one of the main elements of nanoscience, largely due to their unique characteristics and their great potential applications. Indeed, different metal-based nanomaterials are available, differing in their chemical composition, size, shape and crystalline structure. Among all, metal-based ENM of TiO_2, ZnO, CuO and CeO_2 are the most widely used and, perhaps by this reason, those for which there is more available data about their ecotoxicity. Given their widespread application, it becomes important to understand their accumulation patterns, as well as their transport and toxicity in the environment (Boddu et al., 2011).

1.1.1. NiO-nanomaterial (nano-NiO) and Ni-mediated phytotoxicity

Nickel (Ni), firstly discovered by Ronstadt in 1751, is an abundant metal in Earth's crust and occurs in igneous and magmatic rocks (Sunderman and Oskarsson, 1991; Yusuf et al., 2011). Due to its elevated concentrations in soils, Ni is considered a large-scale contaminant (Hussain et al., 2013), being applied in many different areas and technologies, like metallurgical and electroplating industries and as a major component of electrical batteries (Nieboer and Nriagu, 1992).

Nowadays, with the great expansion of nanoscience, not only bulk Ni represents a serious environmental threat, but also its nanosized form, nickel oxide (nano-NiO). Possessing different characteristics than its bulk material, nano-NiO is widely used as catalyzer, battery electrode, fuel additive and gas sensor, and applied in electro-chromic films and magnetic materials (Venkateswara Rao and Sunandana, 2008; Rani et al., 2010; Mu et al., 2011). In this way, the substantial application of nano-NiO on several services and products might pose a serious environmental risk, since NiO nanomaterials

can reach the environment by direct aerial emission or indirect runoffs from land (Wiesner et al., 2006).

As already mentioned, there is an urgent need of testing the effects of nanomaterials on different trophic levels, in attempts to understand the realistic consequences of soil contamination by ENM. When compared to other metal-based nanomaterials, nano-NiO is less studied and its effects for animals and plants remained largely unknown. However, the available data, majorly performed on animal species, suggests that this ENM is able to induce several negative effects and stress conditions (Ispas et al., 2009; Gong et al., 2011; Horie et al., 2011; Kang et al., 2011; Faisal et al., 2013; Nogueira et al., 2015). Also, there is strong evidence that nano-sized NiO releases more Ni ions than its bulk material, and hence aggravating its toxicity to living organisms (Horie et al., 2011). Thus, the evaluation of nano-NiO effects on plants is a matter of great interest, since these organisms can represent a potential pathway for the transport of ENM along food chains (Zhu et al., 2008).

Although toxicity mechanisms of metal-based ENM, such as nano-NiO, are dependent of its features as particles (e.g. size and shape), it is recognized that, once inside plant cells, their toxic effects are pretty much identical to their bulk material. In this sense, given the paucity of studies on the potential phytotoxicity of nano-NiO, the following content will be based mainly on the effects of Ni^{2+} ion, which is the ionic form absorbed by plants regardless of the Ni application mode (bulk material or ENM).

Ni essentiality and distribution in plants

Despite high concentrations of Ni can be extremely toxic for most plant species, the establishment of this metal as an essential micronutrient was performed many years ago (Brown et al., 1987). According to Eskew et al. (1983), in order to a certain mineral be recognized as an essential nutrient, it cannot be replaced by any other element and plants cannot complete their life cycle without adequate levels of it. Indeed, it is well reported that Ni deficiency impairs the normal growth of plants, due to its functions in plant physiology and cellular homeostasis. Ni was already identified as a component of several metalloenzymes, such as urease and superoxide dismutase (Ermler et al., 1998), also being involved in promoting the growth of radicular nodules and the activation of hydrogenase (Polacco et al., 2013; Khoshgoftarmanesh et al., 2014; Harasim and Filipek, 2015).

Thus, given the important functions of Ni in the homeostasis of the cell, it is not surprising that plants have acquired mechanisms for its transport and distribution across all organs (Figure 2). Also, it is important to stress that the rate of Ni uptake by plants is

highly dependent on different factors, such as plant metabolism, Ni concentration in substrate and the presence of another inorganic nutrients, like calcium (Ca) (Chen et al., 2009).

The primary uptake of Ni is performed by roots via two different pathways: passive diffusion and active transport, with energy consumption (Seregin and Kozhevnikova, 2006). In this process, different classes of proteins can be involved, since Ni uptake can be mediated by specific enzymes, such as HoxN – a permease with high affinity for Ni, metallothionein (MT) and metallochaperones (Chen et al., 2009). Also, it is known that Ni uptake can be mediated by other metals' transport system, like copper (Cu), zinc (Zn) and magnesium (Mg) (Chen et al., 2009). In general, the main pathway of Ni transport in plants is from roots to shoots, being finally excreted by transpiration processes (Neumann and Chamel, 1986). However, Ni absorption by leaves of different plant species was also observed (Hirai et al., 1993).

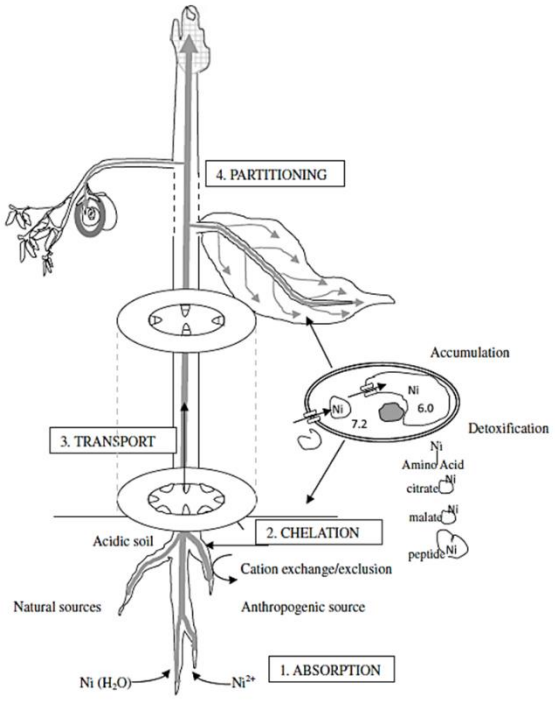

Figure 2. *Ni uptake, transport and distribution in plants.* Extracted from Yusuf et al. (2011)

Once inside the radicular system, Ni is distributed to other plant organs via xylem, in a transport mechanism mediated by different ligands and proteins that specifically bind to Ni. Thus, metal ligands, where nicotinamide (NA) and histidine are included, and organic acids, like citric acid and malate, can be used as intracellular chelators, regulating Ni transport, translocation and differential accumulation in plants (Reeves, 1992; Rauser, 1999; Raskin and Ensley, 2000; Reeves and Baker, 2000).

Overall, more than 50% of Ni is retained in roots and only 20% of its translocated content is found on leaves' cortex. Regarding its subcellular localization, it has been

suggested that Ni is preferentially accumulated in vacuoles and cell walls, although there is no consensus about this matter (Salt et al., 1998).

Ni toxicity in plants

Similarly to other metals, high Ni concentrations can represent a real threat to plants, changing their morphological and physiological traits. In fact, Ni-induced phytotoxicity can be observed at different metabolic pathways and physiological processes, at both organism and cellular levels (Hussain et al., 2013) (Figure 3). Moreover, it appears that Ni toxic effects are largely dependent on the plant species, growth conditions and stage and treatment (e.g.: concentration and exposure period) (Soares et al., 2016). In a general way, for sensitive plant species (where barley is included), Ni toxicity is evidenced upon concentrations above 10 mg kg^{-1} of dry weight (Yusuf et al., 2011).

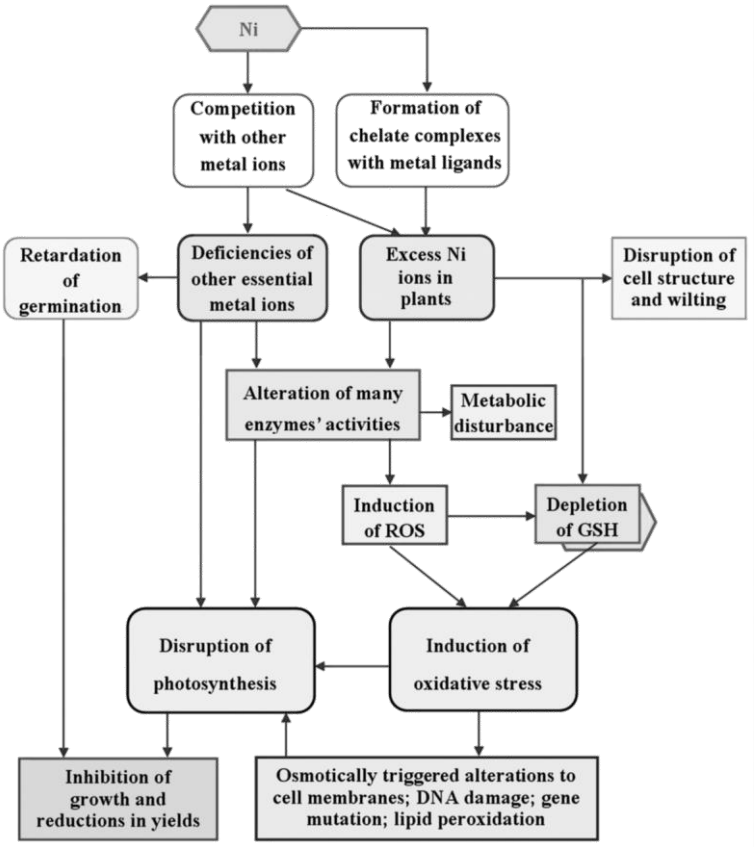

Figure 3. *Effects of Ni-induced phytotoxicity and corresponding metabolic pathways.* Ni in excess can disrupt the proper uptake of other micronutrients and induce different metabolic and physiological disruptions, with repercussions on photosynthesis, enzyme activity and induction of oxidative stress, ultimately leading to losses in growth yield and productivity. Adapted from Chen et al. (2009).

As reviewed by Yusuf et al. (2011), high concentrations of Ni can harshly affect photosynthesis, mineral nutrition, photo-assimilate transport and enzymatic activity. Hence, Ni excess often leads to growth inhibition and induces several toxicity symptoms,

like chlorosis, necrosis and leaf wilting. Furthermore, different bibliographic references indicate that Ni-mediated stress is linked to the establishment of oxidative conditions, even though Ni is not a redox-active metal. Furthermore, although reactive oxygen species (ROS) might not be directly generated by Ni, several studies revealed that this metal is able to affect plant antioxidant system, modulating plant's defense mechanisms (Gomes-Junior et al., 2006; Gajewska et al., 2009; Yusuf et al., 2011; Hussain et al., 2013; Dourado et al., 2015; Soares et al., 2016).

1.2. Human pharmaceuticals

Paired with the development of nanotechnology, pharmaceutical companies have become one of the most promising industries worldwide. In Europe, pharmacy is responsible for the production of 25% of the total chemical substances and about 3000 bioactive pharmaceuticals are used for both veterinary and human medicine practices (Bartha, 2012). Particularly in our country, the public expenditure with drugs and pharmaceuticals is one of the highest across European Union (Furtado and Oliveira, 2011).

Thus, over the last decades, the intensive use and prescription of different medicines have led to their widespread release into the environment, being now considered as EC (Daughton and Ternes, 1999). Unlike many other organic pollutants, such as pesticides, detergents and fuels, drugs possess a high bioactivity factor and are conceived to be stable and to resist to metabolic inactivation. By these reasons, they can accumulate and persist on the environment, thus aggravating their potential hazardous effects on biota (Fent et al., 2006; Glassmeyer et al., 2009).

The delivery of this type of products into the environment can be mediated by several factors, all of them related to the anthropic action and the increasing development of pharmaceutical industries. Within all of these possible input processes, the one that most contributes to the environmental contamination by pharmaceuticals are homemade and hospital discharges. In fact, upon being metabolized in human body, part of pharmaceuticals' bioactive substances, and other produced conjugates, are excreted through urine and/or feces, eventually entering the public water system. Also, the application of animal feces as bio-solids in agricultural practice and the discharges from pharmaceutical companies can increase the level of contamination with these compounds. As a consequence of the constant introduction of pharmaceuticals into the environment and of their resistance to several available methods for water treatment, different drugs and their bioactive residues were already detected in sewage effluents, residual waters and nearby water treatment stations, finally arriving to surface water

resources and, consequently, to the soil habitat (Kinney et al., 2006; Lienert et al., 2007; Bartelt-Hunt et al., 2009).

1.2.1. Acetaminophen (AC) and AC-mediated phytotoxicity

Among the most selling medicines worldwide are non-steroidal anti-inflammatory drugs. AC, commonly known as paracetamol (Figure 4), is one of the most prescribed analgesics in the world, which consumption has been growing over the recent years (Wu et al., 2012). In terms of organic chemistry, AC is named as N-(4-hydroxyphenyl)acetamide and it is a derivate of *p*-aminophenol and its molecular formula is $C_8H_9NO_2$.

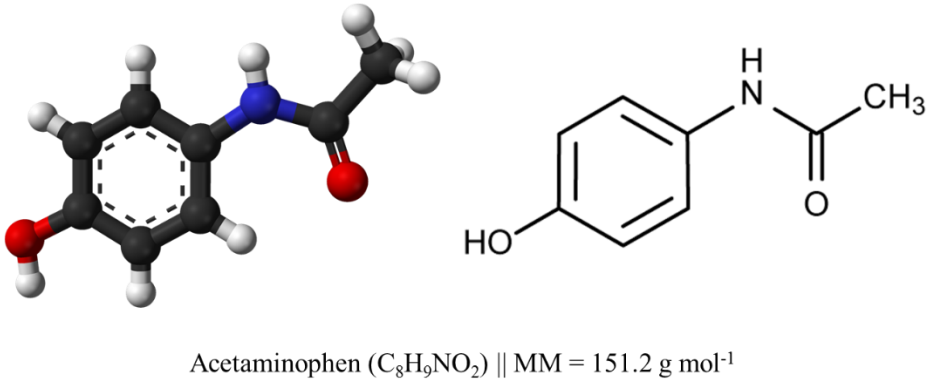

Acetaminophen ($C_8H_9NO_2$) || MM = 151.2 g mol^{-1}

Figure 4. *Acetaminophen.* Chemical structure and molecular mass, expressed in g mol^{-1}.

AC was initially synthetized by Morse in 1878 and its first clinical application was performed by Von Mering a few years later (Morse, 1878; Von Mering, 1893). However, it was due to the experiments of Brodie and Axelrod (Brodie and Axelrod, 1948) that AC became one of the most used drugs all over the world, being now widely used to treat pain and fever (Pandolfini and Bonati, 2005). Despite AC is being used for more than a century, its mode-of-action requires further investigation and remains unclear. Nevertheless, several hypotheses suggest that AC is able to inhibit the nitric oxide pathway, thus increasing the pain threshold; also, its anti-pyretic properties are likely related to its inhibitory effects on prostaglandin production, release and action (Graham and Scott, 2005; Godfrey et al., 2007).

At the moment, fast-growing amounts of paracetamol are being released into the environment and its occurrence was already reported in different media, such as surface waters and sediments. Moreover, based on Kreuzig et al. (2005), AC displays a high tendency to adsorb and persist in the soil, promoting its accumulation and fate in terrestrial and water ecosystems. Although levels of AC found in different water

resources are in the range of ng and μg L^{-1}, there is an increased need to determine its ecotoxicity for soil habitat, especially in plant organisms (Daughton and Ternes, 1999).

Mechanisms of xenobiotic detoxification in plants

Nowadays, it is widely accepted that soil contamination with both organic and inorganic EC can affect plant growth and physiology, thus compromising its productivity and survival (Teixeira et al., 2011). However, as mammals, plants possess different metabolic pathways involved in xenobiotic's detoxification, by converting them into harmless compounds in attempts to minimize their toxic effects. Usually, a three phase-model detoxification process takes place, allowing the proper activation, transformation and accumulation of xenobiotics inside plant cells. Briefly, in phase I, the product undergoes a transformation and activation, followed by its conjugation (phase II) with different chelators and, finally, its accumulation in specific sub-cellular structures (phase III) (Shimabukuro, 1976).

Phase I – Activation and transformation

In this phase, organic contaminants experience a large diversity of chemical modifications, such as oxidations, hydrolysis and reductions. The main purpose of this step is to increase xenobiotics' hydro solubility, by introducing reactive groups in their molecular structure, and prepare them for subsequent metabolism in phases II and III (Coleman et al., 1997).

Among all, hydrolysis and oxidation are the most common reactions in phase I, being catalyzed by different classes of enzymes, like esterases and amidases (hydrolytic reactions) and cytochrome P450 monooxygenases (CYP) (oxidation reactions). Specifically regarding the latter ones, CYP belong to an enzyme superfamily found in different taxa, like animals, plants, fungi and bacteria. In plants, these enzymes, besides being involved in xenobiotic detoxification, actively participate in different physiological processes, catalyzing lignin's, terpenes' and alkaloids' biosynthesis, and mediating plant defense responses against biotic agents, such as pathogens and insects (Schuler and Werck-Reichhart, 2003).

Phase II – Conjugation reactions

Phase II of xenobiotic detoxification is characterized by the covalent linkage of several metabolites to the xenobiotic itself or its activated form. The produced conjugates display a lower biological activity, with reduced toxicity and mobility. The conjugation process

can be mediated by different organic molecules, like glucose, amino acids and glutathione (Coleman et al., 1997; Teixeira et al., 2011).

Glucose-based conjugates include *O*-, *S*-, and *N*-glyxosides and malonyl-glucoses molecules, catalyzed by *O*-, and *N*-glycosyltransferases and malonyltransferases.

The conjugation of xenobiotics with amino acids is also a common response of plants. Among all, aspartate and glutamate are the most used amino acids in the conjugation process, but the involvement of leucine and valine was already suggested. These type of conjugation is frequentely associated to the detoxification of insectides and pesticides and usually results in less biological active substances, with a marked reduction in their mobility (Davidonis et al., 1978).

When electrophilic xenobiotics are regarded, conjugation with the tri-peptide glutathione (γ-Lglutamyl-L-cysteinyl-glycine - GSH) takes place, due to the activity of glutathione S-transferases (GSTs), a multifunctional class of enzymes involved in different cellular and metabolic events (Basantani and Srivastava, 2007). Based on phylogenetic analysis, plant GSTs are grouped in distinct classes: Phi, Tau, Lambda, dehydroascorbatereductase (DHAR), Theta, Zeta, elongation factor 1 gamma (EF1G), and tetrachlorohydroquinone dehalogenase (TCHQD) (Edwards and Dixon, 2005). Besides their function in xenobiotic detoxification, GSTs have also an important roIe in hormone metabolism, vacuolar sequestration of anthocyanins, tyrosine metabolism, regulation of apoptosis and some of them can even act as intracellular peroxidases, modulating plant antioxidant responses to different stressful conditions (Dixon et al., 2010).

Phase III – Compartmentalization

After conjugation processes, intermediated less-toxic compounds can be exported from the cytosol to different organelles, mostly vaculoes and cell wall. Thus, phase III is an important step in the detoxification pathway, allowing the sequestration of xenobiotics from sensitive subcellular structures. In this phase, besides compartmentation, different conjugates can still undergo some modifications and interact with another endogenous compounds (Coleman et al., 1997).

In a general way, soluble residues, like peptide or sugar conjugates, are accumulated inside vacuoles. The transport of these compounds to the vacuole is accomplished by an active transport system, using ATP dependent carriers. On the other hand, insoluble solutes, like aromatic or heterocyclic rings, are sequestred and accumulated in the cell wall, being coupled to lignin, starch, pectin, cellulose or xylan (Sandermann, 1992; Coleman et al., 1997).

AC metabolism in plants and its phytotoxicity

To date, there are only a few records regarding the potential deleterious effects of AC on plant development and not much is known about AC metabolism in plants. Although it is supposed that plant-associated mechanisms are closely linked to the mammal metabolism (Sandermann Jr, 1994; Huber et al., 2009), there are still several differences. In plants, the detoxification of AC is mainly mediated by conjugation with glutathione and the production of glucosides, with these two phenomena acting independently. Thus, according to Huber et al. (2009), who first published the possible metabolism of AC in plants, AC is initially activated by an enzymatic reaction catalyzed by CYP. Right after, most part of activated AC is conjugated with glucose, but can also be transformed into N-acetyl-p-benzoquinone imine (NAPQUI), which then undergoes a conjugation with glutathione, in an enzymatic reaction mediated by GST (Bartha et al., 2010).

The understanding of the effects of AC exposure on plants is only in the beginning and deeper investigation is necessary in order to concretely comprehend its potential toxicity and its repercussions at the cellular level. However, based on the findings reported for different animal species, AC stress is related to the induction of pro-oxidative conditions, favoring the occurrence of oxidative stress (Nunes et al., 2006; Nunes et al., 2008; Hamid et al., 2012; McGill et al., 2012; Xie et al., 2014). In this context, even though bibliography is scare, it seems that a parallel scenario is expected in plants. Indeed, Bartha et al. (2010) found that the exposure of *Brassica juncea* L. to high levels of AC resulted in the establishment of oxidative stress and in the modulation of several antioxidant responses. The same pattern was already reported for *Lemma minor*, where AC-mediated stress led to a rise of lipid peroxidation, accompanied by a decrease of proline accumulation (Nunes et al., 2014) and an increase of reactive oxygen species (ROS) content (Kummerová et al., 2016). Furthermore, AC-mediated inhibition of plant growth and productivity was also detected in wheat and *Lemma minor* (An et al., 2009; Kummerová et al., 2016).

1.3. Oxidative stress and plant antioxidant (AOX) system

Due to their sessile nature, plants are often exposed to a wide range of adverse circumstances that limit their growth and survival performance. In fact, one of the common characteristics of plants growing under stress is the induction of oxidative stress, by an overproduction of reactive oxygen species (ROS). However, throughout evolution, plants have developed an efficient antioxidant (AOX) defense system, composed by both enzymatic and non-enzymatic mechanisms (Gill and Tuteja, 2010).

1.3.1. Reactive oxygen species (ROS)

It is well established that the oxygen-derived atmosphere allowed the appearance of aerobic organisms and several energy generation systems which use O_2 as the final electron acceptor (Temple et al., 2005). However, though molecular oxygen is relatively unreactive, its reduction can lead to the production of reactive substances and it is currently estimated that 1-2 % of the total consumed O_2 is converted to ROS (Bhattacharjee, 2005). ROS are continuously produced as a consequence of the aerobic cell metabolism (Gill and Tuteja, 2010). In plants, ROS play a dual role depending on their concentration: when at low levels, they can be regarded as intracellular signaling agents, inducing a positive response of the antioxidant system; however, when at high levels, all forms of ROS become toxic and capable of interact with all kinds of organic molecules, like proteins and nucleic acids. In fact, if the defense response is not enough to counteract the increased produced amount of ROS, damaging consequences could threat the viability of cells, inducing several consequences, such as lipid and protein oxidation, enzyme inhibition and, ultimately, activation of programmed cell death (PCD) (Mittler, 2002; Gill and Tuteja, 2010; Sharma et al., 2012). Thus, oxidative stress arises from a disproportion between ROS production and elimination, being a complex biochemical and physiological phenomenon (Gill and Tuteja, 2010; Sharma et al., 2012).

ROS can include both molecules and/or free radicals, such as singlet oxygen ($^1O_2$), superoxide anion ($O_2^{\cdot-}$), hydroxyl radical ($OH^{\cdot}$) and hydrogen peroxide (H_2O_2).

$^1O_2$ is a less common ROS, since its production is not related to electron transfer to O_2, but rather linked to the energy dissipation of the chlorophyll triplet state to O_2. Since $^1O_2$ production is frequently associated with high light intensity, its negative effects on photosystem I and II have been largely reported (Gill and Tuteja, 2010). Regarding its chemistry, $^1O_2$ is a highly reactive radical, with a short life-time between 4-100 μs, able to react with different biological molecules, like lipids (Halliwell, 2006).

The superoxide radical is the most typical ROS and the first to be produced, as a consequence of the aerobic metabolism. Based on several references, it is widely accepted that $O_2^{\cdot-}$ production is mainly related to electron transport chains (ETC), whereby the major sources of $O_2^{\cdot-}$ within plant cells are mitochondria and chloroplast in complexes I and III and PSI and II, respectively (Sharma et al., 2012 and references therein). However, its production in other organelles, such as peroxisomes, can also take place. When compared to other ROS, $O_2^{\cdot-}$ is classified as a moderate reactive radical with a short half-time and low mobility, due to its negative charge and consequent inability to cross biological membranes (Demidchik, 2015). Despite $O_2^{\cdot-}$ cannot directly interfere with organic macromolecules, its toxicity is associated with its powerful reducing

ability. In fact, $O_2^{\cdot-}$ can reduce Fe^{3+} to Fe^{2+}, which can later interact with H_2O_2 and arising the production of $OH^{\cdot}$, which is one of the most toxic ROS (Ahmad et al., 2008; Demidchik, 2015). This reaction is globally known as the Haber-Weiss reaction and its last step, where Fe^{2+} interacts with H_2O_2, is referred to as the Fenton's reaction (Demidchik, 2015). Moreover, $O_2^{\cdot-}$ can suffer a process of protonation, inducing the production of $HO_2^{\cdot-}$, a more reactive and stable molecule, permeable through biological membranes.

Along with $O_2^{\cdot-}$, H_2O_2 is considered a primary ROS and, despite being more stable than $O_2^{\cdot-}$, its occurrence can impose a more severe oxidative stress condition (Sharma et al., 2012). However, recent findings suggest that H_2O_2 has a dual role on plant physiology, depending on its intracellular levels. Thus, H_2O_2 can be an important cellular messenger in a broad range of metabolic events and low doses of this molecule can stimulate defense responses for different types of stress; on the other hand, excess of H_2O_2 can cause significant damage to cell homeostasis, conditioning the normal functions of plants (Ahmad et al. 2008; Gill and Tuteja, 2010; Sharma et al., 2012). The high toxicity of H_2O_2 can be easily explained by its chemical nature. Indeed, since it has no unpaired electrons and possesses a relatively long half-time (1 ms), H_2O_2 is able to cross biological membranes and diffuse across long distances, increasing its possible sites of action (Gupta et al., 2015). This molecular ROS can severely inhibit enzyme activity, by triggering the oxidation of thiol groups and the release of metallic ions from different metalloproteins (Scandalios, 1997). Also, according to Scandalios (1993), Calvin cycle-related enzymes are extremely sensitive to H_2O_2 and high levels of this ROS can directly reduce CO_2 assimilation. Regarding its production, many cellular events are involved, namely the electron transport in electron transport chains (ETCs) of different organelles (e.g. mitochondria, chloroplast, endoplasmic reticulum and plasma membrane), photorespiration metabolism and β-oxidation of fatty acids (Sharma et al., 2012).

$^{\cdot}OH$ is the most dangerous and reactive ROS, being produced as a result of the Haber-Weiss reaction, due to the interaction between $O_2^{\cdot-}$ and H_2O_2. Like superoxide anion, $^{\cdot}OH$ has a very short half-time, of around 1 ns (Smirnoff, 2008). Therefore, its major targets and sites of action are closely located to its production source (Sharma et al., 2012). However, even with an extremely short life-time, this can cause serious damage to all organic molecules, leading to harmful consequences in proteins, lipids and nucleic acids. Furthermore, once there is no enzymatic mechanism responsible for its degradation and metabolism, high levels of $OH^{\cdot}$ are able to induce lipid peroxidation and are involved in oxidative stress signaling and PCD (Gill and Tuteja, 2010; Sharma et al., 2012; Demidchik, 2015)

1.3.2. AOX system machinery

As said before, plants possess a complex AOX system, with both enzymatic and non-enzymatic components, which allows the proper scavenging and control of ROS in different organelles of the plant cell (Gill and Tuteja, 2010; Sharma et al., 2012) (Figure 5). Regarding the enzymatic machinery, the main AOX enzymes are superoxide dismutase (SOD), catalase (CAT), GST and enzymes from the ascorbate-glutathione (AsA-GSH) cycle, like ascorbate peroxidase (APX), glutathione reductase (GR), monodehydroascorbate reductase (MDHAR) and dehydroascorbate reductase (DHAR). In what concerns the non-enzymatic AOX component, different metabolites are regarded as important AOX agents. Among all, it is important to stress the involvement of proline (Pro), ascorbate (AsA), glutathione (GSH), carotenoids and flavonoids (Ahmad et al., 2008; Gupta et al., 2015).

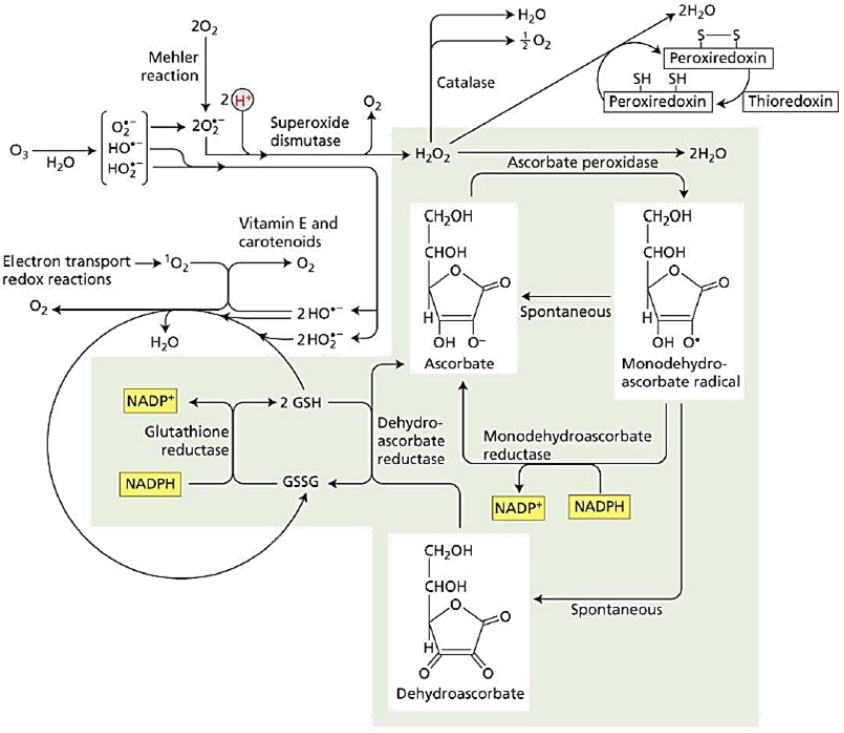

Figure 5. *ROS and AOX defense system in plants – an overview of enzymatic and non-enzymatic components.* The AsA-GSH cycle is highlighted at gray. Aerobic metabolism inevitably leads to the generation of $O_2^{\cdot-}$, which is efficiently scavenged by SOD, with the consequent production of H_2O_2. H_2O_2 levels are then controlled by the catalytic activity of CAT and APX, which requires AsA as the reducing agent. The reduction of AsA is essential to a balanced cell redox condition and can be mediated by two different pathways. First, through the reaction catalyzed by MDHAR, using reducing equivalents from NADPH. Second, by the spontaneous dismutation of MDHA to DHA. Posteriorly, DHA can be enzymatically converted into AsA, in a reaction catalyzed by DHAR, which uses GSH as substrate, oxidizing it into GSSG. GSSG can be restored into GSH, by GR. Other ROS, such as singlet oxygen (^1O) and hydroxyl radical ($OH^{\cdot}$), can be eliminated through non-enzymatic mechanisms, due to the action of vitamins and carotenoids (Taiz et al., 2015).

1.3.2.1. Enzymatic component

Superoxide dismutase (**SOD; EC 1.15.1.1)**

SOD is a ubiquitous protein found in many kinds of aerobic organisms, like bacteria, animals and plants. Firstly isolated from bovine blood, SOD was defined as a blue-greenish protein, responsible for Cu accumulation. However, its catalytic activity was further discovered by McCord and Fridovich in 1969 (Scandalios, 1993). Nowadays, it is largely accepted that SOD acts as the first enzymatic defense line against oxidative stress, catalyzing the $O_2^{\cdot-}$ dismutation in H_2O_2 and molecular oxygen. Actually, SOD assumes a pivotal role in ROS detoxification, not only by determining the levels of both $O_2^{\cdot-}$ and H_2O_2, but also by quickly dismutating O_2.- and preventing its associated-toxicity (Sharma et al., 2012).

In terms of biochemistry, SOD is classified as a metalloenzyme and, depending on the ion present in its active center, three classes of SOD can be considered: Cu/Zn-, Mn- and Fe-SOD (Sharma et al., 2012). Structurally, Fe- and Mn-SOD are much related, although Fe cannot replace the Mn ion in the active center; Cu/Zn-SOD, by possessing two metallic ions in its structure, has distinct chemical and physical properties, which result in differences at the structural level (Scandalios, 1997). The identification of SOD isoforms can be experimentally performed by negative staining in accordance to their sensitivity to KCN and H_2O_2, being Cu/Zn-SOD sensitive to both inhibitors, Fe-SOD sensitive to H_2O_2 and Mn-SOD resistant to KCN and H_2O_2 (Soares et al., 2016). Based on previous phylogenetic studies, it is supposed that the evolution of SODs isoenzymes is related to changes in the availability of the metallic ion. Thus, it appears that Fe-SOD is the oldest group of SODs, since Fe^{2+} was initially more abundant than Cu^{2+} and Mn^{2+} (Alscher et al., 2002).

Although the number of isoenzymes, as well as their relative abundance, are dependent on plant species and environmental circumstances, it is considered that Cu/Zn-SOD is the most abundant form (Gill and Tuteja, 2010) . All types of plant SODs are encoded in the nucleus and the specific location of each class of SOD is determined by a terminal amino acid tag (Kanematsu and Asada, 1989). In this way, SOD isoenzymes can be differentially found in several subcellular compartments: Cu/Zn-SOD is majorly present in the cytosol, chloroplasts, peroxisomes and apoplast; Mn-SOD is fundamentally associated to the mitochondrial matrix, despite it has already been reported its occurrence in the peroxisome; Fe-SOD, a specific plant SOD, is found in the chloroplasts, coupled with thylakoid membranes (Gill and Tuteja, 2010).

Given the high AOX activity of SOD, its occurrence and activation in response to different types of stress has been largely explored (Gill and Tuteja, 2010) and its overexpression in plant species can be an efficient tool to increase abiotic and biotic stress tolerance.

Catalase (CAT; EC 1.11.1.6)

CAT, a tetrameric heme-containing protein, is a common enzyme among different taxa of aerobic organisms and it was the first AOX enzyme to be discovered and functionally characterized (Sharma et al., 2012). The AOX properties of CAT are related to its catalytic activity, being responsible for the intracellular detoxification of H_2O_2, dismutating it into H_2O and O_2 (Gill and Tuteja, 2010).

Although there are several enzymes involved in H_2O_2 degradation, CAT occupies a central role in this scavenging process, since it does not require any reducing power, providing an efficient mechanism to remove H_2O_2 excess from cells (Gill and Tuteja, 2010). Moreover, CAT exhibits one of the highest turn-over rates among AOX enzymes, in which one CAT molecule is able to reduce 6 million H_2O_2 molecules per minute (Gill and Tuteja, 2010). However, despite the high specificity of CAT to H_2O_2, this enzyme's activity is only efficient when high levels of H_2O_2 are present, reason why its affinity for H_2O_2 is relatively lower than other enzymes, such as APX and other peroxidases (Mittler, 2002).

The localization of CAT in plant cells is intrinsically related to the sources of H_2O_2. Given the aerobic metabolism of peroxisomes, CAT is commonly found in this organelle, although several authors have already reported its occurrence in other subcellular compartments, such as mitochondria, chloroplasts and cytosol (Sharma et al., 2012). Thus, though displaying a more restrict location than SOD, CAT is also very important for limiting H_2O_2 diffusion across plant cells (Bowler et al., 1992).

In animals, only one CAT isoenzyme has been reported. Nevertheless, in plant organisms there are three main classes of CATs, classified according to their expression profiles (Ushimaru et al., 2006). In this way, class I CATs are present in photosynthetic tissues and are light-dependent; class II are majorly found in vascular tissues; and class III are detected in seeds and early stages of seedling's development (Gill and Tuteja, 2010).

Likely to SOD, changes in CAT activity are often correlated to the establishment of oxidative stress conditions. Based on different references, it is supposed that CAT behavior is highly dependent on plant species and environmental context. Furthermore, there is a certain disparity between published data. Indeed, several authors defended

CAT's importance in the AOX defense machinery, whilst others do not value their role against stress (Queirós, 2012).

AsA-GSH cycle enzymes

Ascorbate peroxidase (APX; EC 1.11.1.11)

APX is classified as a class I peroxidase, being present in different organisms, such as plants and algae. It was firstly identified from intact chloroplasts and algae by Nakano and Asada (1981) and it plays an essential role in the control of intracellular ROS levels. In fact, being one of the central components of the AsA-GSH cycle, APX functions as an efficient scavenger of H_2O_2, catalyzing its disproportion into water and monodehydroascorbate (MDHA), by using reducing power from AsA (Sharma et al., 2012). In this way, APX activity is greatly dependent on AsA availability, reason why its regeneration is a fundamental process (Foyer and Noctor, 2000). Furthermore, APX possesses a high affinity for H_2O_2 and, in opposite to CAT, can exert its functions even with low amounts of this ROS. By this reason, it is suggested that APX is primarily responsible for H_2O_2 modulation levels for signaling events, whilst CAT is mainly involved in preventing H_2O_2-induced cellular damage by removing its excess (Mittler, 2002).

APXs are codified by a small multigenic family, which transcription is regulated by different stimuli, such as H_2O_2 concentration and redox signals (Gill and Tuteja, 2010). To date, based on amino acid sequences, 5 distinct classes of APX were identified in plants and classified according to their subcellular location. Those include isoenzymes present in the cytosol (cAPX), in the chloroplast (at the stroma – sAPX – and bound to thyllacoid's membrane – tAPX) and in the mitochondria and peroxisomal membranes, mitAPX and pAPX, respectively (Gill and Tuteja, 2010; Sharma et al., 2012). Thus, the importance of APX in ROS detoxification arises from its broad distribution inside plant cells, being present in almost organelles where H_2O_2 is produced.

Overall, APX appears to be one of the main keys of AOX defense system, allowing the proper removal of H_2O_2 in plants. Also, its involvement in the control and regulation of H_2O_2 signaling has been proposed, hence reinforcing its importance in plant cell homeostasis (Gill and Tuteja, 2010; Sharma et al., 2012).

Monodehydroascorbate reductase (MDHAR; EC 1.6.5.4), Dehydroascorbate reductase (DHAR; EC 1.8.5.1) and Glutathione reductase (GR; EC 1.6.4.2)

As a consequence of APX catalytic activity, AsA is oxidized to MDHA, a very unstable radical that can be spontaneously converted into AsA and DHA (Ushimaru et al., 1997).

Yet, MDHA can also be enzymatically reduced by MDHAR, a flavin adenine dinucleotide (FAD) enzyme (Sharma et al., 2012). Present in all plant species, this enzyme is responsible for regenerating the pool of reduced ascorbate in plant cells, by the reduction of the intermediate MDHA, using reducing power from NAD(P)H. As APX, different forms of MDHAR can be found in distinct organelles, such as chloroplasts, mitochondria, peroxisomes and cytosol (Sharma et al., 2012).

Due to the non-enzymatic disproportion of MDHA to AsA and DHA, DHAR is a key element of the AsA-GSH cycle, allowing the regeneration of AsA from its oxidized form – DHA (Taiz et al., 2015). In fact, DHAR requires GSH as reducing agent and has a great specificity for GSH as substrate, not being able to use other reducing compounds (Hossain et al., 1984). This enzyme, classified as a monomeric thiol protein, is essentially found in seed tissues, roots and green organs (Gill and Tuteja, 2010). It is widely accepted that DHAR contributes to the cellular redox balance, with a fundamental role in plant tolerance to abiotic stress (Sharma et al., 2012).

Last, GR is also a relevant component of the AsA-GSH cycle, since it catalyzes the reduction of oxidized glutathione (GSSG) to GSH, allowing the maintenance of GSH/GSSG ratio (Sharma et al., 2012). GR is regarded as a flavoenzyme with a disulfide group and can be found in different taxa of photosynthetic organisms, both prokaryotes and eukaryotes (Sharma et al., 2012). As reviewed by Gill and Tuteja (Gill and Tuteja, 2010), GR is mainly present in the chloroplasts, but it can also be found in mitochondria, cytosol and peroxisomes. Globally, GR importance is intrinsically linked to the maintenance of cell's GSH content and several reverse-genetic studies have highlighted its involvement in plant abiotic stress tolerance (Gill and Tuteja, 2010; Sharma et al., 2012).

Glutathione S-Transferase (GST; EC 2.5.1.18)

GSTs, also named as glutathione transferases, are a class of enzymes present in different types of organisms, including animals and plants (Basantani and Srivastava, 2007). The first report about their occurrence in plant species was made in 1970, in a study conducted with maize (Frear and Swanson, 1970). GSTs are responsible for the conjugation of GSH with different types of xenobiotics, particularly electrophilic substrates (Gill and Tuteja, 2010). Besides their function as important AOX enzymes, GST are also involved in other metabolic events and physiological phenomena, acting as peroxidases under certain conditions and mediating nucleophilic aromatic substitution and isomerization reactions (Basantani and Srivastava, 2007). GSTs show a wide distribution in plant organisms, being present in different development stages and tissues

(McGonigle et al., 2000). The superfamily of plant GSTs is grouped into distinct classes and, generally, are regarded as cytoplasmic proteins, though some isoenzymes were found to be located at chloroplast, microsomes and apoplast (Gill and Tuteja, 2010).

In parallel to what is described for other AOX enzymes, different studies have been exploring the potential of GSTs in increasing plant tolerance to different adverse circumstances. Indeed, it has been suggested that overexpression of GSTs in tobacco plants positively affect the seedling's growth under stressful conditions (Gill and Tuteja, 2010).

1.3.2.2. Non-enzymatic component

Proline (Pro)

The accumulation of compatible solutes by plants is a common response to face stress conditions. By definition, compatible solutes are soluble low molecular mass organic compounds, which can be stored at high concentrations without become toxic. Thus, their increased accumulation provides an excellent tool to prevent oxidative damage and contributes to the cellular osmotic homeostasis and membrane integrity (Hayat et al., 2012). The amino acid Pro, along with sucrose and glycine betaine, is one of the main plant compatible solutes, which has been gaining special attention by plant physiologists as a potent antioxidant (Hayat et al., 2012; Soares et al., 2016).

Pro biosynthesis can be achieved by two different pathways – via glutamic acid or via ornithine. Among them, the production of Pro via glutamic acid is the most frequent, in which PRO is synthetized from glutamate via intermediate Δ'-pyrroline-5-carboxylate (P5C). This reaction involves the catalytic activity of two different enzymes, Δ'-pyrroline-5-carboxylate synthetase (P5CS) and Δ'-pyrroline-5-carboxylate reductase (P5CR) (Gill and Tuteja, 2010).

Although for a long time, Pro was only regarded as an inert osmolyte, able to protect different subcellular structures and macromolecules from osmotic stress, it is, nowadays, recognized that Pro is a powerful AOX, potentially inhibiting programmed cell death (PCD) and directly scavenging ROS, including $^1O_2$ and $OH^{\cdot}$. Indeed, over the past years, a great number of studies regarding the effects of proline on abiotic stress tolerance have been performed, strengthening its role as one of the main non-enzymatic antioxidants (Gill and Tuteja, 2010).

Ascorbate (AsA)

AsA, commonly known as vitamin C or ascorbic acid, is the most abundant AOX metabolite in plant cells, where it can reach up to concentrations of 300 mM (Smirnoff, 2008). This water soluble AOX is found in distinct subcellular compartments, with chloroplasts representing 30-40% of cell's total AsA content (Gill and Tuteja, 2010).

Regarding its biosynthesis, AsA is produced in the mitochondria by L-galactono-γ-lactonedehydrogenase, being posteriorly transported to other organelles, via active transport or facilitated diffusion (Sharma et al., 2012).

Upon normal conditions, the major content of ascorbic acid corresponds to its reduced form, which pool is maintained due to the activity of MDHAR and DHAR. Since it is regarded as the most powerful AOX in plants, the mechanisms responsible for its regeneration play a crucial role in AOX defense system and are essential for plant cell redox balance (Gill and Tuteja, 2010). The importance of AsA in AOX performance is related to its ability to act as an electron donor in a series of enzymatic and non-enzymatic biochemical reactions; also, AsA is capable of directly interact with different ROS, neutralizing the toxic effects of $^1O_2$, $O_2^{\cdot -}$ and $OH^{\cdot}$, and reduce the content of H_2O_2, through the activity of APX (Ahmad et al. 2008; Smirnoff, 2008; Gill and Tuteja, 2010; Sharma et al., 2012).

With effect, in complement to AsA pivotal role in plant AOX defense against pro-oxidative conditions, there are a great number of studies which suggest its involvement in a wide spectrum of other metabolic adjustments. Currently, it is known that AsA also actively participates in the control of mitosis, cellular elongation, senescence and cell death, and can also act as an enzyme stabilizer, protecting enzymes with prosthetic metallic ions (Ahmad et al. 2008; Gill and Tuteja, 2010; Queirós, 2012).

Glutathione (GSH)

The tripeptide GSH is listed as one of the main components of the non-enzymatic AOX system, possessing different properties and being involved in an extensive variety of physiological processes (Ahmad et al. 2008; Gill and Tuteja, 2010; Queirós, 2012). GSH is a non-protein thiol, synthetized in the cytosol and chloroplasts, by specific enzymes - γ-glutamylcysteine synthetase (γ-ECS) and glutathione synthetase (Gill and Tuteja, 2010). The location of GSH is not restricted to any specific organelle and its presence in vacuoles, endoplasmic reticulum, chloroplast, mitochondria and cytosol was already observed (Mittler and Zilinskas, 1992; Jiménez et al., 1998).

In parallel to what is described for AsA, the ratio between GSH and GSSG (oxidized form) gives valuable data about the redox state of the cell. Indeed, GSH acts as a cellular

buffer, contributing to the maintenance of the reduced state of several cell components during both normal and stressful conditions (Foyer and Noctor, 2005). The increased amount of GSH relative to GSSG is accomplished by the action of GR, by increasing GSH biosynthesis and/or GSSG degradation or, alternatively, due to the long-distance transport of GSH and GSSG. Indeed, based on the results of Noctor et al. (2002), glutathione transport across long distances is a common response to balance the differences in GSH production of different plant organs and also mediates the distribution of sulphur (S) from leaves to other parts of the plant.

The AOX activity of GSH arises from its ability to chemically react with $O_{2}^{\cdot -}$, $OH^{\cdot}$ and H_2O_2, functioning as an efficient radical scavenger (Sharma et al., 2012). In addition, GSH plays a significant role in AsA regeneration, since it is the substrate for DHAR. Thus, it has been postulated that GSH can protect several classes of biomolecules, like proteins and lipids, whether by directly removing excess of ROS and/or by reacting with electrophiles (glutathiolation) (Asada et al., 1994).

Overall, GSH is defined as an important water soluble AOX metabolite, but its functions are not confined to the redox state. Indeed, due to GSH reducing power, its importance in cell growth, protein synthesis, enzymatic regulation and expression of stress-responsive genes has been largely documented (Gill and Tuteja, 2010; Sharma et al., 2012).

1.4. Silicon dioxide nanomaterial (nano-SiO_2) - a tool to improve abiotic stress tolerance

As previously mentioned, soil contamination with different types of EC, like nanomaterials and pharmaceuticals, is a matter of great concern and its effects on plant species remain largely unknown. Thus, more than understanding EC-mediated phytotoxicity, it is also essential the development of new tools to increase crop's tolerance to soil degradation.

Silicon (Si) is the second most abundant mineral in soils and, although its establishment as an essential macronutrient is not a consensus (Marschner, 2011; Taiz et al., 2015), it is a beneficial element for plant growth, especially under stressful circumstances (Epstein, 1999, 2009). Thus, over the last couple of years, efforts in investigating the possible mode of action of Si in plants were reinforced, in attempts to better understand the mechanisms behind Si-induced tolerance to biotic and abiotic stress (Liang et al., 2007). According to a high number of previous studies, the positive role of Si in plant stress tolerance might result from an improvement of the plant antioxidant system efficiency, as well as the protection of the photosynthetic apparatus

and the complexation of metals with Si (Liang et al., 2007). In this context, several approaches have been designed and Si application is often used as a tool to increase plant resistance to stress.

Nowadays, nanotechnology is one of the most important tools in modern agriculture, providing new agrochemicals to improve crop's productivity and nutritional safety. In this way, nanofertilizers can be completely and quickly absorbed by plants and suited as an excellent tool to face the low availability of traditional fertilizers (Mousavi and Rezaei, 2011).

Given the positive effects of Si on plant growth and resistance to multiple stress situations, Si nanomaterial could provide new solutions for improving plant tolerance and for agronomic procedures. From the available data, silicon dioxide nanomaterial (nano-SiO_2) has been efficient in mitigating salinity- and metal-induced phytotoxicity. According to Wang et al. (2015), exogenous application of nano-Si improved the growth and nutritional balance of rice seedlings under Cd stress; also, the positive role of Si in regulating salinity responses was highlighted in a study with tomato plants (Haghighi and Pessarakli, 2013). Nevertheless, to the best of our knowledge, only few papers have explored the potential of nano-SiO_2 and its mode-of-action requires further investigation. Moreover, up to now, no reports about the possible beneficial effects of Si on plant tolerance to xenobiotics have been found.

1.5. *Hordeum vulgare* L.

Hordeum vulgare L., commonly known as barley (Figure 6), is one of the most important crops worldwide and one of the first plant species to be domesticated. Nowadays, it is used for both human and animal feeding and malt barley is the main raw material for beer production (Katerji et al., 2006). According to FAOSTAT (2013), barley's global grain production from 2005 to 2009 reached about 140 million ton.

Beyond being an economically important crop, *H. vulgare* also possesses several characteristics which make it a perfect model species for plant science and agronomic studies. Actually, barley is a fast-growing monocot species with the ability to grow in marginal environments, which are often characterized by soil degradation and other stress agents (Katerji et al., 2006). Moreover, in 2012, the total genome sequence of

barley was published (Consortium, 2012), simplifying many molecular, proteomics and metabolomics approaches.

Figure 6. *Hordeum vulgare* L. (a) intact plant; (b) spike; (c) seeds. Extracted from: http://luirig.altervista.org/schedenam/fnam.php?taxon=hordeum+vulgare

1.6. Main objectives

In this project, we are interested in understanding the ecotoxicity of nano-NiO and AC to *Hordeum vulgare* L. and unraveling the beneficial effects of nano-SiO_2 application on its tolerance. For this purpose, several questions underlying this master dissertation need to be answered: What is the ecotoxicological relevance of nano-NiO and AC for barley? How does nano-NiO and AC toxicity affect barley plants productivity? What are the main biochemical and molecular mechanisms underlying this toxicity? How can nano-SiO_2 improve barley's tolerance to both contaminants?

In order to achieve these main objectives, different approaches will be considered, and the studies were focused in:

I. ***Performing a characterization of the phytotoxicity and the physiological effects of AC and nano-NiO on barley plants***, giving particular attention to standard procedures and physiological endpoints;

II. ***Assessing if the co-treatment with nano-SiO_2 results in a higher tolerance of barley to these contaminants***, focusing on different growth-related parameters and physiological evaluations, particularly those related to the induction of oxidative stress and AOX defense;

III. ***Understanding the mode of action of nano-SiO_2, as well as the biochemical and molecular basis of AC- and nano-NiO phytotoxicity***, in what regards the crosstalk between the generation of ROS and the performance of the plant AOX, both at transcript and protein levels.

2. MATERIAL & METHODS

2.1. Tested chemicals and test substrate

Nickel oxide nanomaterial (nano-NiO) (nearly spherical with a particle size of 100 nm, a surface area of 6 m^2 g^{-1} and a 99% purity), silicon dioxide nanomaterial (nano-SiO_2) (hydrophilic with a particle size of 7-14 nm, a surface area of 200 m^2 g^{-1} and a 99.8% purity) and acetaminophen (AC) were purchased from Nanostructured & Amorphous Materials Inc. (Houston, TX, USA), PlasmaChem GmbH© (Germany) and Sigma-Aldrich® (Sigma-Aldrich, Germany), respectively, as powders. The test substrate was an artificial soil, composed of 72.5% (w/w) sand, 12.5% (w/w) kaolin and 5% (w/w) organic matter.

2.2. Characterization of nano-NiO and nano-SiO_2 powders

The characterization of nano-NiO and nano-SiO_2, in order to obtain their size and shape, was evaluated by transmission electron microscopy (TEM) using a Hitachi H8100 with a LaB6 filament operated at an acceleration voltage of 200 kV. The images were acquired by an Olympus KeenView digital Camera with the iTEM software. The powder sample was suspended in ethanol and, then, a drop was allowed to dry on a Cu grid with a formvar film.

2.3. Test species

Seeds of *Hordeum vulgare* L., obtained from a local supplier, were individually observed to discard the damaged ones and, then, surface sterilized with 70 % (v/v) ethanol for 15 min and 20 % (v/v) commercial bleach for 10 min, followed by three series of washing with sterilized deionized water.

2.4. Experimental setup

2.4.1. Ecotoxicological assays with nano-NiO and AC

2.4.1.1. Tested concentrations and treatments

To all the experiments, a series of sequential doses of each contaminant (nano-NiO and AC) was applied, ranging from 0 to 1000 mg kg^{-1} soil, with a dilution factor of 1.5, giving the following concentrations: 87.8, 131.7, 197.5, 296.5, 444.4, 666.7 and 1000 mg kg^{-1} soil. In the case of the Petri dishes' assay, the same procedure was followed, but the concentrations were expressed in mg L^{-1}. The maximum concentration was based on ISO instructions, which suggest that 1000 mg kg^{-1} should be the maximum concentration

tested in ecotoxicological studies (ISO, 2012). Above this level chemical substances should be considered as no toxic.

2.4.1.2. Germination assays in Petri plates

After sterilization, seeds were placed in Petri plates with filter paper embedded in 0.25x modified Hoagland solution (HS) (Taiz et al., 2015), with or without the different concentrations of each tested contaminant. Then, seeds were allowed to germinate for 5 days at 24 °C in a growth chamber, in the dark, during the first 2 days, and at a photoperiod of 16 h - light/8 h - dark thereafter. After the growth period, the germination rate and radicle length were recorded, as well as macroscopic symptoms of toxicity. For each treatment, three biological replicates were considered, with 10 seeds each.

2.4.1.3. Ecotoxicological assays in plastic pots

The seed germination and plant growth ecotoxicological assays were performed in plastic pots with 200 g $_{dw}$ of the artificial soil (5% organic matter, pH 5.5), spiked with aqueous solution/suspension of each contaminant, based on the OECD guidelines (OECD, 2006). The maximum water holding capacity (WHC_{max}), previously determined (ISO, 2005), was adjusted to 40%. The adequate water volume for the WHC_{max} adjustment was used to prepare contaminant's suspensions or solutions, in order to obtain the range of concentrations described above. In order to guarantee the maintenance of soil moisture, a cup filled with distilled water was placed under each test pot. The communication between these was achieved by letting a cotton rope to pass through a hole in the bottom of the test pot. Regarding the assay, briefly, 20 barley seeds, surface sterilized as stated before, were placed in each pot and kindly covered with the soil. At this moment, in order to ensure the availability of nutrients, 120 mL of HS were added to the cup of each pot, only once and in the beginning of the assay. For each experimental condition, 8 replicates (pots) were considered, as well as a negative control, grown in OECD artificial soil without any of the contaminants, thus only moisten with water.

The assay started after 50% of the control seeds germinate and lasted 14 days. Only the 5 first germinated seeds were left in each pot to avoid intraspecific competition between organisms. Plants were maintained in a greenhouse, with controlled conditions of temperature (21 ºC), photoperiod (16 h - light/8 h - dark) and PAR (60 µmol m^{-2} s^{-1}) and the water content of each pot was adjusted when necessary. At the end of the experiment, plants were collected and separated into roots and leaves. Randomly, part of the plant material from 4 replicates was used for the evaluation of the standard

endpoints (root length, fresh and dry weights) and the other 4 replicates were used for biochemical analysis, where the second and third leaves of one plant per biological replicate were randomly selected. The evaluation of fresh biomass was achieved by weighting roots and leaves immediately after collecting the plant material, which was then oven-dried at 60 ºC until constant weight for analysis of the dry biomass.

2.4.2. Selection of nano-SiO_2 concentration

Based on some previous reports (Haghighi and Pessarakli, 2013; Liu et al., 2013; Liu et al., 2015; Wang et al., 2015), four different concentrations (3, 30, 60 and 120 mg kg^{-1} soil) of nano-SiO_2 were tested in order to determine the optimal dose to be used in the final growth assay. Thus, after selecting nano-NiO and AC concentrations (based on standard OECD procedures), the assays above described (2.4.1.3.) were performed once again, testing 3, 30, 60 and 120 mg kg^{-1} soil nano-SiO_2 with and without a selected concentration of each contaminant previously tested (nano-NiO: 120 mg kg^{-1} soil; AC: 400 mg kg^{-1} soil). Nano-SiO_2, nano-NiO and AC were added to the soil, by preparing a solution/suspension of each mixture in the adequate water volume according to the WHC_{max} value. After the growth period the same biometric parameters were evaluated.

2.4.3. Final growth trial

After the selection of the concentration of nano-NiO, AC and nano-SiO_2 to be used in the final assay, barley plants were grown for 14 days in OECD soil as previously described, in order to understand the possible protective role of nano-SiO_2 on the tolerance of barley exposed to both contaminants. For this purpose, different experimental conditions were considered:

- **CTL** – OECD soil;
- **Nano-SiO_2 treatment** – OECD soil + nano-SiO_2;
- **Nano-NiO treatment** – OECD soil + nano-NiO;
- **Nano-NiO + nano-SiO_2 treatment** – OECD soil + nano-NiO + nano-SiO_2;

- **CTL** – OECD soil;
- **Nano-SiO_2 treatment** – OECD soil + nano-SiO_2;
- **AC treatment** – OECD soil + AC;
- **AC + nano-SiO_2 treatment** – OECD soil + AC + nano-SiO_2.

Given that both assays were performed simultaneously, CTL and nano-SiO_2 treatments were the same for both experiments. For each condition, four replicates were prepared. After 14 days, plants from each treatment and replicate were harvested and separated onto roots and leaves. Some individuals from each condition (n=5) were used for biometric parameters, by the evaluation of fresh and dry weights and root elongation. Part of the plant material was immediately processed for biochemical analysis, while the remaining was frozen and grinded in liquid N_2 and stored at -80 ºC to be used for biochemical and molecular techniques.

2.5. Quantification of Ni content

Plants exposed to nano-NiO alone or in the co-presence of nano-SiO_2 were analyzed for the quantification of Ni content in both roots and leaves. Thus, after the growth period, roots and leaves of nano-NiO exposed plants were washed with tap water, immersed in deionized water and dried at 60 ºC until constant weight was recorded. The dried material was mechanically powdered in a mortar, digested with a mixture of HCl:HNO_3, (1:3) and re-suspended in water. Five aliquots of each digested sample were used to prepare solutions to the Ni quantification via multiple standard addition procedure. Ni content in each sample was measured by flame-atomic absorption spectroscopy (Perkin Elmer, AAnalyst 200 model). The recovery rates oscillated from 95 to 106%.

2.6. Quantification of biochemical and cellular parameters

2.6.1 Extraction and quantification of chlorophylls and carotenoids

The evaluation of photosynthetic pigments was performed based on the protocol of Lichtenthaler (1987). Briefly, frozen aliquots of leaves (200 mg) were homogenized in 80% (v/v) acetone and centrifuged for 10 min at 1400 *g*. After collecting the supernatant (SN), the absorbance at 470, 647 and 663 nm was recorded and the concentrations of chlorophyll a (Chl a) and b (Chl b) and carotenoids (Car) were calculated according to the following equations (Lichtenthaler, 1987):

$$\text{Chl a}\,(\text{mg/L}) = 12.25\ \times \text{Abs}\ 663\ \text{nm}\ - 2.79\ \times \text{Abs}\ 647\ \text{nm}$$

$$\text{Chl b}\,(\text{mg/L}) = 21.50\ \times \text{Abs}\ 647\ \text{nm}\ - 5.10 \times \text{Abs}\ 663\ \text{nm}$$

$$Car\ (mg/L) = \frac{1000\ \times Abs\ 470\ nm - 1.82\ \times Chl\ a - 85.02\ \times Chl\ b}{198}$$

2.6.2. Chlorophyll fluorescence analysis

Chlorophyll fluorescence measurements were performed in the second and third expanded leaves of barley plants, using the portable fluorometer Minipan Photosynthesis Yield Analyser (Walz, Effeltrich, Germany). After 20 min of dark adaptation of leaves, several fluorescence parameters were analyzed on the middle region of leaves' adaxial page. Thus, different records were registered: minimum Chl fluorescence in the dark adapted state (F_0), when all the reaction centers of photosystem II (PSII) are opened; maximum Chl fluorescence in the dark adapted state (F_m), after a pulse of actinic light has closed all the reaction centers of PSII; the steady state Chl fluorescence in the light adapted state (F_0); and the maximum Chl fluorescence in the light adapted state (F'_m) after the same pulse of actinic light has been applied. By measuring these values, it was possible to determine PSII efficiency (quantum yield) (ΦPSII) and the maximum quantum yield (F_v/F_m), based on the following formulas:

$$\Phi\,(PSII)\; = \frac{(F'm - Ft)}{F'm}$$

$$\frac{Fv}{Fm} = \frac{Fm - F0}{Fm}$$

2.6.3. Extraction and quantification of soluble proteins

Total soluble proteins were extracted from root and leaf tissues, using frozen aliquots of 0.5 g, in 2 mL of extraction buffer, containing 60 mM Tris-HCl (pH 6.8), Complete™, Mini, EDTA-free – protease inhibitor cocktail tablets (1.4 tablets/10 mL extraction medium), and 1 % (w/v) polyvinylpolypyrrolidone (PVPP). Following the homogenization process, extracts were centrifuged at 16 000 *g* for 25 min at 4 ºC and after collecting the SN, the total soluble protein content was quantified according to Bradford (1976). Basically, 2 µL of extract were combined with 800 µL of dd-H_2O and 200 µL of Protein Assay Dye Reagent Concentrate (BioRad®). After mixing all reaction tubes, an incubation of 15 min was performed at room temperature (RT), followed by the spectrophotometric analysis of each sample at 595 nm. The protein content was calculated based on a calibration curve, using different known concentrations of bovine serum albumin (BSA) as standards, and expressed in mg g^{-1} of fresh weight.

2.6.4. Extraction and quantification of nitrogen (N) metabolism-related enzymes

2.6.4.1. Nitrate Reductase (NR; EC 1.6.6.1) activity assay

The quantification of NR activity was performed in roots and leaves of barley plants, following the protocol of Kaiser and Brendle-Behnisch (1991). Frozen plant material samples, of around 500 mg, were homogenized, at 4 ºC, in 50 mM HEPES-KOH buffer (pH 7.8), supplemented with 1 mM phenylmethylsulfonyl fluoride (PMSF), 10 mM $MgCl_2$ and 1% PVPP. After homogenization, all samples were centrifuged for 25 min, at 15 000 *g* and 4 ºC and, then, SN were collected to new tubes and used for protein quantification (see above in 2.6.3.) and enzyme activity assays.

For NR activity, 100 µL of SN were mixed with 900 µL of a reaction solution, containing 20 mM HEPES-KOH (pH 7.8), 500 µM NADH, 10 µM FAD and 2 mM KNO_3. Then, NADH consumption was followed by spectrophotometry at 340 nm for 1 min and 40 sec, in 20 sec intervals. The levels of NR activity were estimated using NADH extinction coefficient (39.4 mM^{-1} cm^{-1}) and expressed as mmol mg^{-1} of protein.

2.6.4.2. Glutamine Synthetase (GS; EC 6.3.1.2) activity assay

GS activity was determined in both plant organs, using samples from frozen root and leaf tissues. According to the protocol of Shapiro and Stadtman (1970), aliquots were homogenized, at cold conditions, in 2 mL of 25 mM Tris-HCl (pH 6.4) buffer, supplemented with 10 mM $MgCl_2$, 1 mM dithiothreitol (DTT), 10% (v/v) glycerol, 0.05% (v/v) Triton X-100 and 1% (w/v) insoluble PVPP. Afterwards, homogenates were centrifuged for 20 min at 15 000 *g* (4 ºC) and the SN collected and used for protein quantification (see above in 2.6.3) and GS assay.

GS activity was determined by the transferase assay, based on a colorimetric assay, by recording the absorbance at 500 nm. Shortly, 50 µL of SN were combined with 50 µL of 6.4% (w/v) sodium arsenate (pH 6.4) and 400 µL of a reaction mixture (pH 6.4), composed of 100 mM Tris-HCl buffer, 12.5 mM L-glutamine, 6.3 mM hydroxylamine, 5 mM $MnCl_2.4H_2O$ and 2.3 µM adenosine 5′-diphosphate (ADP). In parallel, a blank tube was prepared, by substituting the SN by the extraction buffer. Afterwards, all tubes were incubated for 30 min, at 30 ºC and, then, the reaction was stopped by adding 500 µL of stop solution [2.6 (w/v) $FeCl_3$, 4% (w/v) trichloroacetic acid (TCA) and 33% (v/v) HCl]. After measuring the absorbance, the activity of GS was calculated and expressed as nkat mg^{-1} of protein.

2.6.5. Evaluation of lipid peroxidation

The membrane injury was evaluated in terms of lipid peroxidation (LP), by the quantification of malondialdehyde (MDA) content, according to Heath and Packer (1968). Frozen aliquots of roots and leaves (≈ 250 mg) were homogenized in 1.5 mL of 0.1% (w/v) TCA and centrifuged at 10 000 *g* for 5 min. Afterwards, 1000 µL of 0.5% (w/v) thiobarbituric acid (TBA) in 20% (w/v) TCA were mixed with 250 µL of SN. In parallel, a blank tube was prepared, by mixing 250 µL 0.1% (w/v) TCA instead of SN. Then, tubes were incubated at 95 ºC for 30 min and subsequently cooled on ice (15 min). After centrifugation (10 000 *g*; 15 min) the absorbance of each sample was recorded at 532 and 600 nm. The obtained absorbance values at 600 nm were subtracted to the ones of 532 nm, in order to minimize unspecific turbidity effects. The MDA content, expressed as nmol g^{-1} of fresh weight, was determined using the extinction coefficient of 155 mM^{-1} cm^{-1}.

2.6.6. Quantification of ROS

2.6.6.1. H_2O_2

The quantification of H_2O_2 content was performed as previously described by Jana and Choudhuri (1982). Frozen plant samples of around 200 mg were homogenized, at RT, in 1.5 mL of 50 mM potassium phosphate (PK) buffer (pH 6.5). Then, samples were centrifuged for 25 min (6 000 *g*) and SN aliquots of 1 mL were mixed with 1 mL of a reaction solution containing 0.1% (w/v) $TiSO_4$ in 20% (v/v) H_2SO_4. In parallel, a blank tube was also prepared, by mixing 1 mL of 50 mM PK buffer (pH 6.5) with 1 mL of the reaction solution. After vortexing all tubes for 15 sec, a new centrifugation was performed (6 000 *g*; 15 min) and, then, the absorbance at 410 nm of each sample was recorded. Using the extinction coefficient of 0.28 μM^{-1} cm^{-1}, the content of H_2O_2 was calculated and expressed as ρmol g^{-1} of fresh weight.

2.6.6.2. $O_2^{\cdot-}$

The content of $O_2^{\cdot-}$ was spectrophotometrically assayed following the procedures of Gajewska and Sklodowska (2007), by the reduction of the nitroblue tetrazolium (NBT) reagent. Briefly, equal and small pieces of leaves and roots (ca. 300 mg) were immersed and incubated in 3 mL of a solution composed of 0.01 M sodium phosphate (pH 7.8), 0.05% (w/v) NBT and 10 mM NaN_3 for 60 min in dark conditions. Posteriorly, 2 mL of this reaction solution were collected and transferred to new tubes. A new incubation at 85 ºC

took place for 15 min and the tubes were, subsequently, cooled on ice. Then, after vortexing the tubes and a brief centrifugation (15 sec; maximum speed), the absorbance at 580 nm of each SN was measured. The levels of $O_2^{\cdot -}$, represented by the reduction of the NBT, were expressed as the $Abs_{580\ nm}\ h^{-1}\ g^{-1}$ of fresh weight.

2.6.7. Total and non-protein thiols quantification

The determination of total and non-protein thiols levels was accomplished by spectrophotometry, following the method of Zhang et al. (2009). In cold conditions (4 ºC), frozen aliquots of roots and leaves were homogenized in a mortar and a pestle with quartz sand and extraction buffer, containing 20 mM ethylenediaminetetraacetic acid (EDTA) and 20 mM ascorbic acid (roots: 200 mg/1mL of extraction buffer; leaves: 200 mg/2 mL of extraction buffer). Next, all samples were centrifuged for 20 min at 12 000 *g* (4 ºC). After recovering the SN, part of it was used to determine the total thiols and other left to quantify the non-protein thiols.

Regarding total thiols, 200 µL of SN were mixed with 960 µL of 200 mM Tris-HCl (pH 8.2) and 40 µL of 10 mM 5,5´-dithiobis(2-nitrobenzoic acid) (DTNB). The reaction mixture was incubated at RT for 15 min and, then, the absorbance (412 nm) of each sample was read.

In order to quantify the non-protein thiol groups, 500 µL of SN were mixed with 500 µL of 10% (w/v) sulfosalicylic acid, in duplicates, followed by an incubation at RT for 15 min and a centrifugation at 3 000 *g* (4 ºC) for 15 min. Then, the SN of both tubes was recovered and mixed together. To each 500 µL of SN, 475 µL of 400 mM Tris-HCl (pH 8.9) and 25 µL of DTNB were added. Color was allowed to develop for 5 minutes at RT and the absorbance was read at 412 nm.

Total and non-protein thiol groups were calculated using the extinction coefficient of 13 600 $M^{-1}\ cm^{-1}$ and expressed as nmol g^{-1} of fresh weight. The protein thiol groups were estimated, by subtracting the non-protein to the total thiol groups.

2.6.8. Cell death histochemical detection

In order to detect possible changes in barley's cellular viability in response to nano-NiO and AC, the second and third leaf of each plant were immersed in a 0.25 % (w/v) Evans Blue solution during 24 h (Romero-Puertas et al., 2004). Posteriorly, leaves were incubated in boiling 96% (v/v) ethanol to remove the pigments. At this point, cell death, stained as blue spots on leaves, was photographically recorded using a digital camera. Then, leaves were cut in small and equal pieces and incubated in a solution of 1% (w/v) sodium dodecyl sulfate (SDS) in 50% (v/v) ethanol, for 18 h at 50 ºC, in order to solubilize

the dye agent. After this period, the absorbance of each sample was recorded at 600 nm and the results expressed as $Abs_{600\ nm}\ g^{-1}$ of fresh weight.

2.6.9. Extraction and quantification of AOX metabolites

2.6.9.1. Proline

The evaluation of Pro levels was performed according to the protocol described by Bates et al. (1973). In a mortar, containing some quartz sand, samples of plant material, previously frozen at -80 ºC, were homogenized in 3% (w/v) sulfosalicylic acid, in a proportion of 1 mL for 0.100 g of sample. The homogenates were centrifuged at 500 *g* for 10 min and, then, SN of each sample was collected. Subsequently, 200 µL of SN were combined with 200 µL of glacial acetic acid and 200 µL of acid ninhydrin (3 technical replicates/homogenate). All reaction mixtures were incubated at 96 ºC for 1 h and posteriorly cooled on ice. In order to extract the proline, 1 mL of toluene was added to each tube, followed by a vigorous vortexing (15 sec). After total separation of phases, the reddish upper one was collected to new tubes and its absorbance at 520 nm was measured, using toluene as blank.

The Pro content was estimated through a calibration curve, obtained by different solutions of known concentration of proline. Results were expressed as µg g^{-1} of fresh weight.

2.6.9.2. Ascorbate – reduced and oxidized forms

Levels of reduced and oxidized AsA were quantified by spectrophotometry, based on α-α'-bipyridyl-based colorimetric assay (Gillespie and Ainsworth, 2007).

Aliquots from both roots and leaves were homogenized, on ice, in 6% (w/v) TCA and centrifuged, at 4 ºC and 6 000 *g*, for 5 min. Then, 100 µL of SN were mixed with 50 µL of 75 mM PK buffer (pH 7.0). In parallel, two blank tubes were prepared (one for total ascorbate and another for AsA), by replacing the SN for 6% (w/v) TCA. These reaction mixtures were used for the estimation of total and reduced ascorbate contents.

For the total ascorbate assay, reaction mixtures were combined with 50 µL of 10 mM DTT and incubated at RT for 10 min, in order to reduce the pool of oxidized AsA. Then, 50 µL of 0.5% (w/v) N-ethylmaleimide (NEM) were added to remove the excess of DTT. In contrast, to quantify the reduced ascorbate, the exact volumes of DTT and NEM were substituted by adding 100 µL of dd-H_2O to the respective tubes.

Afterwards, all assay tubes were supplemented with 250 µL of 10% (w/v) TCA, 200 µL of 43% (v/v) H_3PO_4, 200 µL of 4% (w/v) 4,4'-bipyridyl (BIP) and 100 µL of 3% (w/v)

$FeCl_3$, vigorously shaken and subsequently incubated for 1 h at 37 ºC. Then, the absorbance at 525 nm of each sample was recorded.

The concentration of both total and reduced ascorbate was estimated through a calibration curved, obtained by the above described protocol and prepared with known concentrations of AsA. DHA was calculated as the difference between the content of total ascorbate and AsA. Total ascorbate, AsA and DHA levels were expressed in terms of μmol g^{-1} of fresh weight.

2.6.10. Extraction and quantification of AOX enzymes

2.6.10.1. Extraction procedure

Samples of plant material (ca. 0.5 g), stored at -80 ºC, were homogenized, on ice, with some quartz sand and 2 mL of extraction buffer, containing 100 mM PK (pH 7.3), 8% (v/v) glycerol, Complete™, Mini, EDTA-free – protease inhibitor cocktail tablets (1.4 tablets/10 mL extraction medium), 1 mM PMSF, 1 mM EDTA, 5 mM L-ascorbic acid and 1% (w/v) PVPP. The extracts were centrifuged, at 4 ºC, for 25 min at 16 000 *g* and the resulting SN were divided into aliquots, used for protein quantification (see 2.6.3.) and enzyme activity assays. Regarding specifically SOD activity assay, SN aliquots were combined with NaN_3 and glycerol to final concentrations of 10 μM and 40% (v/v), respectively.

2.6.10.2. SOD activity assay

The total activity of SOD was quantified by spectrophotometry, based on the inhibition of the photochemical reduction of NBT, following the protocol of Donahue et al. (1997). For each sample, an appropriate volume of extract (50 μg of protein) was added to a reaction mixture containing 100 mM PK (pH 7.8), 0.093 mM EDTA, 12.05 mM L-methionine, 0.0695 mM NBT and 0.0067 mM riboflavin in a final volume of 3 mL. The enzymatic reaction was started by adding the riboflavin to the tubes, which were immediately placed under 6 fluorescent 8W lamps for 10 min. After this period, the light source was removed in order to stop the reaction. In parallel, for each sample, a blank tube was prepared by replacing the protein extract by the homogenization buffer. After recording the absorbance of each sample at 560 nm, SOD activity was expressed as units of SOD mg^{-1} of protein, in which one SOD unit corresponds to the amount of enzyme that inhibits by 50 % the photochemical reduction of NBT at 560 nm.

2.6.10.3. APX activity assay

APX activity was quantified according to Nakano and Asada (1981), with slight modifications. The assays were performed in a UV-microplate well and in a final volume of 200 µL. Briefly, in each well, 170 µL of 50 mM PK buffer (pH 7.0), containing 0.6 mM AsA, were mixed with 20 µL of protein extract and 10 µL of 254 mM H_2O_2. The same procedure was followed to prepare a blank, in which the protein extract was replaced by the extraction buffer. Afterwards, the UV-microplate was shaken for 5 sec and the AsA oxidation, at 290 nm, was monitored in intervals of 10 sec over 1 min. The total activity of APX was calculated using the AsA extinction coefficient of 0.49 mM^{-1} cm^{-1} and expressed as µmol oxidized AsA min^{-1} mg^{-1} of protein.

2.6.10.4. CAT activity assay

The quantification of CAT activity was performed in roots and leaves, following the protocol of Aebi (1984) with slight modifications. As in APX, all procedures were executed in a final volume of 200 µL and in a UV-microplate. Basically, 160 µL of PK buffer (pH 7.0) were combined with 20 µL of sample and 20 µL of 100 mM H_2O_2. After shaking the UV-microplate for 5 sec, the rate of H_2O_2 degradation was followed over 30 sec, in 5-sec intervals, at 240 nm. Based on the Lambert-Beer law, and knowing that H_2O_2 extinction coefficient is 39.4 mM^{-1} cm^{-1}, CAT activity was determined and expressed as nmol H_2O_2 min^{-1} mg^{-1} of protein.

2.7. Expression profile of AOX enzymes – SOD, CAT and APX

2.7.1. RNA extraction and cDNA synthesis

Total RNA from both root and leaf tissues was extracted and used to quantify the expression of specific genes using quantitative PCR analysis.

RNA extraction, isolation and purification was performed using the NZYol reagent (NZYTech®, Portugal), following the instructions of the manufacture. Briefly, aliquots of around 100 mg were mixed with 1 mL of NZYol, vigorously vortexed by 3 min and centrifuged at 12 000 *g* for 10 min (2-8 ºC). In order to allow the phase separation, an incubation at RT for 5 min was performed and, then, 200 µL of chloroform were added to each tube, followed by a new incubation (RT; 2-3 min) and centrifugation (12 000 *g*; 15 min; 2-8 ºC). After this process, the aqueous phase was carefully transferred to new

Eppendorf tubes and the RNA was precipitated by adding 500 µL of cold isopropyl alcohol. Once again, tubes were incubated at RT for 10 min and subsequently centrifuged at 12 000 *g* for 10 min (2-8 ºC). Posteriorly, SN was removed and the pellet washed with 1 mL of 75% (v/v) ethanol, followed by a new centrifugation for 10 min at 7 500 *g*. Then, the pellet was air-dried and re-suspended in 40 µL of RNase free water and 1 µL of Ribolock RNase Inhibitor. In order to avoid genomic DNA contamination, each sample was treated with NZY DNase I (NZYTech®,Portugal). After this, RNA was once again precipitated, washed with ethanol and re-suspended in RNase free water.

Posteriorly, after RNA quantification and assessing its integrity by agarose gel electrophoresis, cDNA synthesis was performed with SuperScript® IV Reverse Transcriptase (ThermoFisher Scientific®), following the manufacture's guidelines. The reactions were performed in a final volume of 20 µL, using the R9 primer (5'-CCA GTG AGC AGA GTG ACG AGG ACT CGA GCT CAA GCT TTT TTT TTT TTT TTT-3'), which contains a poly-T region to anneal to the template RNA. Afterwards, cDNA solutions were diluted (1:10) and used in quantitative PCR analysis.

2.7.2. q-PCR amplification

The transcript levels of the main AOX enzymes (*HvSOD, HvCAT1, HvCAT2 and HvAPX*) was analyzed by monitoring their expression rate with quantitative real time PCR, performed in a CFX96 Real-Time Detection System (BioRad®, Portugal). All reactions were performed in triplicate using SsoFast™ EvaGreen®Supermix (BioRad®, Portugal). In order to allow the normalization of gene expression, *HvACTIN* was used as the internal control. The PCR conditions consisted of an initial denaturation at 95 ºC for 3 min, followed by 40 cycles (95 ºC for 30 sec; 58 ºC for 45 sec; 72 ºC for 45 sec).

The obtained data was analyzed by CFX Manager Software (BioRad®, Portugal) and the quantification of mRNA levels was achieved by applying the $2^{\Delta\Delta Ct}$ method of Livak and Schmittgen (Livak and Schmittgen, 2001). All primer pairs used in all q-PCR reactions are listed in Table 1, as well as their melting temperature (T_m) and amplicon size.

Table 1. *Gene-specific primers used in q-PCR analysis.*

Gene name	Acession number	Primer sequence	T_m (°C)	Amplicon (bp)	Reference
SOD (HvSOD)	AK252295	5'-CCGAAGATGAAATCCGCCA-3' 5'-CGGCCAATGATTGAATGTGG-3'	55.42/54.71	126	Shagimardanova et al., 2010
CAT1 (HvCAT1)	U20777	5-TGAAGTGCCTCTTGGAT-3' 5-AGACGGTGCCTTTGGGT–3'	50.41/57.01	373	Chen et al., 2010
CAT2 (HvCAT2)	U20778	5'-CAAACTACCTGATGCTC-3' 5'-CTT CTC CCT CTT TCC AA-3'	47.04/47.94	191	Chen et al., 2010
cAPX (HvAPX)	AJ006358	5'-CCTCATCGCCGAGAAGAA-3' 5'-TGTCCAGGGTCCCTCAAA-3'	54.30/55.77	466	Chen et al., 2010
Actin (HvACTIN)	AY145451	5'-ATGTTTTTTTCCAGACG-3' 5'-ATCAAGCCAACCCAAGT-3'	44.75/51.41	149	Chen et al., 2010

2.8. Statistical analysis

All biometric, biochemical and molecular measurements were, at least, carried out in triplicate for each replica (in a total of 3 replicas for each parameter) and the results expressed as mean ± standard deviation of the mean (STDEV).

Regarding the ecotoxicological assays with increased concentrations of nano-NiO and AC, in attempts to discriminate differences between each tested-concentration and the control, and after checking the homogeneity of variances by using the Levene's test, a one-way ANOVA was performed, followed by a Dunnet post-hoc test, when significant differences were recorded ($p < 0.05$). Since one-way ANOVA is regarded as a robust and strong analysi,s parametric tests were always used instead of nonparametric tests (Zhar, 1996). The statistical analysis was accomplished by using the software GraphPad® Prism 6 (GraphPad Software Inc.,USA). The calculation of ECx (effective concentration for a x% of effect) values, and the corresponding 95% confidence limits, was performed using the nonlinear least squares regression model procedure by the Statistica software (version 13).

Regarding the final growth trial, where plants were exposed to contaminants alone and in the presence of nano-SiO_2, after checking variance homogeneity and performing a one-way ANOVA, Tukey's multiple range tests were used for determining significant differences among means in nano-NiO and AC experiments. Once again, all statistical data was generated by GraphPad® Prism 6 (GraphPad Software Inc.,USA).

3. RESULTS

In this section, statistical results of ANOVA analysis for each evaluated parameter are presented in Tables 1, 2, 3 and 4, found in Annex I.

3.1. Ecotoxicity of nano-NiO and AC to barley plants

In this study, we firstly aimed to determine the ecotoxicological relevance of nano-NiO and AC to *H. vulgare*. With this purpose, and also in order to select the proper concentrations of nano-NiO and AC to be tested in the final assay, an independent experiment was designed and performed, in which barley plants were cultivated in the presence of increasing concentrations of each contaminant.

3.1.1. Characterization of nano-NiO by TEM analysis

As can be seen in Figure 7, nano-NiO are nearly spherical, with an irregular surface, and despite some smaller nanoparticles were present (< 100 nm), overall the nanomaterial showed a maximum size between 100 nm in all the dimensions, corroborating the manufacture's information. However, although this NM has tendency to aggregate when suspended in water (Nogueira et al., 2015), the aggregation observed in the figure was likely caused by the preparation of the grids for TEM observations.

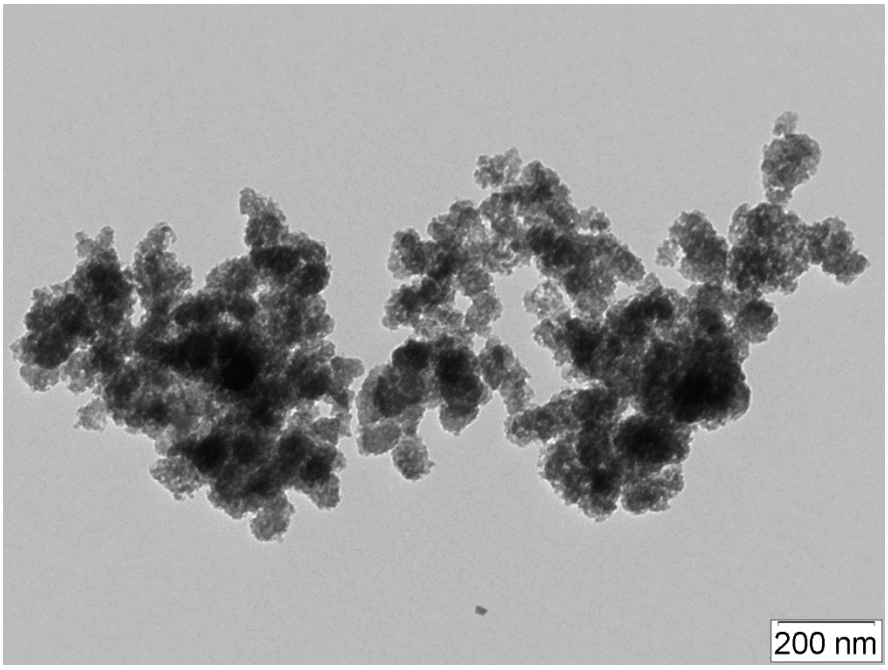

Figure 7. *Transmission electron microscopy (TEM) images of nano-NiO.*

3.1.2. Effects of nano-NiO and AC on germination and seedling growth

The exposure of *H. vulgare* to increasing concentrations of nano-NiO and AC did not affect seed germination, since no significant differences were found among all tested concentrations and the control situation.

However, as can be seen in Figure 8, seedlings growing in the presence of different nano-NiO and AC concentrations resulted in a significant inhibition of root elongation, with increasing concentrations of both contaminants. It is also evident that nano-NiO induced a more pronounced response than AC, with lower ECx and LOEC values (Tables 2 and 3).

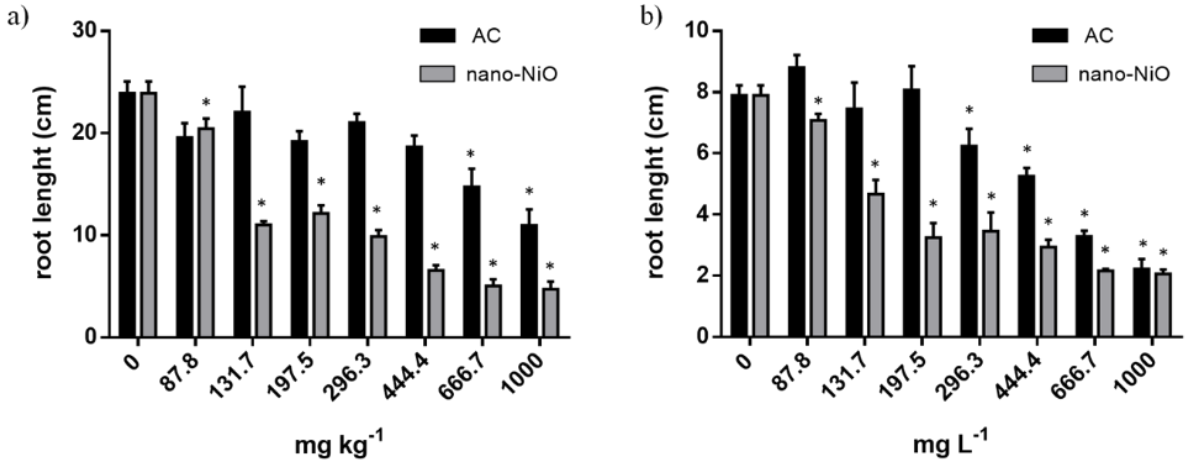

Figure 8. *Root length of barley plants exposed to different concentrations of nano-NiO and AC for 14 days in OECD soil (a) and for 5 days in Petri plates (b).* Data presented are mean ± STDEV (n ≥ 3). * above bars indicates significant statistical differences from control at $p \leq 0.05$.

3.1.3. Effects of nano-NiO and AC on biometric parameters of soil-grown barley

After screening the potential toxicity of both contaminants on barley seedlings development during 5 days, barley plants were cultivated in OECD soil for 14 days, testing the same doses of nano-NiO and AC.

After 14 days of growth, the exposure of barley to increased concentrations of nano-NiO and AC led to a significant decrease in root length (Figure 8). However, likely to what was reported for Petri plate assay, nano-NiO exhibited a more pronounced negative effect than AC.

Furthermore, as shown in Figure 9 and 10, the exposure of barley plants to each contaminant induced a decrease in biomass production of both organs, even though different patterns between nano-NiO and AC on fresh and dry weight of seedlings have been observed.

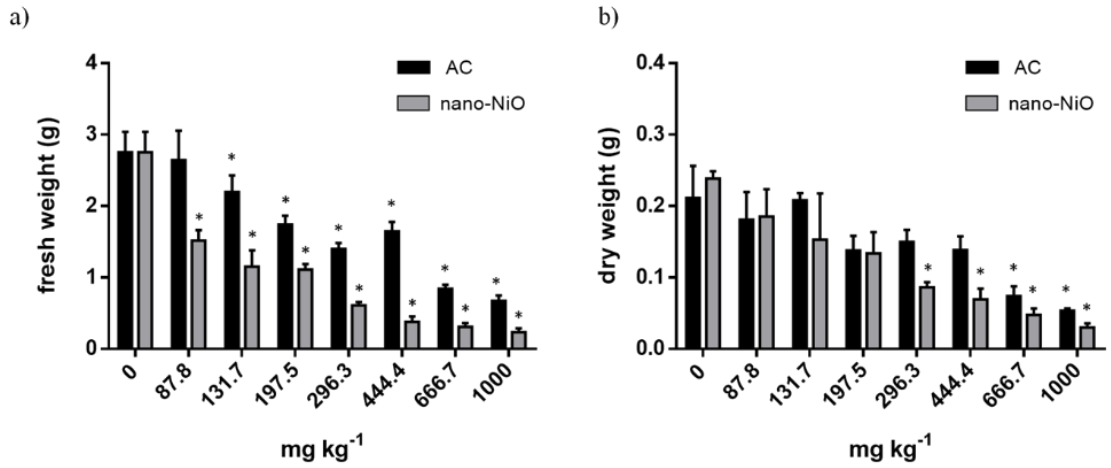

Figure 9. *Roots' fresh (a) and dry (b) weights of barley plants exposed to different concentrations of nano-NiO and AC for 14 days in OECD soil.* Data presented are mean ± STDEV (n ≥ 3). * above bars indicates significant statistical differences from control at $p \leq 0.05$.

Relatively to nano-NiO, as the Figures 9 and 10 suggest, a strong adverse effect on biomass production was recorded in roots and leaves, especially for leaves fresh weight (Table 2). Also, the development of toxicity symptoms (data not shown) in nano-NiO-treated leaves was observed. Regarding AC experiment, significant differences were only detected for higher concentrations of the contaminant in both roots and leaves, being roots the most sensitive organ (Figure 9 and 10) (Table 3).

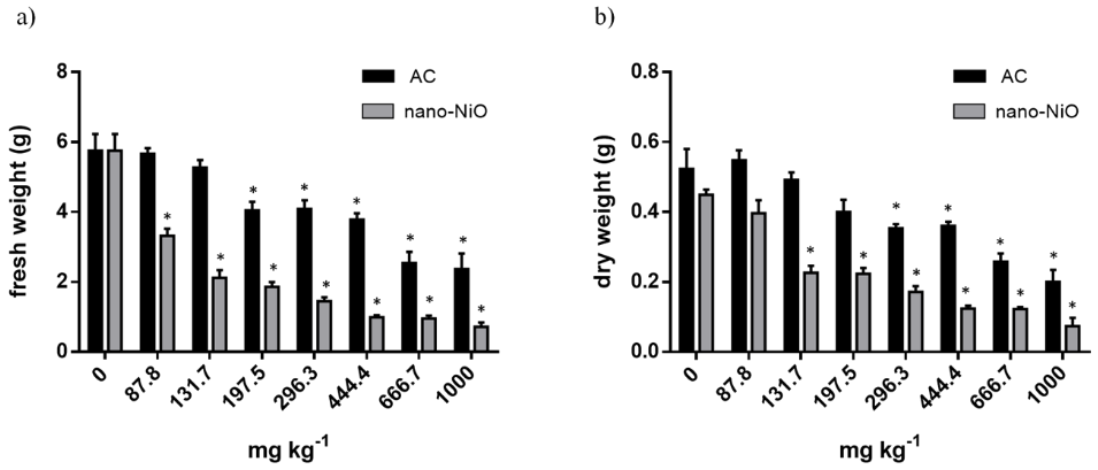

Figure 10. *Leaves' fresh (a) and dry (b) weights of barley plants exposed to different concentrations of nano-NiO and AC for 14 days in OECD soil.* Data presented are mean ± STDEV (n ≥ 3). * above bars indicates significant statistical differences from control at $p \leq 0.05$.

Based on these results, and considering the lowest EC_{50} value for each contaminant, the concentrations of 120 and 400 mg kg^{-1} of nano-NiO and AC, respectively, were selected for the further experiments (Tables 2 and 3), since these concentrations induced significant macroscopic toxic effects, without completely compromising plant development and biomass production.

Table 2. *Summary of ecotoxicological data obtained for nano-NiO experiment.* Concentrations, and corresponding 95% confidence intervals, are expressed as mg kg^{-1} of soil, excepting in Petri dish assays, where values are expressed as mg L^{-1}.

Endpoint		nano-NiO					
		NOEC	LOEC	Units of estimated model (p; r)	EC_{10}	EC_{20}	EC_{50}
Germination rate		≥1000	–	–	–	–	–
Root lenght	Petri plate	–	≤87.8	0.85; 0.92	23.9 (0.08–47.72)	54.9 (14.7–95.1)	227.2 (141.0–313.4)
	OECD soil	–	≤87.8	0.90; 0.95	28.6 (10.3–46.9)	58.8 (30.7–86.9)	201.5 (150.1–252.9)
Root fresh weight		–	≤87.8	0.90; 0.95	18.6 (5.1–32.2)	37.2 (17.0–57.4)	121.1 (87.5–154.7)
Root dry weight		197.5	296.3	0.73; 0.86	39.2 (−5.0 to 83.5)	73.5 (10.7–136.3)	214.5 (112.0–317.0)
Leaf fresh weight		–	≤87.8	0.95; 0.97	13.8 (5.9–21.7)	30.9 (17.8–44.1)	122.6 (96.9–148.3)
Leaf dry weight		87.8	131.7	0.86; 0.93	29 (8.1–49.9)	59.2 (27.5–90.9)	200.5 (142.5–258.5)
Chlorophylls		131.7	197.5	0.76; 0.87	45.1 (−10.1 to 100.2)	128.3 (21.5–234.9)	764.2 (438.3–1090.1)
Carotenoids		–	≤87.8	0.74; 0.86	29.2 (−18.8 to 77.3)	143.6 (5.9–281.2)	2175.5 (308.7–4042.3)
Lipid peroxidation		–	≤87.8	–	–	–	–
O_2^-		–	≤87.8	–	–	–	–
H_2O_2		–	–	–	–	–	–
O_2^-/H_2O_2		–	≤87.8	–	–	–	–
Cell death		–	≤87.8	–	–	–	–

NOEC – Non-observed-effect concentration; ***LOEC*** – Lowest-observed-effect concentration; ***ECx*** – effective concentration causing x% of the effect.

Table 3. *Summary of ecotoxicological data obtained for AC experiment.* Concentrations, and corresponding 95% confidence intervals, are expressed as mg kg^{-1} of soil, excepting in Petri dish assays, where values are expressed as mg L^{-1}.

Endpoint		AC					
		NOEC	LOEC	Units of estimated model (p; r)	EC_{10}	EC_{20}	EC_{50}
Germination rate		≥1000	–	–	–	–	–
Root lenght	Petri plate	197.5	296.3	0.87; 0.93	194 (95.5–292.4)	288.2 (182.7–393.7)	566.4 (459.0–674.0)
	OECD soil	444.4	666.6	0.62; 0.79	323.6 (100.7–546.5)	490.9 (75.1–706.5)	999.9 (733.8–1265.9)
Root fresh weight		87.8	131.7	0.76; 0.87	63.2 (−0.8 to 127.2)	124.6 (33.0–216.3)	397.4 (242.4–552.3)
Root dry weight		444.4	666.6	0.70; 0.83	65.6 (−11.7 to 142.9)	131.1 (18.3–243.9)	427.7 (236.9–618.4)
Leaf fresh weight		131.7	197.5	0.79; 0.89	87.7 (15.0–160.3)	180.6 (75.4–285.7)	620 (438.9–801.1)
Leaf dry weight		197.5	296.3	0.77; 0.88	108.5 (16.3–200.6)	207.7 (84.2–331.2)	630.4 (443.9–816.9)
Chlorophylls		≥1000	–	–	–	–	–
Carotenoids		≥1000	–	–	–	–	–
Lipid peroxidation		–	≤87.8	–	–	–	–
O_2^-		–	≤87.8	–	–	–	–
H_2O_2		≥1000	–	–	–	–	–
O_2^-/H_2O_2		–	≤87.8	–	–	–	–
Cell death		–	≤87.8	–	–	–	–

NOEC – Non-observed-effect concentration; *LOEC* – Lowest-observed-effect concentration; *ECx* – effective concentration causing x% of the effect.

3.1.4. Effects of nano-NiO and AC on physiological and redox status of soil-grown barley

In attempts to gain a better insight about the possible mechanisms underlying nano-NiO- and AC-induced phytotoxicity, the levels of photosynthetic pigments were quantified and the occurrence of oxidative stress was evaluated, by estimating $O_2^{\cdot-}$ and H_2O_2 content, as well as lipid peroxidation (LP) and cell death.

As shown in Figure 11, excess of nano-NiO induced a clear negative response in photosynthetic pigments, since a significant reduction of both chlorophylls and carotenoids contents was observed. When comparing the two photosynthetic pigments, Table 2 suggests that carotenoids represent a more sensitive biomarker than chlorophylls for nano-NiO-mediated stress. In opposite to this situation, the exposure of *H. vulgare* up to 1000 mg kg^{-1} of AC did not affect neither total chlorophyll nor carotenoids content.

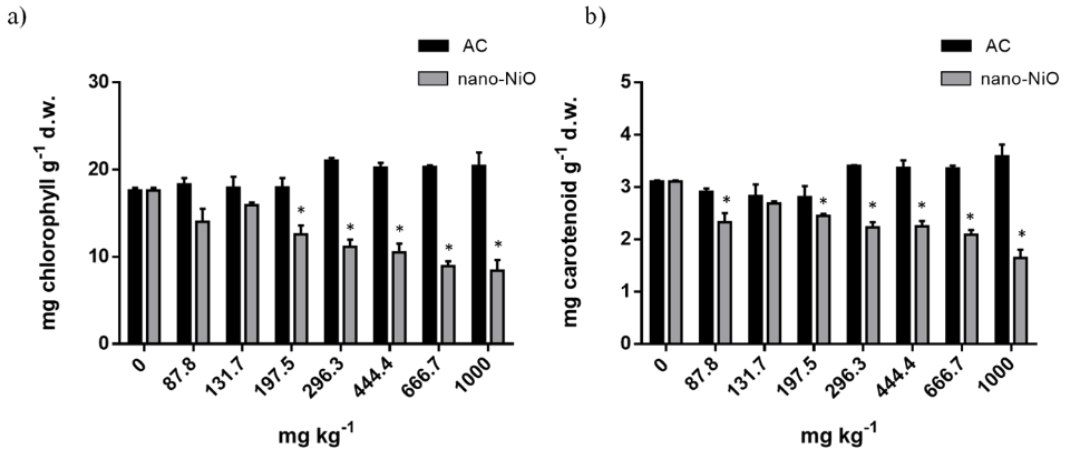

Figure 11. *Total chlorophylls (a) and carotenoids (b) in leaves of barley plants exposed to different concentrations of nano-NiO and AC for 14 days in OECD soil.* Data presented are mean ± STDEV (n ≥ 3). * above bars indicates significant statistical differences from control at $p \leq 0.05$.

The lipid peroxidation damage was measured in terms of MDA content in leaves of barley plants treated and non-treated with the different concentrations of each contaminant.

When nano-NiO-treated plants are concerned, significant changes from the CTL were observed for all tested-concentrations (Figure 12).

Plants grown under the exposure to increasing doses of AC exhibited higher values of MDA than the control situation (Figure 12). For the three lowest concentrations (87.8, 131.7 and 197.5 mg kg^{-1}soil) a tendency for decreased lipid peroxidation levels was found, although levels were always higher than the CTL. Regarding the four higher AC

concentrations (296.5, 444.4, 666.7 and 1000 mg kg^{-1} soil), a gradual increment in MDA content was noticed.

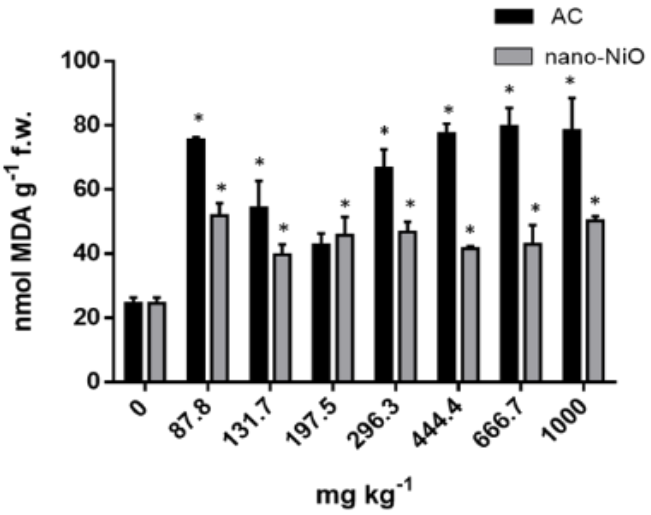

Figure 12. *MDA content in leaves of barley plants exposed to different concentrations of nano-NiO and AC for 14 days in OECD soil.* Data presented are mean ± STDEV (n ≥ 3). * above bars indicates significant statistical differences from control at $p \leq 0.05$.

As can be seen in Figure 13a, the levels of $O_2^{\cdot-}$ were increased in response to AC treatments, even in the lowest applied dose. Regarding nano-NiO experiment, the same pattern was observed, with higher values of this ROS in all tested-concentrations relatively to the CTL, in a dose-dependent manner (Figure 13a).

a)

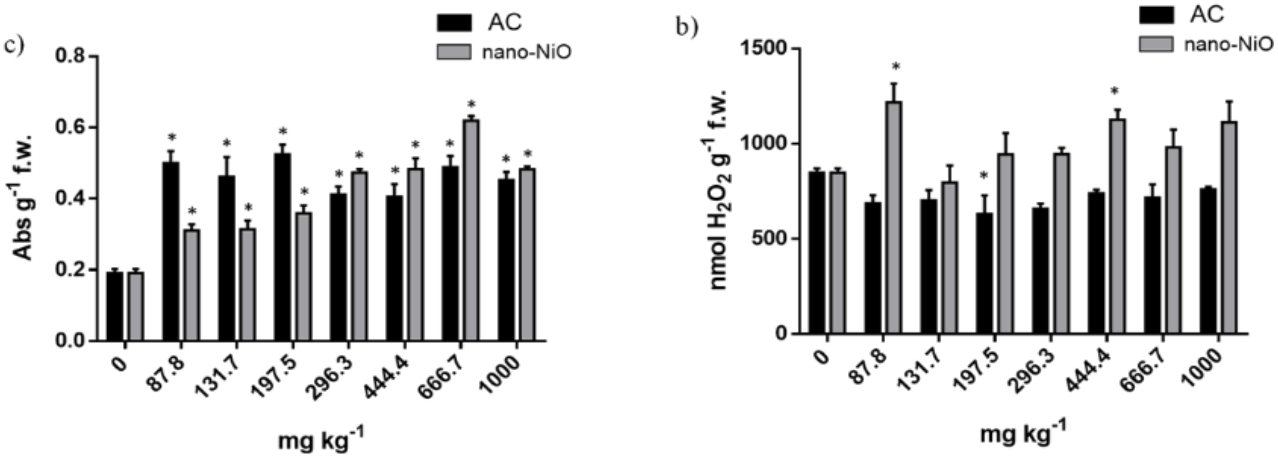

Figure 13. *$O_2^{\cdot-}$ (a) and H_2O_2 (b) content in leaves of barley plants exposed to different concentrations of nano-NiO and AC for 14 days in OECD soil.* Data presented are mean ± STDEV (n ≥ 3). * above bars indicates significant statistical differences from control at $p \leq 0.05$.

The exposure of barley to AC did not affect the total content of H_2O_2, since no significant differences were found between the applied doses and the CTL situation

(Figure 13b). On the other hand, nano-NiO affected the production of H_2O_2, but, as displayed in Figure 13b, it was not observed a consistent response among treatments.

The ratio between $O_2^{\cdot-}/H_2O_2$ was changed in response to both nano-NiO and AC treatments (Figure 14). Regarding nano-NiO experiment, higher values of $O_2^{\cdot-}/H_2O_2$ in all tested-concentrations were found relatively to the CTL, in a dose-dependent manner (Figure 14), except for the highest concentration where a decreasing tendency was observed. The application of sequential doses of AC to soil-grown barley also resulted in an increase of this proportion for all the tested concentrations (Figure 14).

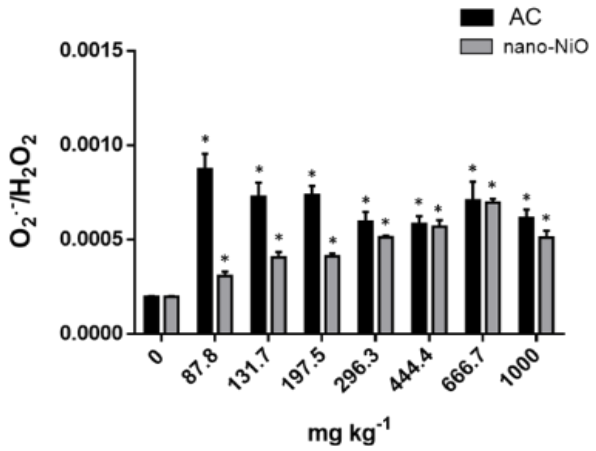

Figure 14. *$O_2^{\cdot-}/H_2O_2$ ratio in leaves of barley plants exposed to different concentrations of nano-NiO and AC for 14 days in OECD soil.* Data presented are mean ± STDEV (n ≥ 3). * above bars indicates significant statistical differences from control at $p \leq 0.05$.

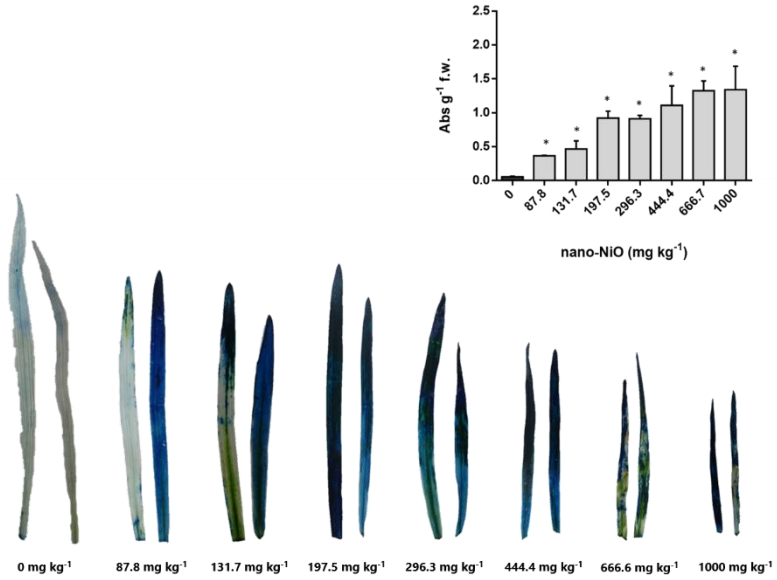

Figure 15. *Cell death staining and quantification in leaves of barley plants exposed to different concentrations of nano-NiO for 14 days in OECD soil.* Data presented are mean ± STDEV (n ≥ 3). * above bars indicates significant statistical differences from control at $p \leq 0.05$.

Cell death was analyzed by histochemical detection, along with spectrophotometry in leaves of barley plants treated and non-treated with the different concentrations of each contaminant (Figures 15 and 16). An increase in cell death of barley leaves was observed for all tested-concentrations of both nano-NiO and AC, in a concentration-dependent manner (Figures 15 and 16).

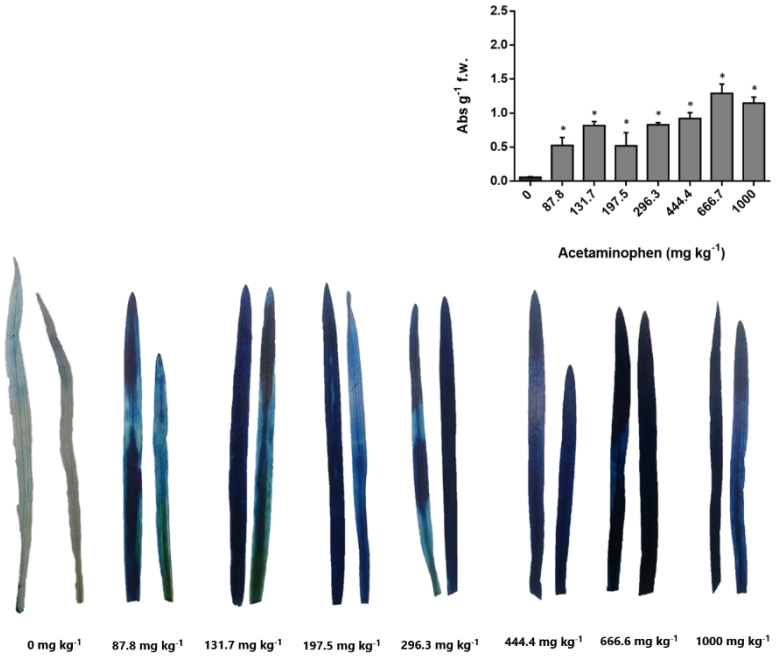

Figure 16. *Cell death staining and quantification in leaves of barley plants exposed to different concentrations of AC for 14 days in OECD soil.* Data presented are mean ± STDEV (n ≥ 3). * above bars indicates significant statistical differences from control at $p \leq 0.05$.

3.2. Effects of nano-SiO_2 on the tolerance of barley under nano-NiO and AC stress

After selecting nano-NiO and AC concentrations, four concentrations of nano-SiO_2 were applied alone and in the presence of each contaminant to select the dose with great potential for ameliorating the toxic effects of the other contaminants.

3.2.1. Characterization of nano-SiO_2 by TEM analysis

As can be seen in Figure 17, nano-SiO_2 showed a spherical shape and, overall, the nanomaterial showed a medium size of around 25 nm, corroborating the manufacture's information. Furthermore, as reported for nano-NiO, a great tendency for nano-SiO_2 to form aggregates was also observed.

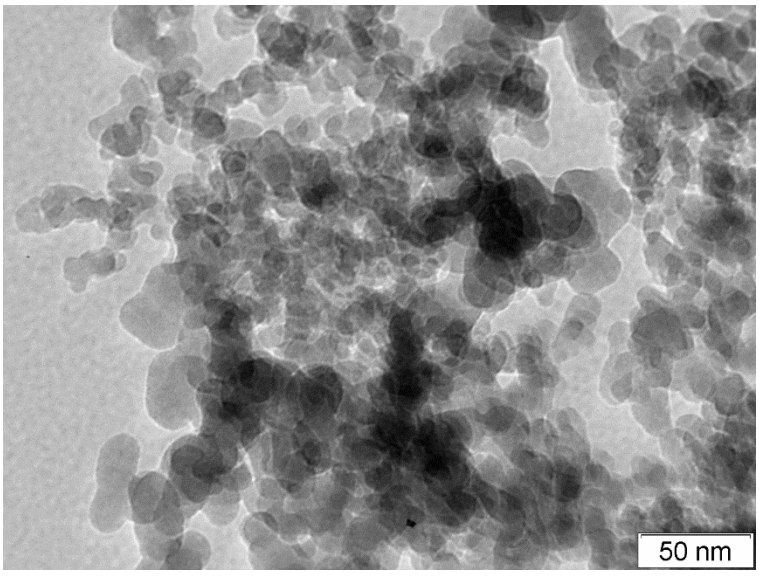

Figure 17. *Transmission electron microscopy (TEM) images of nano-SiO_2.*

3.2.2. Selection of nano-SiO_2 concentration

Results displayed in Figure 18 show that the treatment of plants with increased concentrations of nano-SiO_2 did not change the root length in any experimental condition, since no statistical significance was found.

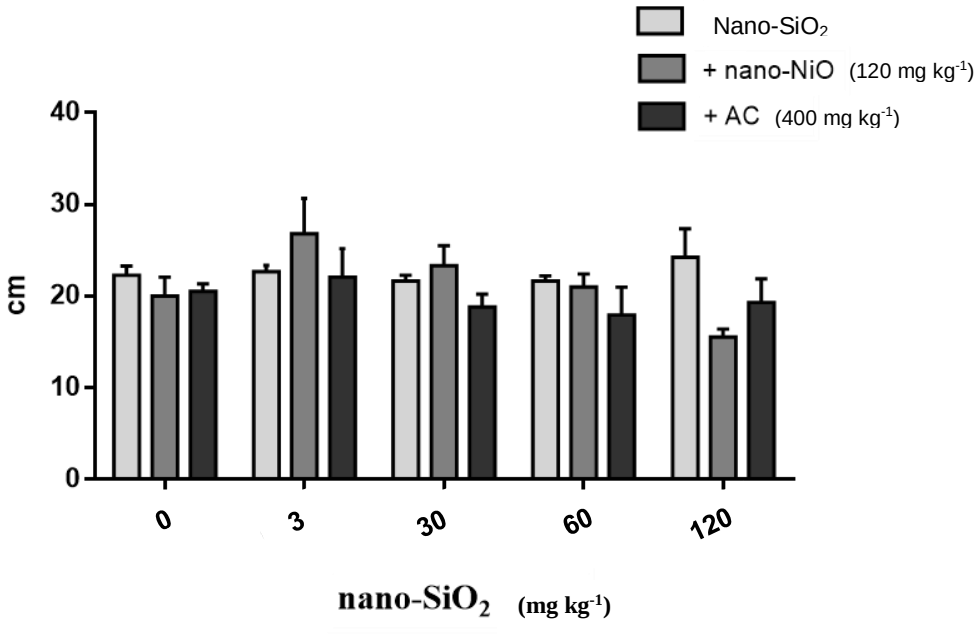

Figure 18. *Root lenght of barley plants exposed for 14 days in OECD soil to constant concentrations of nano-NiO and AC, each one mixed with a range of concentrations of nano-SiO_2.* Data presented are mean ± STDEV (n ≥ 3). * above bars indicates significant statistical differences from control at $p \leq 0.05$. The control corresponds to the first light gray bar without nano-SiO_2 and without both contaminants.

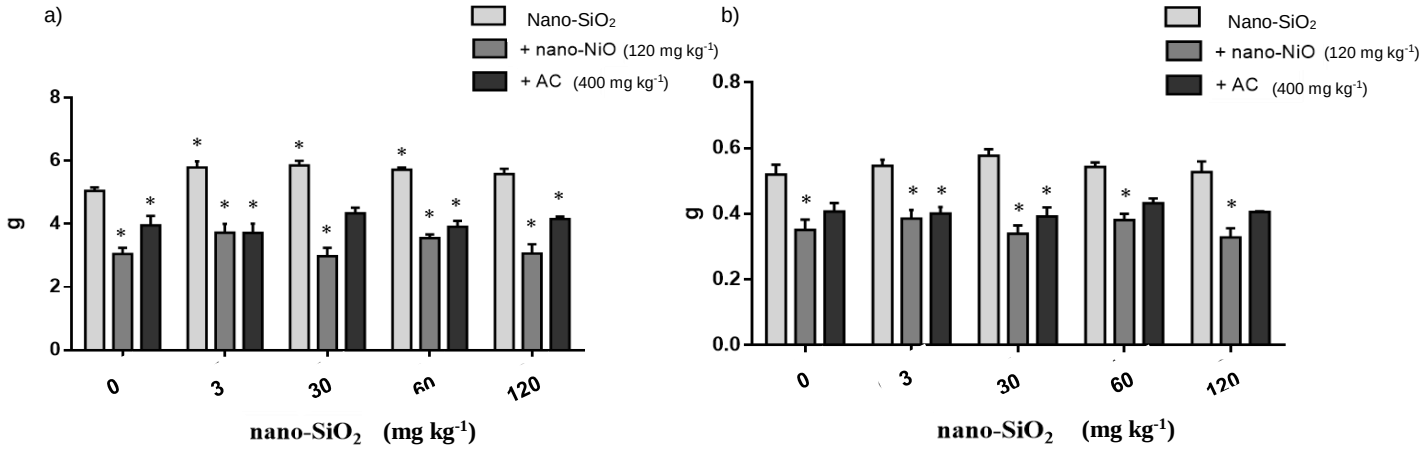

Figure 19. *Leaves' fresh (a) and dry (b) weight of barley plants exposed for 14 days in OECD soil to constant concentrations of nano-NiO and AC, each one mixed with a range of concentrations of nano-SiO_2.* Data presented are mean ± STDEV (n ≥ 3). * above bars indicates significant statistical differences from control at $p \leq 0.05$. The control corresponds to the first light gray bar without nano-SiO_2 and without both contaminants.

In general, results regarding the biomass production revealed that nano-SiO_2 co-exposure did not change the inhibition caused by any of the contaminants (Figures 19 and 20). However, especially for nano-NiO-treated plants, it was possible to observe that the treatment with 3 mg kg^{-1} nano-SiO_2 somehow led to a better response in the analyzed endpoints (root length and leaves' and roots' biomass production), along with a reduction in macroscopic symptoms induced by nano-NiO (data not shown).

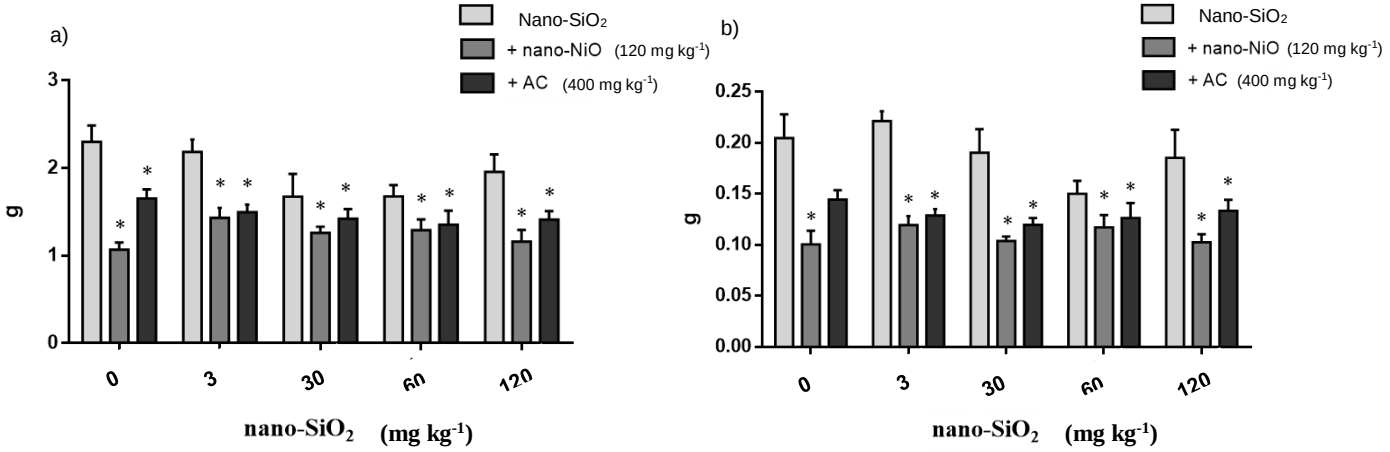

Figure 20. *Roots' fresh (a) and dry (b) weight of barley plants exposed for 14 days in OECD soil to constant concentrations of nano-NiO and AC, each one mixed with a range of concentrations of nano-SiO_2.* Data presented are mean ± STDEV (n ≥ 3). * above bars indicates significant statistical differences from control at $p \leq 0.05$. The control corresponds to the first light gray bar without nano-SiO_2 and without both contaminants.

By these reasons, the concentration of 3 mg kg^{-1} nano-SiO_2 was selected to be used in the final assay in attempts to understand its possible role in mitigating nano-NiO- and AC-induced stress. Thus, in the final growth trial, barley plants were cultivated under six distinct experimental conditions, namely: CTL (only water was added to the soil), nano-SiO_2 (3 mg kg^{-1}), nano-NiO (120 mg kg^{-1}), nano-NiO (120 mg kg^{-1}) + nano-SiO_2 (3 mg kg^{-1}), AC (400 mg kg^{-1}) and AC (400 mg kg^{-1})+ nano-SiO_2 (3 mg kg^{-1}).

3.2.3. Biometric parameters and biomass production

Results highlighted in Figure 21 showed that the exposure of barley to nano-NiO and AC did not affect root length, since no significant differences were found among all groups of plants. However, when looking to Figure 22, it is clear that 120 mg kg^{-1} nano-NiO led to the appearance of several phytotoxicity symptoms, manifested as foliar chlorosis and necrosis, along with a significant decrease of leaves' length. However, these phytotoxic effects were partially recovered by nano-SiO_2 co-application. On the other hand, 400 mg kg^{-1} of AC did not severely induced macroscopic toxicity signs and co-treatment with nano-SiO_2 did not change this pattern.

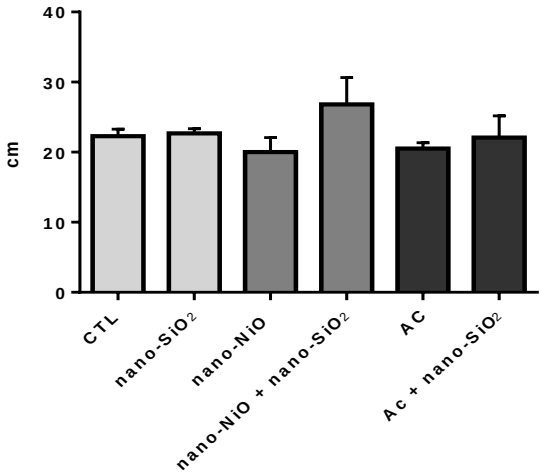

Figure 21. *Root length of barley plants cultivated for 14 days in OECD soil only moistened with water (CTL), in OECD soil spiked with nano-SiO_2 (3 mg kg^{-1}) suspension and in OECD soil spiked with nano-NiO (120 mg kg^{-1}) or AC (400 mg kg^{-1}) with and without nano-SiO_2.* Data presented are mean ± STDEV (n ≥ 3). * above bars indicates significant statistical differences from control at $p \leq 0.05$.

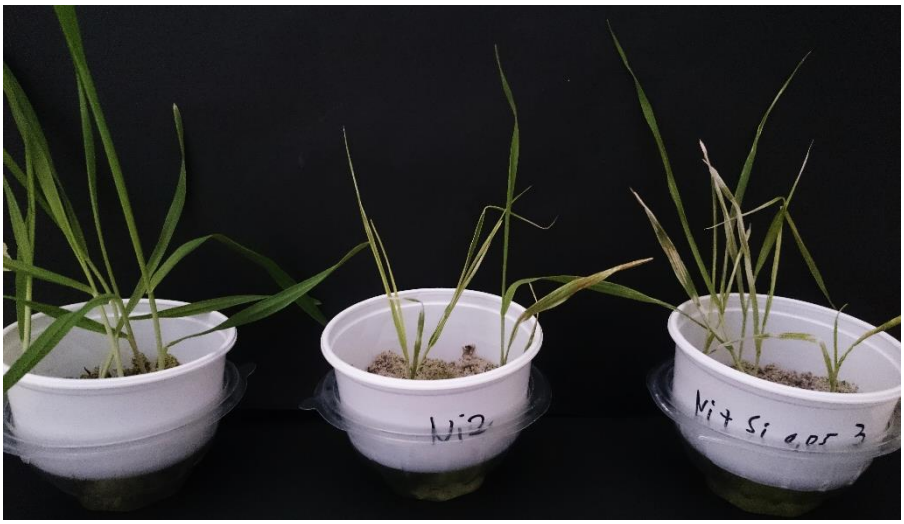

Figure 22. *Macroscopic symptoms of nano-NiO toxicity in barley plants after 14 days of growth.* Left: CTL plants; Center: nano-NiO plants; Right: nano-NiO + nano-SiO_2 plants.

Biomass production was markedly affected by exposure of barley to both nano-NiO and AC (Figure 23). Indeed, when compared to the control and as expected, fresh weight of nano-NiO-treated plants was 40% and 54% lower in leaves and roots, respectively. However, nano-SiO_2 co-application somehow reverted this situation, with lower reductions in fresh weight (leaves – 26%; roots – 38%) relatively to CTL plants (Figure 23a). When dry weight is concerned, as shown in Figure 23b, the same pattern of fresh biomass production was recorded, with reductions of about 32% and 57% in nano-NiO treatment and 25% and 49% in nano-NiO + nano-SiO_2 treatment in leaves and roots, respectively.

Regarding AC experiment, changes in both fresh and dry weights were observed, regardless of the co-application of nano-SiO_2 (Figure 23). Thus, fresh weight was reduced in response to AC stress in both leaves (22%) and roots (28%), relatively to the CTL; dry weight followed the same tendency, with reductions of about 22% in leaves and 38% in roots. In summary, nano-SiO_2 did not revert the significant reduction in both parameters caused by the contaminant.

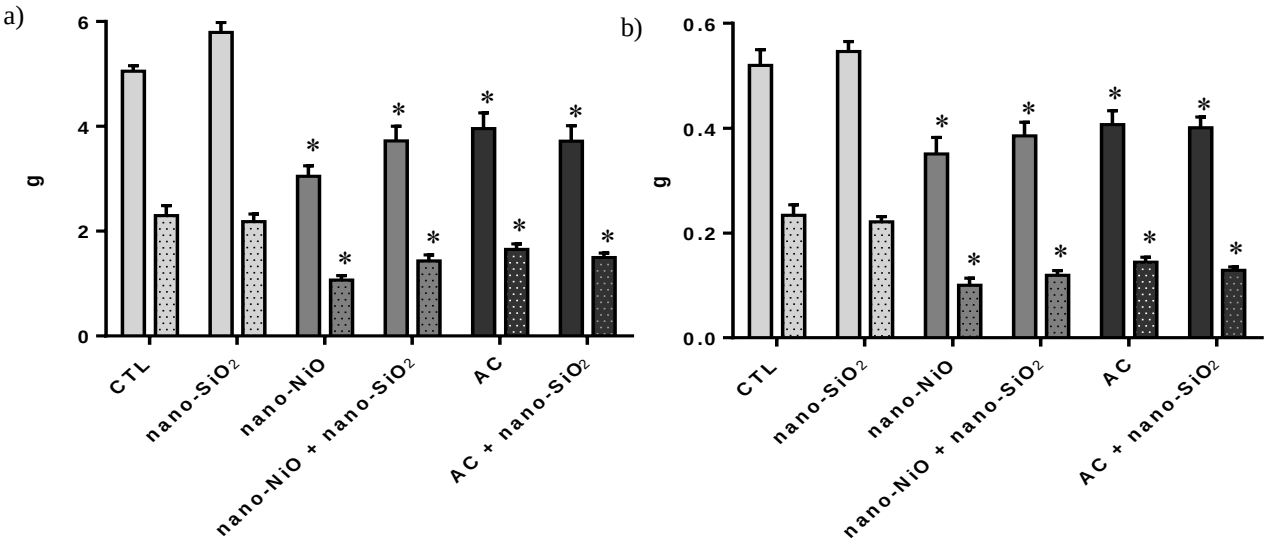

Figure 23. *Fresh (a) and dry (b) weight of barley plants cultivated for 14 days in OECD soil only moistened with water (CTL), in OECD soil spiked with nano-SiO_2 (3 mg kg^{-1}) suspension and in OECD soil spiked with nano-NiO (120 mg kg^{-1}) or AC (400 mg kg^{-1}) with and without nano-SiO_2.* Bars without pattern – leaves; Bars with pattern – roots. Data presented are mean ± STDEV (n ≥ 3). * above bars indicates significant statistical differences from control at $p \leq 0.05$.

3.2.4. Ni quantification

The accumulation of Ni in plant tissues was investigated after 14 days of growth. As seen in Figure 24, Ni content in CTL leaves and roots was < 0.01 mg g^{-1} plant $material_{dw}$. However, upon Ni exposure, a boost up to and 1.7- and 123-fold was found in leaves and roots, respectively. When plants were co-cultivated with nano-SiO_2, a tendency for

slightly lower Ni levels in leaves was detected, but a higher content in roots was found (173-fold higher than the CTL).

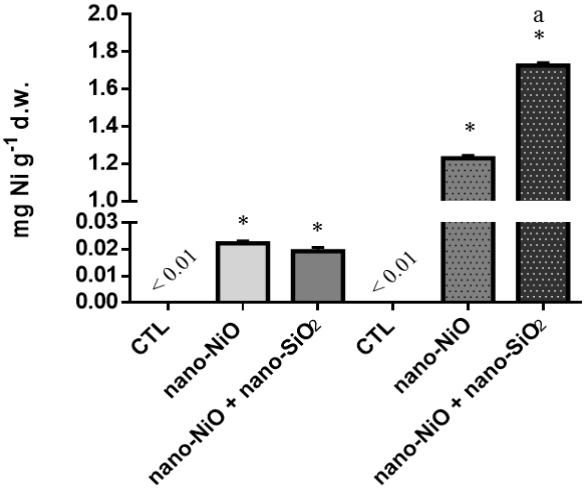

Figure 24. *Ni content of barley plants cultivated for 14 days in OECD soil only moistened with water (CTL), in OECD soil spiked with nano-SiO_2 (3 mg kg^{-1}) suspension and in OECD soil spiked with nano-NiO (120 mg kg^{-1}) or AC (400 mg kg^{-1}) with and without nano-SiO_2.* Bars without pattern – leaves; Bars with pattern – roots. Data presented are mean ± STDEV (n ≥ 3). * above bars indicates significant statistical differences from control at p ≤ 0.05. [a] above bars indicates significant statistical differences from control at $p \leq 0.05$.

3.2.5. Photosynthetic pigments and chlorophyll fluorescence analysis

As shown in Figure 25, only plants exposed to nano-NiO alone showed a significant reduction of about 16% in total chlorophylls relative to the control. Regarding carotenoids, no statistical differences were found among treatments.

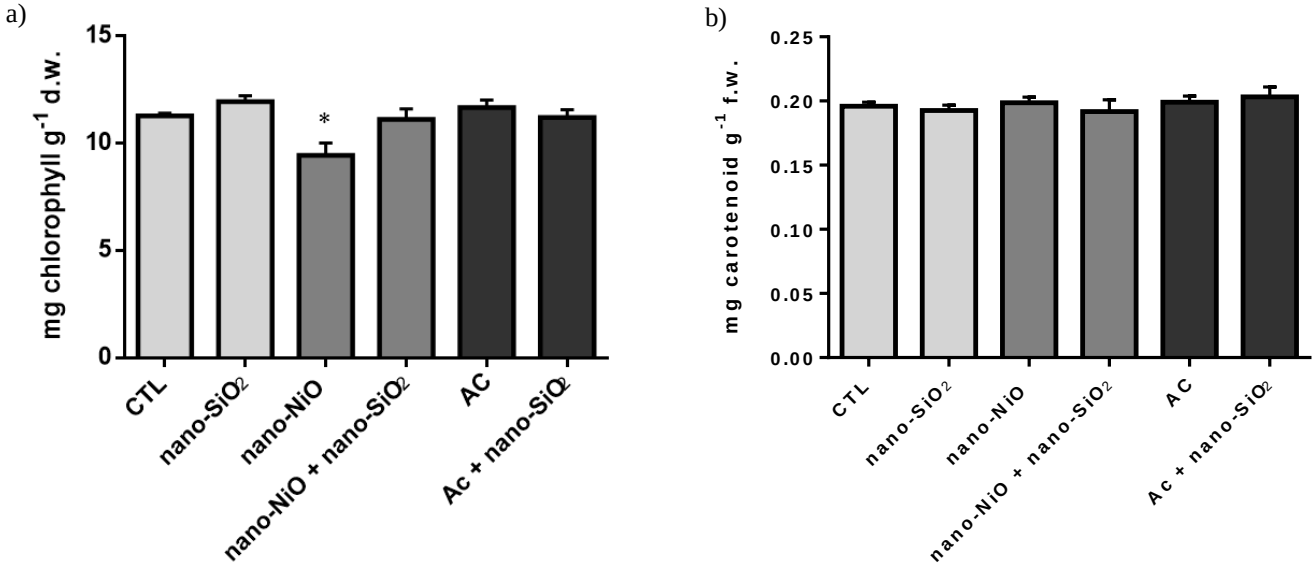

Figure 25. *Total chlorophylls (a) and carotenoids (b) contents of barley plants cultivated for 14 days in OECD soil only moistened with water (CTL), in OECD soil spiked with nano-SiO_2 (3 mg kg^{-1}) suspension and in OECD soil spiked with nano-NiO (120 mg kg^{-1}) or AC (400 mg kg^{-1}) with and without nano-SiO_2.* Data presented are mean ± STDEV (n ≥ 3). * above bars indicates significant statistical differences from control at $p \leq 0.05$.

Figures 26 and 27 report the results obtained for F_v/F_m, ΦPSII and electron transport rate (ETR). After adapting the second and third leaves for 20 min to the dark, results showed that nano-NiO induced a slight decrease in F_v/F_m , but the co-treatment with nano-SiO_2 reverted this situation, reestablishing the values for those found in the CTL. Regarding AC, no significant changes were recorded for this parameter in both plants exposed to AC and to AC mixed with nano-SiO_2.

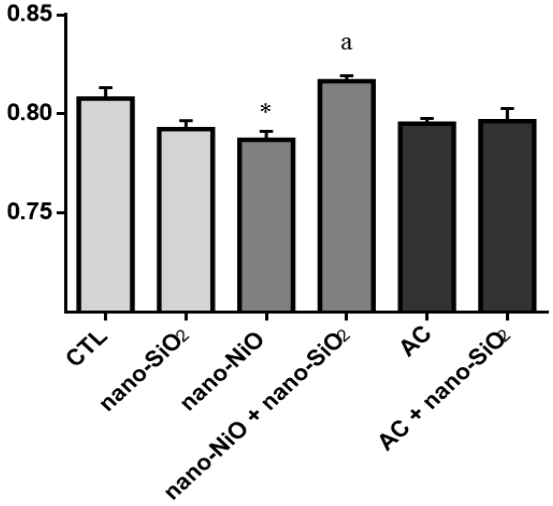

Figure 26. *F_v/F_m values of barley plants cultivated for 14 days in OECD soil only moistened with water (CTL), in OECD soil spiked with nano-SiO_2 (3 mg kg^{-1}) suspension and in OECD soil spiked with nano-NiO (120 mg kg^{-1}) or AC (400 mg kg^{-1}) with and without nano-SiO_2.* Data presented are mean ± STDEV (n ≥ 3). * above bars indicates significant statistical differences from control at P ≤ 0.05. [a] above bars indicates significant statistical differences from nano-NiO at $p \leq 0.05$.

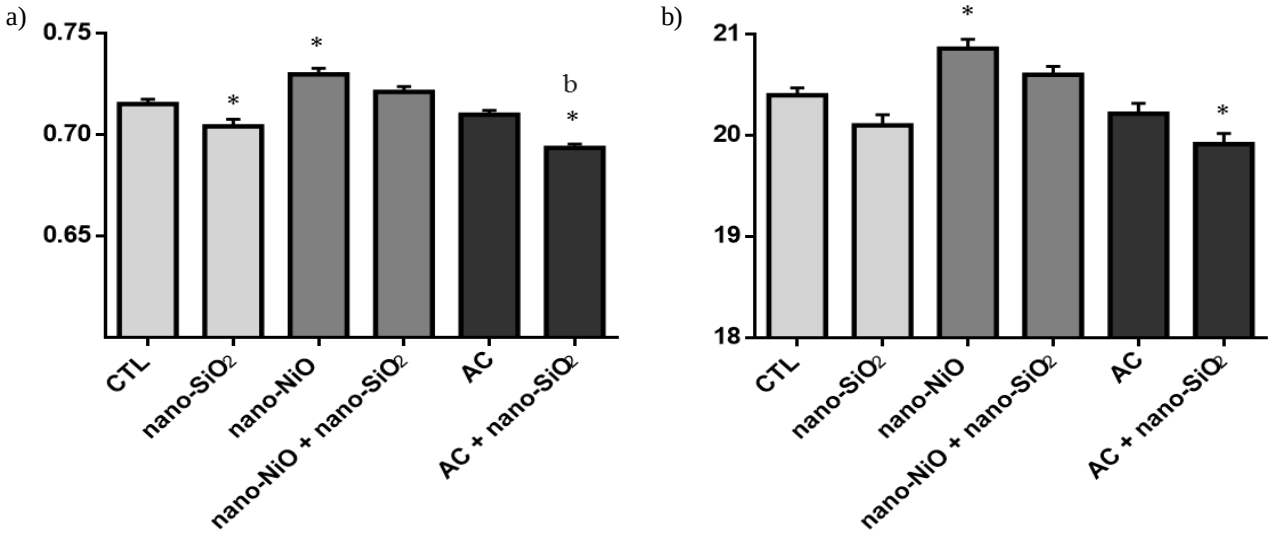

Figure 27. *ΦPSII (a) and ETR (b) of barley plants cultivated for 14 days in OECD soil only moistened with water (CTL), in OECD soil spiked with nano-SiO_2 (3 mg kg^{-1}) suspension and in OECD soil spiked with nano-NiO (120 mg kg^{-1}) or AC (400 mg kg^{-1}) with and without nano-SiO_2. Data presented are mean ± STDEV (n ≥ 3).* * above bars indicates significant statistical differences from control at P ≤ 0.05. [b] above bars indicates significant statistical differences from AC at $p \leq 0.05$.

After measuring the Fv/Fm, plants were adapted to light conditions for 10 min in order to evaluate the ΦPSII and the ETR. As seen in Figure 27, the two parameters revealed an identical response among all treatments, with nano-NiO plants exhibiting an increase of 2%, relatively to the CTL, in both ΦPSII and the ETR. Also, although no changes were recorded for plants under AC alone, a decrease of 3% was found for those treated with both AC and nano-SiO_2.

3.2.6. Nitrogen nutrition – GS and NR activity

In order to assess if any of the treatments was interfering with the normal N nutrition, the activity of GS and NR was studied in both roots and leaves of barley plants.

Regarding GS, differential responses were recorded between organs and contaminants (Figure 28). Indeed, in what concerns to nano-NiO, GS activity in leaves was positively affected (25%) by the presence of this nano-material, but no significant changes were found in roots. However, co-application of nano-SiO_2 restored the GS activity levels to the ones of control in leaves. A higher activity of this enzyme was also observed in roots, with a rise of 53% and 60%, when compared to CTL and nano-NiO, respectively.

Under AC stress, barley plants exhibited significant higher GS activity in leaves (AC: 74%; AC + nano-SiO_2: 83%), but not in roots, relatively to the CTL, regardless of being or not co-treated with nano-SiO_2 (Figure 28).

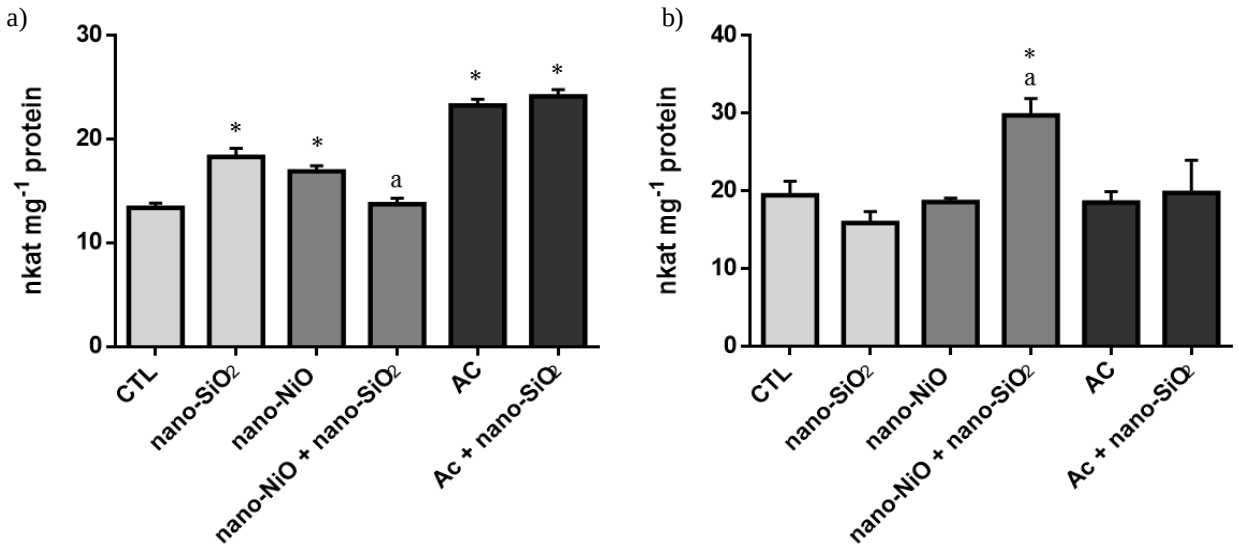

Figure 28. *GS activity in leaves (a) and roots (b) of barley plants cultivated for 14 days in OECD soil only moistened with water (CTL), in OECD soil spiked with nano-SiO_2 (3 mg kg^{-1}) suspension and in OECD soil spiked with nano-NiO (120 mg kg^{-1}) or AC (400 mg kg^{-1}) with and without nano-SiO_2.* Data presented are mean ± STDEV (n ≥ 3). * above bars indicates significant statistical differences from control at p ≤ 0.05. [a] above bars indicates significant statistical differences from nano-NiO at $p \leq 0.05$.

NR activity was always higher in roots than in leaves and the exposure of plants to nano-SiO_2 alone resulted in a significant increase of NR activity in roots in relation to the CTL. As can be seen in Figure 29, nano-NiO induced a great boost in NR activity (2.4-fold) relatively to the control, in leaves, with an even more pronounced rise upon nano-SiO_2 co-exposure (2.9-fold). Regarding roots, although so statistical differences were found, a tendency for nano-NiO to inhibit NR was recorded, being this effect partially recovered by nano-SiO_2, with values around the CTL situation. However, no significant differences were recorded among treatments.

Concerning AC, no changes were detected in leaves, but a decline in NR activity was found in roots (44%). Nano-SiO_2 co-exposure changed the activity pattern of NR under AC stress, inducing a significant decrease of 27% in leaves and a significant increase of 48% in roots (Figure 29).

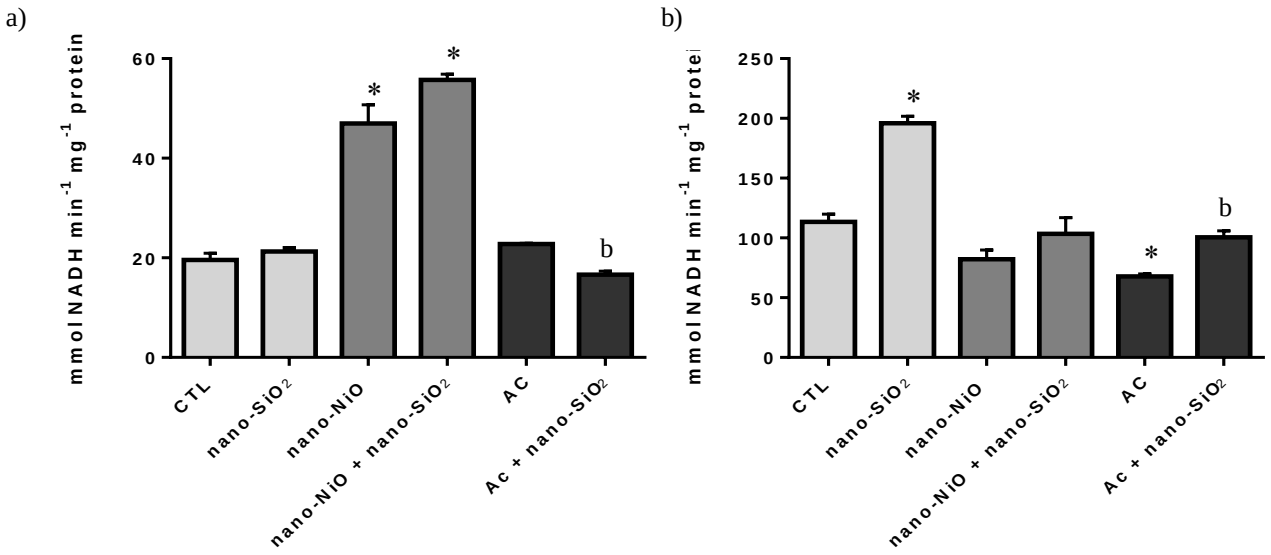

Figure 29. *NR activity in leaves (a) and roots (b) of barley plants cultivated for 14 days in OECD soil only moistened with water (CTL), in OECD soil spiked with nano-SiO_2 (3 mg kg^{-1}) suspension and in OECD soil spiked with nano-NiO (120 mg kg^{-1}) or AC (400 mg kg^{-1}) with and without nano-SiO_2.* Data presented are mean ± STDEV (n ≥ 3). * above bars indicates significant statistical differences from control at $p \leq 0.05$. [b] above bars indicates significant statistical differences from AC at $p \leq 0.05$

3.2.7. Oxidative stress markers – LP, thiols (total and protein-bond), $O_2^{\cdot-}$ and H_2O_2

LP, evaluated by the quantification of MDA, was used as an oxidative stress marker. As Figure 30 suggests, 120 mg kg^{-1} soil nano-NiO led to a significant increase of about 29% of LP levels in leaves, relatively to the control. However, this negative effect of nano-NiO on LP was strongly ameliorated in plants co-treated with nano-SiO_2, since similar values of LP were found in plants from both control nano-NiO + nano-SiO_2 treatments. Regarding roots, no statistical differences were found.

On the other hand, AC did not significantly change the levels of MDA neither in roots or leaves, though co-treatment with nano-SiO_2 resulted in a decrease of 31% of MDA in roots relative to the CTL (Figure 30).

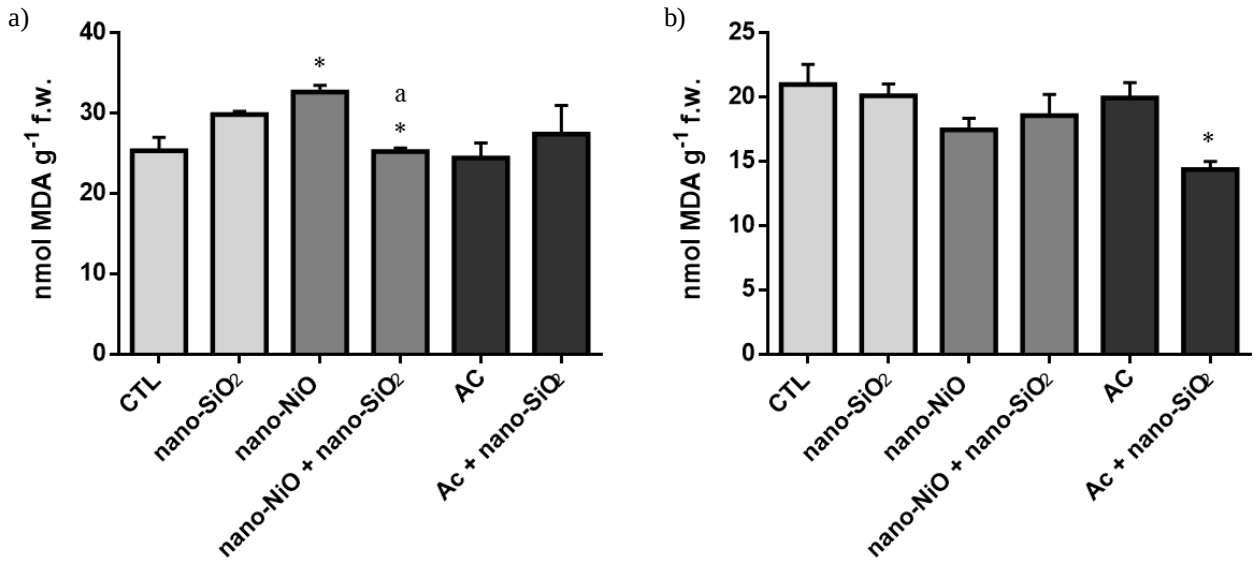

Figure 30. *MDA content in leaves (a) and roots (b) of barley plants cultivated for 14 days in OECD soil only moistened with water (CTL), in OECD soil spiked with nano-SiO_2 (3 mg kg^{-1}) suspension and in OECD soil spiked with nano-NiO (120 mg kg^{-1}) or AC (400 mg kg^{-1}) with and without nano-SiO_2.* Data presented are mean ± STDEV (n ≥ 3). * above bars indicates significant statistical differences from control at $p \leq 0.05$. [a] above bars indicates significant statistical differences from nano-NiO at $p \leq 0.05$

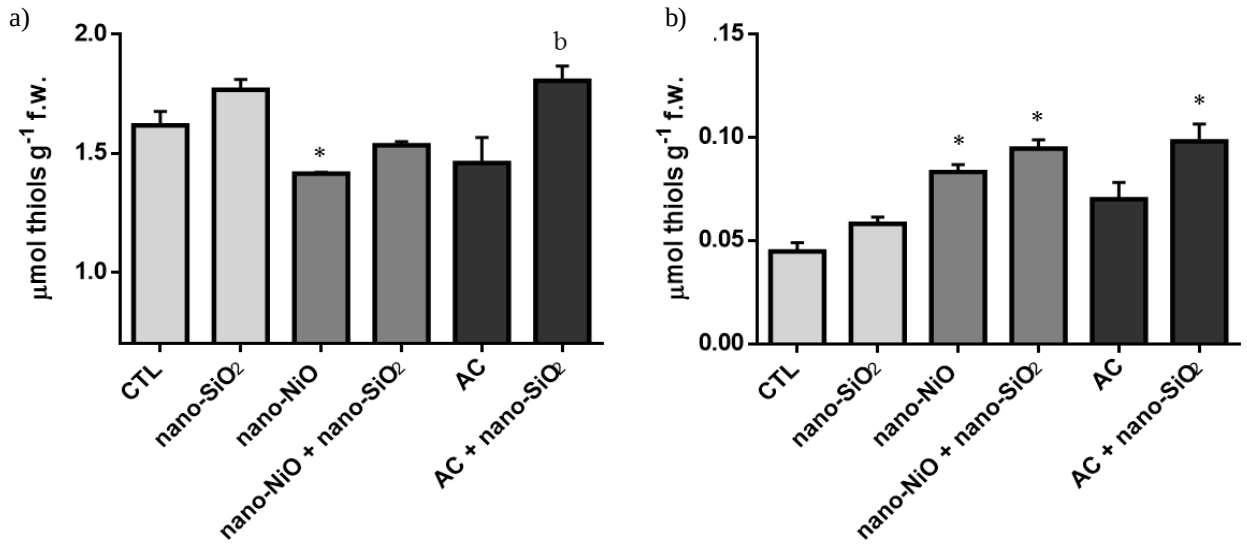

Figure 31. *Total thiols levels in leaves (a) and roots (b) of barley plants cultivated for 14 days in OECD soil only moistened with water (CTL), in OECD soil spiked with nano-SiO_2 (3 mg kg^{-1}) suspension and in OECD soil spiked with nano-NiO (120 mg kg^{-1}) or AC (400 mg kg^{-1}) with and without nano-SiO_2.* Data presented are mean ± STDEV (n ≥ 3). * above bars indicates significant statistical differences from control at $p \leq 0.05$. [b] above bars indicates significant statistical differences from AC at $p \leq 0.05$.

The effects of nano-NiO and AC on total and protein-bond thiols are represented in Figures 31 and 32.

As can be seen, the cultivation of plants in the presence of nano-NiO alone led to a reduction of about 13% in leaves' total thiols. However, in roots, the opposite behavior was detected, with a rise of 88% and 112% in response to nano-NiO alone and co-treated with nano-SiO_2, respectively and in relation to the control. Regarding AC treatments, no changes were found in response to AC single exposure, but an increase of about 24% (relatively to AC alone) and 120% (relatively to control) was recorded upon nano-SiO_2 treatment in leaves and roots, respectively.

In relation to protein-bond thiols, in leaves, no significant changes from the control situation were found, although co-treatment of nano-NiO with nano-SiO_2 led to an increase of 14% relatively to nano-NiO alone. In roots, the same pattern of total thiols was observed, with statistical differences in nano-NiO (increase of 106%) and nano-NiO + nano-SiO_2 (increase of 134%) plants, along with a rise of 161% in plants grown in the presence of both AC and nano-SiO_2, relatively to the control (Figure 32).

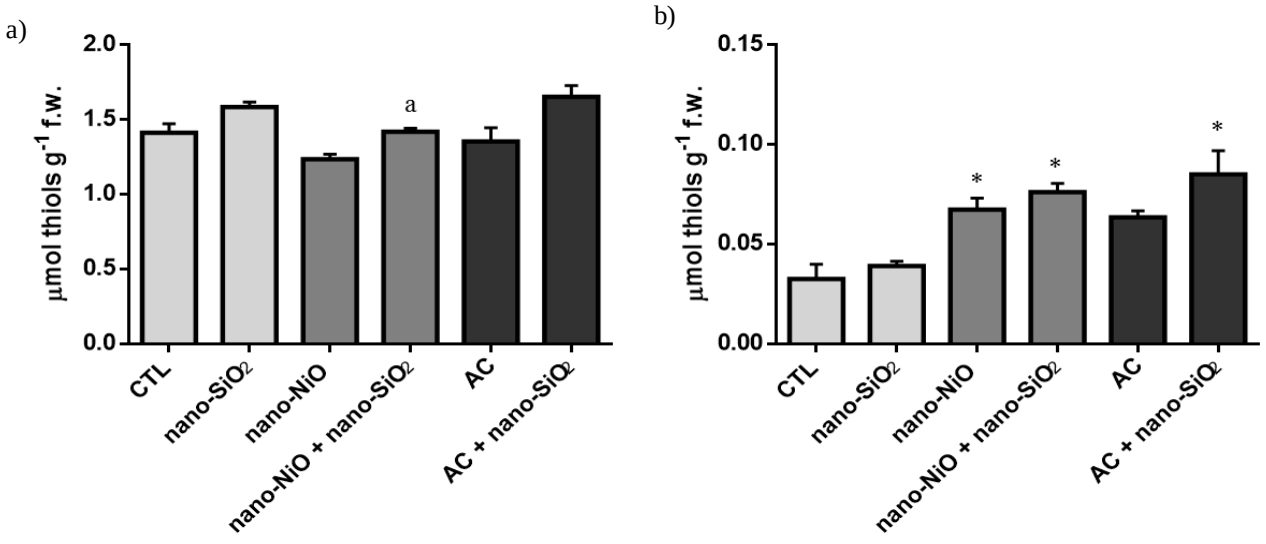

Figure 32. *Protein-bond thiols levels in leaves (a) and roots (b) of barley plants cultivated for 14 days in OECD soil only moistened with water (CTL), in OECD soil spiked with nano-SiO_2 (3 mg kg^{-1}) suspension and in OECD soil spiked with nano-NiO (120 mg kg^{-1}) or AC (400 mg kg^{-1}) with and without nano-SiO_2.* Data presented are mean ± STDEV (n ≥ 3). * above bars indicates significant statistical differences from control at $p \leq 0.05$. [a] above bars indicates significant statistical differences from nano-NiO at $p \leq 0.05$.

Obtained data for $O_2^{\cdot-}$ quantification, documented in Figure 33, showed that significant changes were recorded in both leaves and roots of barley plants. Upon nano-SiO_2 application alone, levels of this ROS were higher than those of CTL, though statistical differences were only found in leaves.

In what concerns nano-NiO, a strong rise of $O_2^{\cdot-}$ content was found in both studied organs (77% in leaves and 136% in roots). As a result of nano-SiO_2 co-application, although foliar levels of $O_2^{\cdot-}$ suffered an increase of 116% relatively to CTL, no statistical differences were recorded in roots, with values around those of CTL situation.

Regarding AC exposure, while in leaves a strong rise of $O_2^{\cdot-}$ content was found regardless of the co-application of nano-SiO_2, no changes were recorded in roots relatively to the CTL situation.

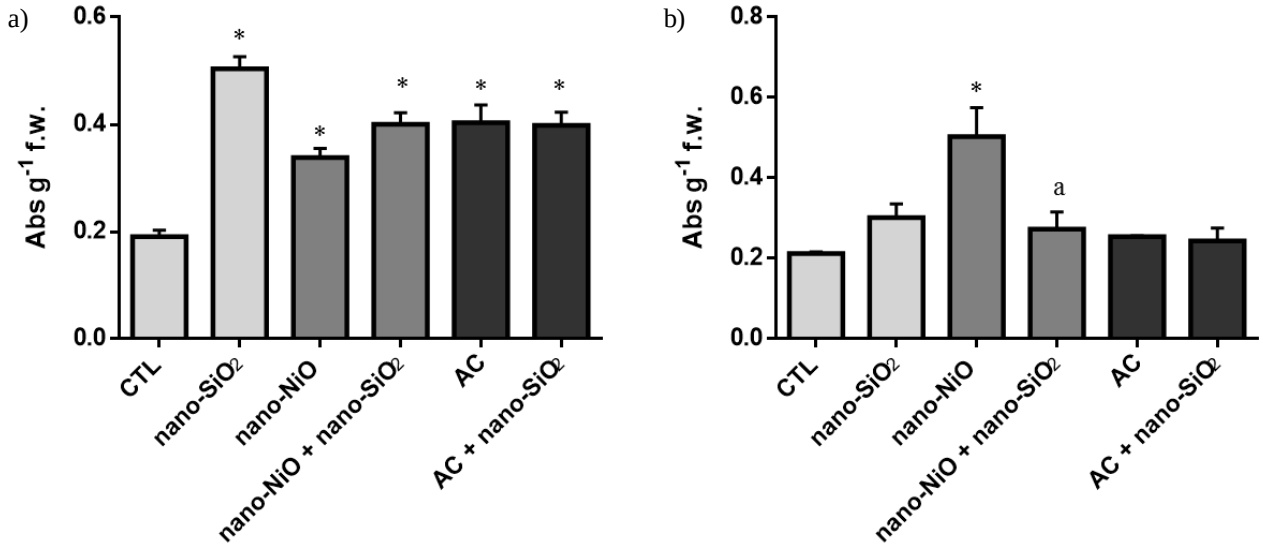

Figure 33. *$O_2^{\cdot-}$ levels in leaves (a) and roots (b) of barley plants cultivated for 14 days in OECD soil only moistened with water (CTL), in OECD soil spiked with nano-SiO_2 (3 mg kg^{-1}) suspension and in OECD soil spiked with nano-NiO (120 mg kg^{-1}) or AC (400 mg kg^{-1}) with and without nano-SiO_2.* Data presented are mean ± STDEV (n ≥ 3). * above bars indicates significant statistical differences from control at $p \leq 0.05$. [a] above bars indicates significant statistical differences from nano-NiO at $p \leq 0.05$.

As Figure 34 reports, the content of H_2O_2 showed differential responses between organs and experimental conditions, being always higher in leaves than in roots.

Thus, although nano-NiO did not induce a rise in H_2O_2 levels, upon nano-SiO_2 co-application, barley plants exhibited a decline of 14% in H_2O_2 content of leaves, relatively to the CTL.

Regarding AC, no statistical significance was found in leaves, while in roots AC led to an increase of around 35%, independently of being or not co-applied with nano-SiO_2 (Figure 34).

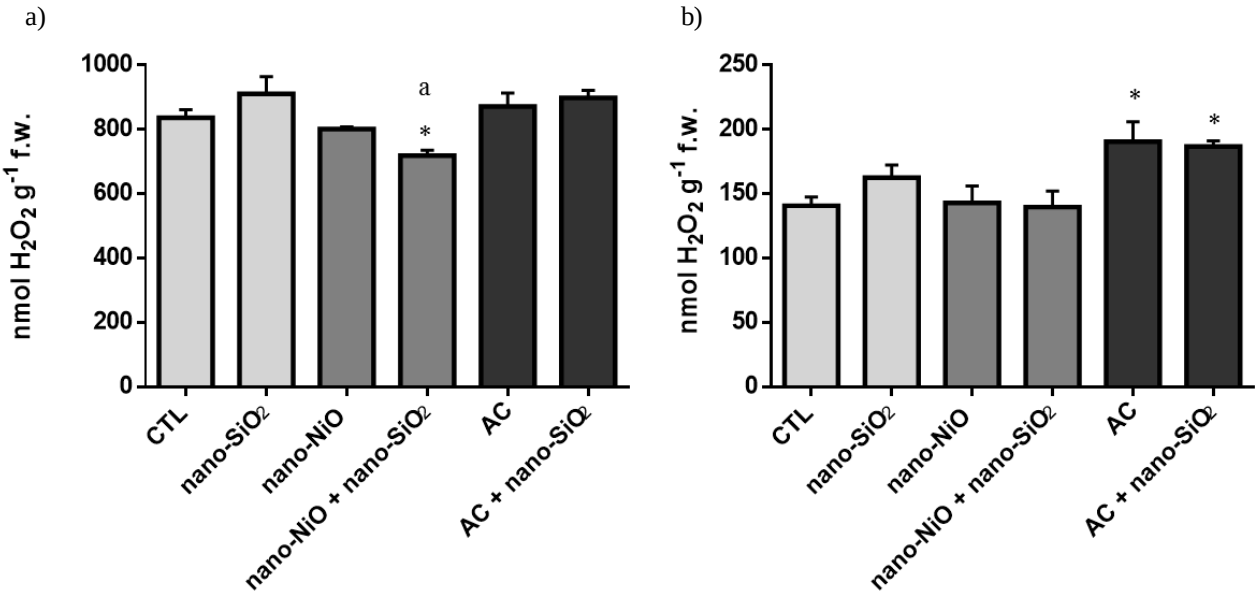

Figure 34. *H_2O_2 levels in leaves (a) and roots (b) of barley plants cultivated for 14 days in OECD soil only moistened with water (CTL), in OECD soil spiked with nano-SiO_2 (3 mg kg^{-1}) suspension and in OECD soil spiked with nano-NiO (120 mg kg^{-1}) or AC (400 mg kg^{-1}) with and without nano-SiO_2.* Data presented are mean ± STDEV (n ≥ 3). * above bars indicates significant statistical differences from control at $p \leq 0.05$. [a] above bars indicates significant statistical differences from nano-NiO at $p \leq 0.05$.

3.2.8. Non-enzymatic AOX system – Pro and AsA

As reported in Figure 35, Pro content was increased in response to nano-NiO excess, with a rise of 3.5-fold and a decline of 0.4-fold in leaves and roots, respectively compared to the CTL. However, upon nano-SiO_2 co-treatment, Pro levels were restored to the ones of CTL plants in both organs. Regarding AC stress, a marked increase in Pro levels was detected in leaves (by about 80%), but no significant changes were recorded in roots. In this case, the co-application of nano-SiO_2 also resulted in an increase of about 100% in leaves, although in roots a reduction of proline levels (around 30%) was found compared to AC-treated plants. However in both AC treatments no significant differences from the roots of CTL plants were recorded.

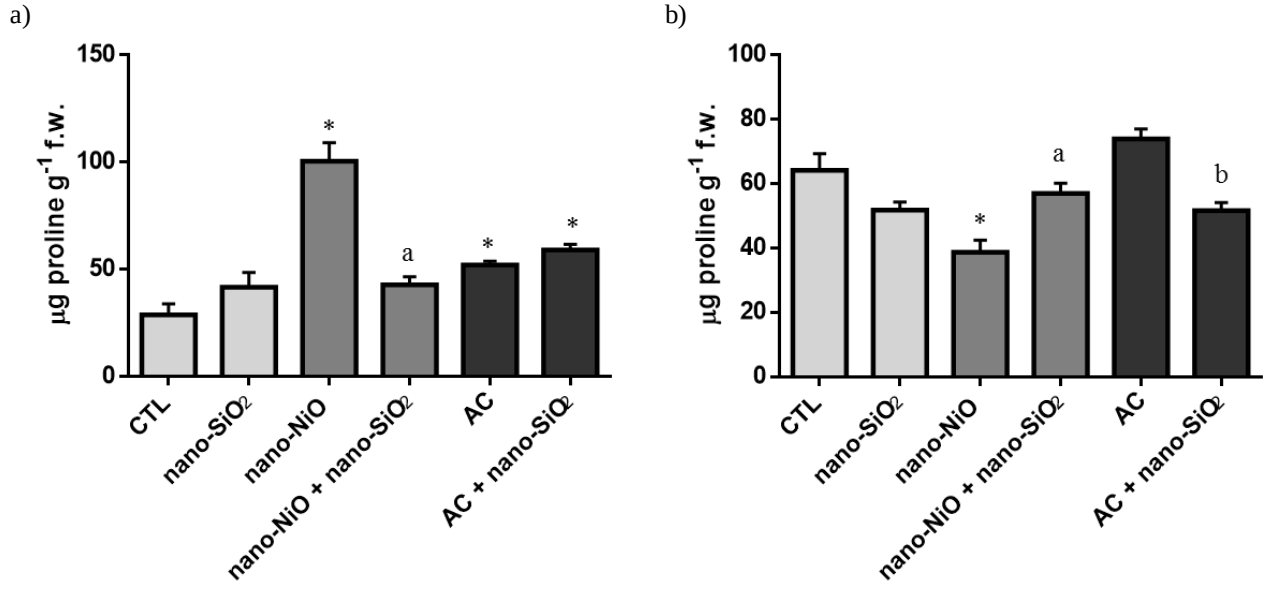

Figure 35. *Proline levels in leaves (a) and roots (b) of barley plants cultivated for 14 days in OECD soil only moistened with water (CTL), in OECD soil spiked with nano-SiO_2 (3 mg kg^{-1}) suspension and in OECD soil spiked with nano-NiO (120 mg kg^{-1}) or AC (400 mg kg^{-1}) with and without nano-SiO_2.* Data presented are mean ± STDEV (n ≥ 3). * above bars indicates significant statistical differences from control at $p \leq 0.05$. [a] above bars indicates significant statistical differences from nano-NiO at $p \leq 0.05$. [b] above bars indicates significant statistical differences from AC at $p \leq 0.05$.

The results regarding total ascorbate, AsA and DHA contents are represented in Figure 36 and Table 4.

As can be seen, no significant changes in the total pool of ascorbate were recorded in leaves. However, a strong tendency for nano-NiO-exposed plants to show decreased levels of ascorbate was noticed, being this negative effect reverted upon nano-SiO_2 co-treatment. When roots are concerned, a decline in this parameter was detected among all experimental conditions, with an inhibition effect up to 40%, which was not reverted by the co-treatment with nano-SiO_2 (Figure 36).

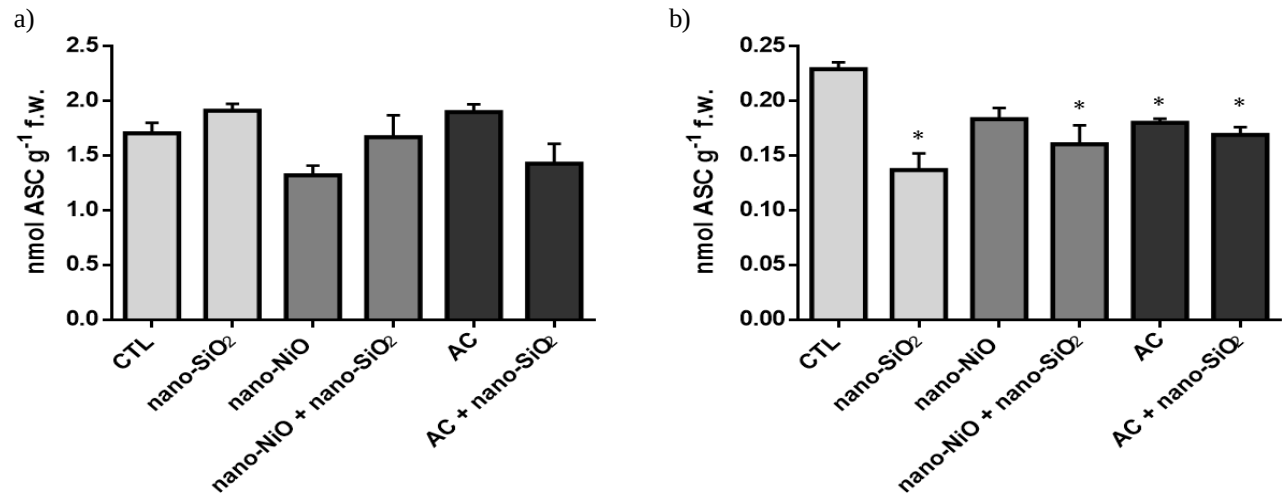

Figure 36. *Total ascorbate content in leaves (a) and roots (b) of barley plants cultivated for 14 days in OECD soil only moistened with water (CTL), in OECD soil spiked with nano-SiO_2 (3 mg kg^{-1}) suspension and in OECD soil spiked with nano-NiO (120 mg kg^{-1}) or AC (400 mg kg^{-1}) with and without nano-SiO_2.* Data presented are mean ± STDEV (n ≥ 3). * above bars indicates significant statistical differences from control at $p \leq 0.05$.

Table 4. *Relative content of AsA and DHA in leaves and roots of barley plants cultivated for 14 days in OECD soil only moistened with water (CTL), in OECD soil spiked with nano-SiO2 (3 mg kg-1) suspension and in OECD soil spiked with nano-NiO (120 mg kg-1) or AC (400 mg kg-1) with and without nano-SiO_2.* Data presented are mean ± STDEV (n ≥ 3). * above bars indicates significant statistical differences from control at $p \leq 0.05$. [a] above bars indicates significant statistical differences from control at $p \leq 0.05$.

	Leaves		Roots	
	AsA/Total	**DHA/Total**	**AsA/Total**	**DHA/Total**
CTL	0.97 ± 0.011	0.049 ± 0.0061	0.41 ± 0.028	0.59 ± 0.028
nano-SiO_2	1.03 ± 0.047	0.037 ± 0.0035	0.41 ± 0.029	0.59 ± 0.029
nano-NiO	0.92 ± 0.0053	0.080 ± 0.0053 *	0.45 ± 0.031	0.55 ± 0.031
nano-NiO + nano-SiO_2	0.97 ± 0.0047	0.029 ± 0.00039 *a	0.43 ± 0.020	0.56 ± 0.020
AC	0.96 ± 0.0051	0.044 ± 0.0051	0.33 ± 0.012	0.67 ± 0.011
AC + nano-SiO_2	0.93 ± 0.0078	0.063 ± 0.0032	0.33 ± 0.021	0.67 ± 0.021

Regarding the relative content of AsA, no statistical significant differences were found among all the groups of plants, neither in leaves nor roots (Table 4). However, a marked increase of DHA relative content was found in leaves of nano-NiO-treated plants (by 60%), effect that was significantly attenuated by the co-application of nano-SiO_2, with a decline of 64% when compared to plants exposed to nano-NiO alone. In roots, no differences were found (Table 4).

3.2.9. Enzymatic AOX system – SOD, CAT and APX

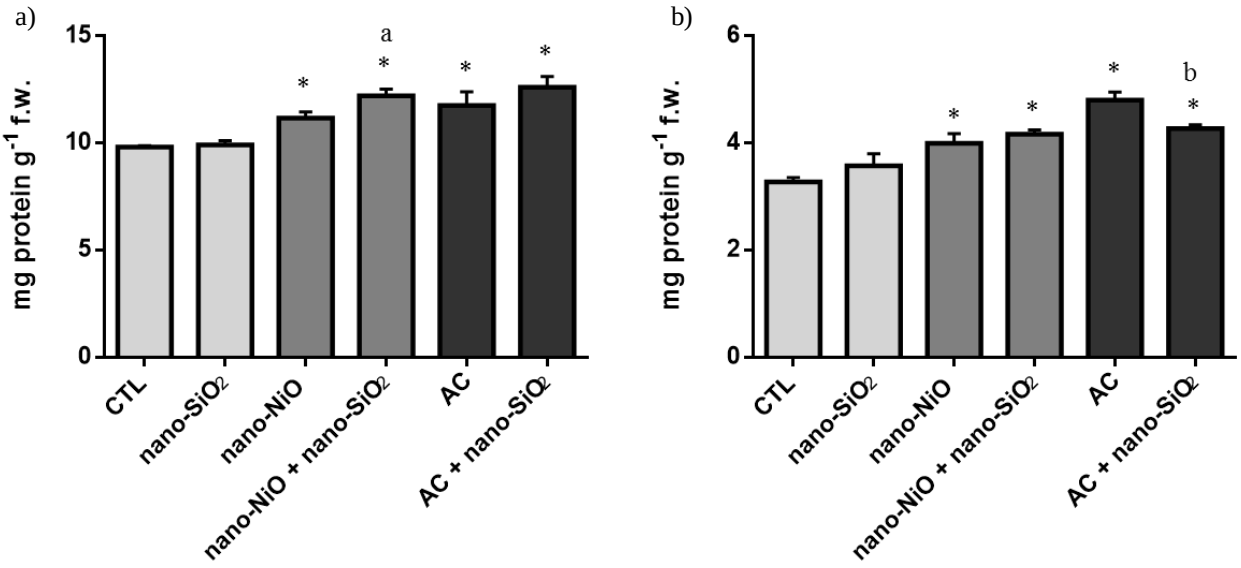

Figure 37. *Total soluble protein content in leaves (a) and roots (b) of barley plants cultivated for 14 days in OECD soil only moistened with water (CTL), in OECD soil spiked with nano-SiO_2 (3 mg kg^{-1}) suspension and in OECD soil spiked with nano-NiO (120 mg kg^{-1}) or AC (400 mg kg^{-1}) with and without nano-SiO_2.* Data presented are mean ± STDEV (n ≥ 3). * above bars indicates significant statistical differences from control at $p \leq 0.05$. [a] above bars indicates significant statistical differences from nano-NiO at $p \leq 0.05$. [b] above bars indicates significant statistical differences from AC at $p \leq 0.05$.

Aiming to understand the involvement of the enzymatic AOX system, the activity of SOD, CAT and APX was measured in leaves and roots of barley plants and expressed per mg of soluble protein.

The levels of soluble protein are represented in Figure 37. As can be seen, a rise in protein content was found among all experimental treatments, with increases up to 28% in leaves and 49% in roots.

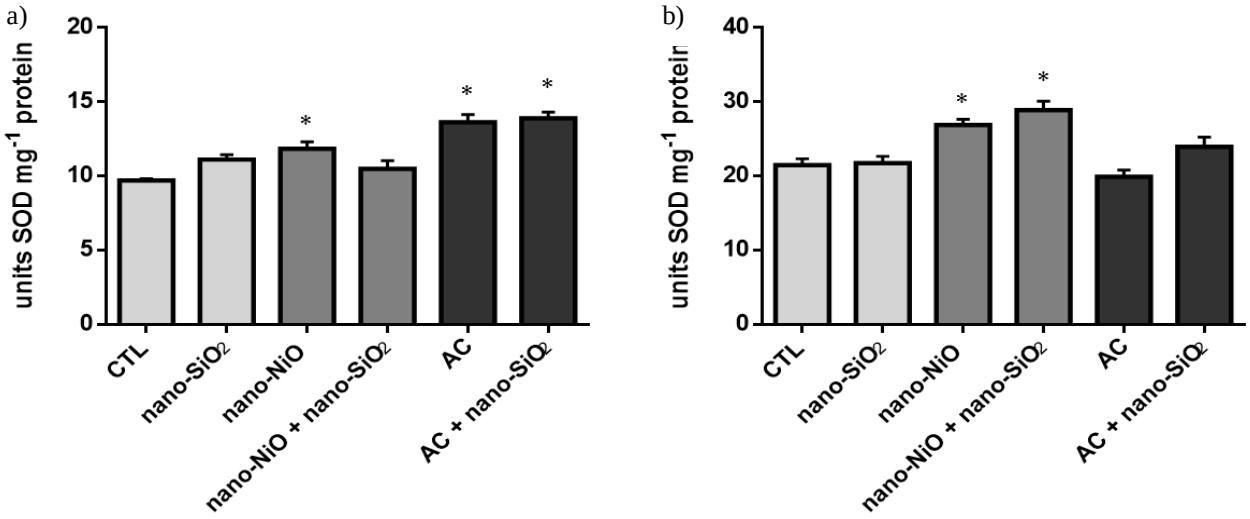

Figure 38. *Total activity of SOD in leaves (a) and roots (b) of barley plants cultivated for 14 days in OECD soil only moistened with water (CTL), in OECD soil spiked with nano-SiO_2 (3 mg kg^{-1}) suspension and in OECD soil spiked with nano-NiO (120 mg kg^{-1}) or AC (400 mg kg^{-1}) with and without nano-SiO_2.* Data presented are mean ± STDEV (n ≥ 3). * above bars indicates significant statistical differences from control at $p \leq 0.05$.

As shown in Figure 38, leaves of barley plants exposed to high levels of nano-NiO and AC exhibited a significant increase in SOD activity. The activity of this enzyme was kept significant high in leaves when this drug was mixed with nano-SiO_2. Regarding roots, only statistical significant differences were observed for plants grown under nano-NiO, with a rise of 25% and 35% upon single exposure and nano-SiO_2 co-exposure, respectively.

As Figure 39 suggests, the presence of high concentrations of nano-NiO induced a slightly increase in the total activity of CAT in leaves; furthermore, when plants were grown in soil spiked with the mixture of the metallic nanomaterial and nano-SiO_2, a significant increase of 21% and 18% was found relatively to the nano-NiO and CTL exposed plants, respectively. In contrast, leaves of AC-treated plants showed a reduction in CAT activity levels of about 20%, regardless of the presence of nano-SiO_2. Concerning roots, CAT activity was only detected in CTL and nano-SiO_2-treated plants, as reported in Figure 39.

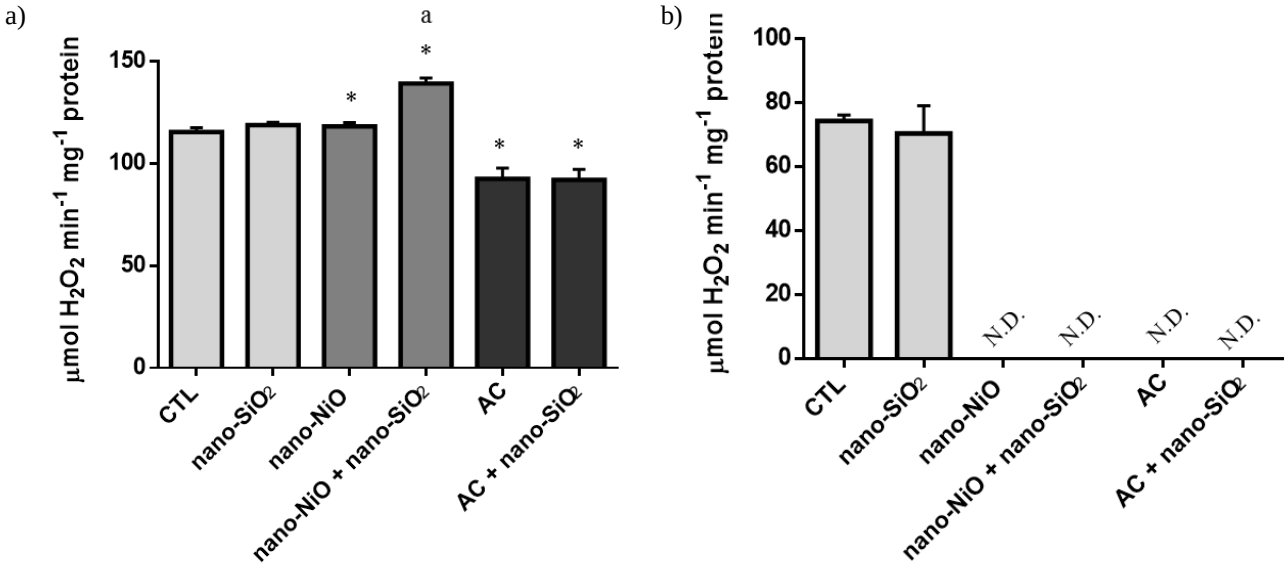

Figure 39. *Activity of CAT in leaves (a) and roots (b) of barley plants cultivated for 14 days in OECD soil only moistened with water (CTL), in OECD soil spiked with nano-SiO_2 (3 mg kg^{-1}) suspension and in OECD soil spiked with nano-NiO (120 mg kg^{-1}) or AC (400 mg kg^{-1}) with and without nano-SiO_2.* N.D – non-detected. Data presented are mean ± STDEV (n ≥ 3). * above bars indicates significant statistical differences from control at $p \leq 0.05$. [a] above bars indicates significant statistical differences from nano-NiO at $p \leq 0.05$.

As for CAT, APX activity of leaves was not affected by nano-NiO single exposure, but a significant increase of about 30% was detected in response to nano-SiO_2 co-treatment. No changes were noticed in barley leaves exposed to AC (Figure 40).

In what concerns roots, a strong positive effect of nano-NiO on APX activity was measured, with increases up to 78% under single exposure and 118% under co-exposure with nano-SiO_2. Regarding AC, only changes were recorded upon co-treatment with nano-SiO_2, with a rise of 63% and 47% in relation to the CTL and AC-treated plants, respectively (Figure 40).

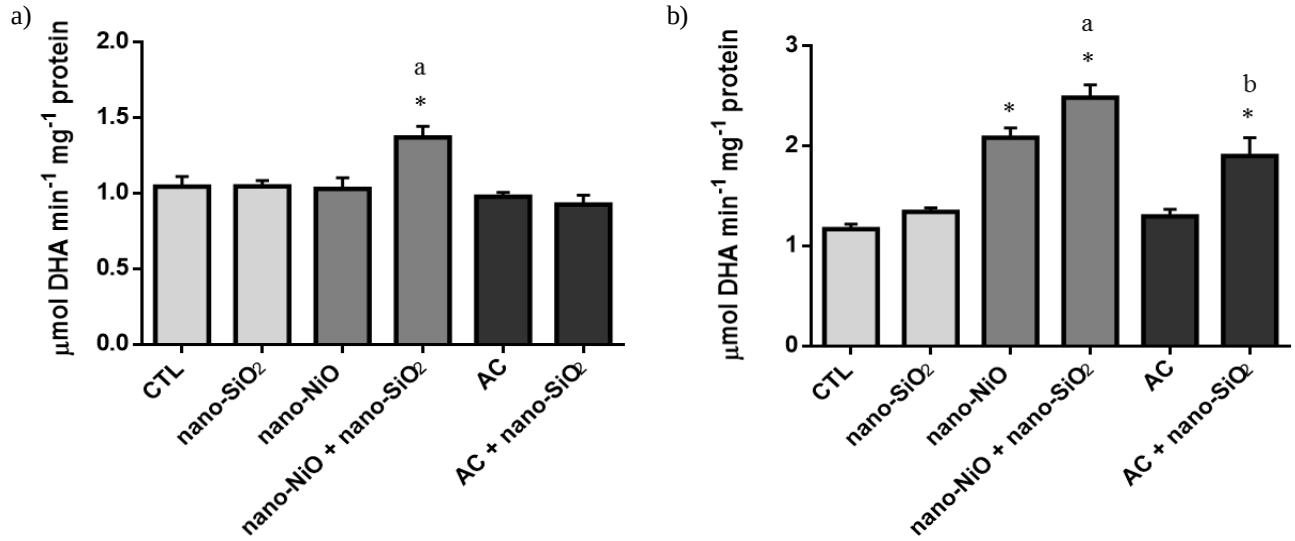

Figure 40. *Activity of APX in leaves (a) and roots (b) of barley plants cultivated for 14 days in OECD soil only moistened with water (CTL), in OECD soil spiked with nano-SiO_2 (3 mg kg^{-1}) suspension and in OECD soil spiked with nano-NiO (120 mg kg^{-1}) or AC (400 mg kg^{-1}) with and without nano-SiO_2.* Data presented are mean ± STDEV (n ≥ 3). * above bars indicates significant statistical differences from control at $p \leq 0.05$. [a] above bars indicates significant statistical differences from nano-NiO at $p \leq 0.05$. [b] above bars indicates significant statistical differences from AC at $p \leq 0.05$.

3.2.10. Expression profile of SOD, CAT and APX

The transcript accumulation of SOD, CAT and APX was assessed by qPCR in leaves of barley plants (Figures 41 and 42). As can be seen, generally, nano-SiO_2 stimulated the mRNA levels of the three studied enzymes when compared to the CTL situation.

Upon nano-NiO stress, it was possible to observe an increase in transcripts of SOD, CAT1 and APX (up to 1.4-fold); however, when plants were co-exposed to nano-NiO and nano-SiO_2, mRNA levels were reestablished to those of CTL plants.

The exposure of barley to AC also resulted in a strong up-regulation of genes coding for SOD, CAT and APX, with rises up to 3.2-fold; however, the co-application with nano-SiO_2 reverted this patter, for levels similar to the control.

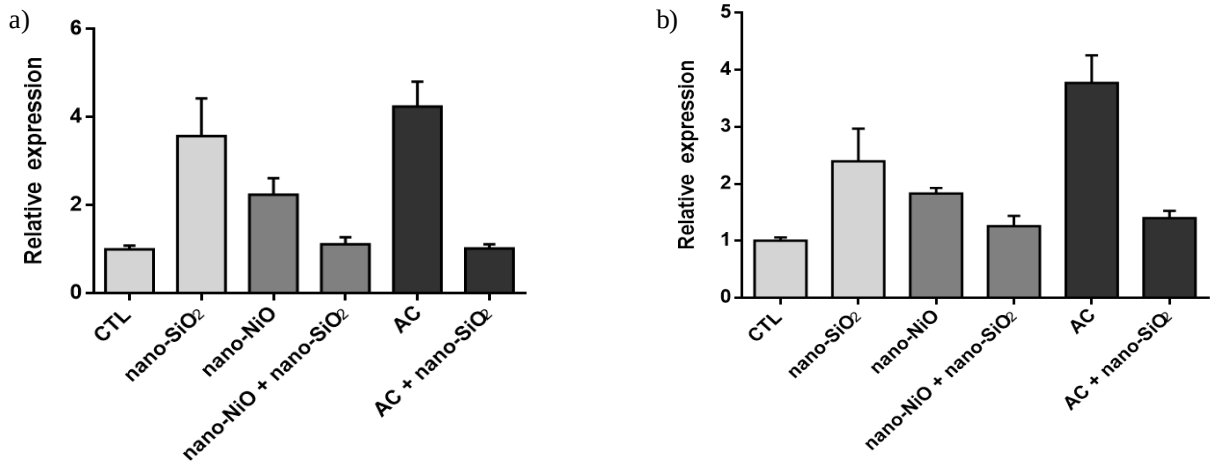

Figure 41. *Expression profile of SOD (a) and APX (b) in leaves of barley plants cultivated for 14 days in OECD soil only moistened with water (CTL), in OECD soil spiked with nano-SiO_2 (3 mg kg^{-1}) suspension and in OECD soil spiked with nano-NiO (120 mg kg^{-1}) or AC (400 mg kg^{-1}) with and without nano-SiO_2.* Data presented are mean ± STDEV (n ≥ 3).

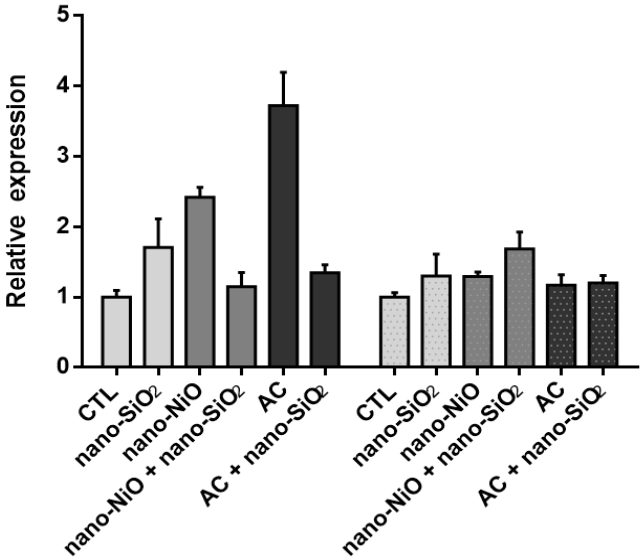

Figure 42. *Expression profile of CAT1 (bars without pattern) and CAT2 (bars with pattern) in leaves of barley plants cultivated for 14 days in OECD soil only moistened with water (CTL), in OECD soil spiked with nano-SiO_2 (3 mg kg^{-1}) suspension and in OECD soil spiked with nano-NiO (120 mg kg^{-1}) or AC (400 mg kg^{-1}) with and without nano-SiO_2.* Data presented are mean ± STDEV (n ≥ 3).

4. DISCUSSION

4.1. Ecotoxicity of nano-NiO and AC to barley plants

Currently, the responsible evaluation of different stress factors in plant's development, growth and physiology is a matter of major importance. Thus, phytotoxicology is now an essential part of ecotoxicology research (Eullaffroy, 2013).

In this section of the present work, focus was centered on the possible phytotoxicity significance of two different emerging contaminants (nano-NiO and AC) for soil-grown barley, at both organism and cellular levels. In attempts to achieve a deeper and more reliable analysis, different methodologies were combined and comparisons between endpoints evaluated on standard protocols and other physiological parameters were performed.

Standard methods – biometric and growth-related parameters

As sessile organisms, plants are constantly and directly exposed to contaminated soils since the early steps of germination throughout all of their life-cycle stages. Thereby, seed germination is often used to estimate pollution effects on plant organisms (Miralles et al., 2012). However, our results clearly showed that the application of both nano-NiO and AC did not affect this parameter, even at the highest tested concentration (1000 mg kg^{-1}). In agreement with these data, several authors also reported the lack of sensitiveness of seed germination on ecotoxicological studies for both inorganic and organic compounds (An et al., 2009; Gavina et al., 2013; Bouguerra et al., 2016). Indeed, the potential risk of metals and other contaminants in the impairment of seed germination is highly dependent on their ability to reach embryogenic tissues, which are strongly protected by seed coats, structures with differential permeability to different types of substances (Seregin and Kozhevnikova, 2005; Akinci and Akinci, 2010).

Together with the evaluation of the germination, it is also common to analyze parameters related to growth, since plant's growth measurements are important bioassay endpoints to evaluate the toxicity of a specific compound (Kapanen and Itävaara, 2001; Adrees et al., 2015a) and its impacts on soil functions. Here, barley plants were grown in OECD soil for 14 days with nano-NiO and AC at different concentrations, ranging from 87.8 to 1000 mg kg^{-1}. In addition to the OECD standard assay, a parallel experiment was performed in Petri plates, where seeds were allowed to germinate and seedlings' development was evaluated after 5 days. Although these experiences may not reflect the real conditions of plants exposure to contaminants, since their availability is expected to be higher than in the soil, we observed a good correlation

between the results from Petri plate's and soil's assay for nano-NiO, with very similar $EC_{10,\ 20,\ 50}$ values between them. In what concerns AC, the same pattern was not observed and the $EC_{10,\ 20,\ 50}$ were always lower in Petri plate's assay than in the soil. In fact, even in soil substrate, the bioavailability of certain compounds can be changed in response to different soil properties. Particularly focusing on metals, it is widely accepted that soil pH and the presence of another ions, such as phosphate, can alter metal's bioavailability, thus changing its possible effects on biota (Olaniran et al., 2013). Also, recent findings uncovered that phosphate and nitrogen can affect several xenobiotics' availability in soil (Allison et al., 2013). Thus, it appears that these kind of approaches are highly species-, contaminant- and substrate-dependent and, by this reason, rather than exclude one or another, combined strategies could represent an advantage to risk assessment and, so, Petri dish assays could be useful for a first screening of the toxicity of new contaminants. Our results demonstrated that both tested contaminants, particularly nano-NiO, induced a marked decrease in root length. The reduction of root length is a common response of plants exposed to different types of stresses, including metals, like Ni. Although very few studies are available concerning the effects of nano-NiO on plants, the inhibition of root growth as a consequence of Ni excess was detected in a wide range of plant species (see works reviewed by Hussain et al., 2013). Regarding AC, An et al. (2009) found that the exposure of wheat plants to paracetamol negatively affected root elongation, with an EC_{50} of about 670 mg L^{-1}. In accordance, based on the results of Petri plate's assay, an EC_{50} of around 550 mg L^{-1} was estimated on root length, corroborating the previous results with wheat, which is also a monocotyledonous species like barley.

Simultaneously with the reduction of root growth, the exposure of barley to nano-NiO and AC induced a significant decrease in the biomass production of roots and leaves, evaluated in terms of both fresh and dry weights. Interestingly, for both contaminants and organs, fresh weight was always more sensitive than dry weight, with lower $EC_{10,\ 20,\ 50}$ values. Moreover, it was clear that nano-NiO caused deleterious effects at lower concentrations that AC. However, we cannot completely assume that nano-NiO is more toxic than AC; indeed, it seems that AC-mediated toxicity is related to its degradation pathways in soil. According to Li et al. (2014), AC is rapidly degraded in soil, with microorganisms playing a central role in this process. Thus, we cannot exclude the hypothesis that AC may be being metabolized by soil microbial community and, by this reason, only higher concentrations led to negative effects on barley's growth performance. Actually, bearing in mind the different $EC_{10,\ 20,\ 50}$ of AC in Petri plate and OECD soil assays, it is likely that in Petri plates assays the maintenance of aseptic conditions prevented AC degradation, aggravating its toxicity.

When plants are growing onto contaminated soils, the first main target of stress is the radicular system, reason why the evaluation of root responses can help us to understand the potential hazards of different contaminants. However, in many ecotoxicology studies with plants, the evaluation of root's development and biomass is not considered. Here, we noticed a differential discriminatory power between roots and leaves growth in a contaminant-dependent manner, being the biomass of roots more sensitive than leaves for AC and less sensitive for nano-NiO. This fact might be related to the different chemical nature of AC and nano-NiO, as well as their possible effects on plant physiology. Indeed, although high levels of Ni are phytotoxic, this metal is regarded as an essential micronutrient for plant growth, and plants have specific translocation pathways for Ni. So, we can hypothesize that nano-NiO is absorbed by the radicular system and, then, translocated to leaves, as a protection mechanism for roots. This idea was also proposed by different authors and publications (see review by Yusuf et al., 2011) and strengthened by the macroscopic phytotoxicity symptoms observed in our study in nano-NiO-treated leaves (data not shown). On the other hand, though AC is not found in normal plant metabolism, it is supposed that plants may possess an effective detoxification pathway for different xenobiotics, like AC (Bartha et al., 2010). Since there are no records regarding the toxic effects of this antipyretic drug on plant growth, we suggest that roots are the main targets of AC-mediated stress, although a marked decrease of leaves fresh and dry weight was also observed for high doses. Paired with this hypothesis, several studies with other organic contaminants, like fungicides and pesticides, also reported a decrease in plant biomass, particularly in roots (Tiyagi et al., 2004; Parween et al., 2011; Teixeira et al., 2011; Yildiztekin et al., 2015).

Physiological endpoints – photosynthetic pigments and oxidative stress markers

As said before, one of the major objectives of this work was to assess if the inclusion of diverse biochemical endpoints could improve the sensitivity of ecotoxicological tests. Therefore, aiming to have a better insight about the effects of nano-NiO and AC on the physiological status of barley plants and of their mechanisms of action, the levels of photosynthetic pigments were quantified. Although no significant changes were found regarding AC treatments, a gradual decrease of both chlorophylls and carotenoids was reported in nano-NiO-exposed plants. Indeed, several references point out that Ni excess can lead to a lower photosynthetic pigments content (Lin and Kao, 2007; Ahmad et al., 2011; Dubey and Pandey, 2011; Soares et al., 2016), possibly due to a higher activity of chlorophyllase and/or inhibition of chlorophyll production (Ali et al., 2008). Moreover, it is known that Ni can replace the Mg ion in the chlorophyll molecule, leading

to a lower photosynthetic activity (Küpper et al., 1996). In general, when looking at the LOEC and $EC_{10,20,50}$ values obtained, we can assume that the inclusion of photosynthetic pigments analysis did not contribute to a higher discriminatory evaluation of the potential risks of AC and nano-NiO.

One of the main common characteristics of the exposure of plants to different kinds of stress, including soil pollution, is the induction of oxidative stress, by an overproduction of ROS (Gill and Tuteja, 2010; Sharma et al., 2012). Although ROS are continuously produced as a consequence of the aerobic and photosynthetic metabolism, an exacerbated rise in their production can trigger great damage to plant cells, leading, in last, to cell apoptosis (Gill and Tuteja, 2010). In this study, particular emphasis was given to different types of oxidative stress indicators, namely the content of $O_2^{\cdot-}$ and H_2O_2, as well as lipid peroxidation and cell death histochemical detection.

Although Ni is not considered a catalyst of the Haber-Weiss reaction, due to not being a redox-active metal, the relationship between Ni excess and the occurrence of oxidative stress in plants is well described in literature (Gomes-Junior et al., 2006; Gajewska et al., 2009; Yusuf et al., 2011; Hussain et al., 2013; Dourado et al., 2015; Soares et al., 2016). Here, in general, contents of both $O_2^{\cdot-}$ and H_2O_2 were frankly increased by nano-NiO treatments. Indeed, even that large amounts of hydrogen peroxide can lead to toxic effects to plant cells, the role of this ROS as a signaling molecule is being progressively recognized, so its production can be also related to a mechanism of cell signaling (Sharma et al., 2012). Therefore, three hypotheses can be considered to explain the maintenance of H_2O_2 levels between CTL and stressed plants: this molecule could be used as an intracellular messenger, be efficiently removed by the AOX enzymatic system and/or react with $O_2^{\cdot-}$ favoring the production of $OH^{\cdot}$. Regarding AC, as in nano-NiO situation, $O_2^{\cdot-}$ was a more sensitive marker than H_2O_2. Despite the lack of information about AC possible effects on plant oxidative status, we can suggest that excess of this pharmaceutical triggers the production of $O_2^{\cdot-}$, which is usually the first ROS to be produced (Gill and Tuteja, 2010; Sharma et al., 2012; Gupta et al., 2015). In accordance to this hypothesis, Kummerová et al. (2016) reported an increase of ROS content, particularly $O_2^{\cdot-}$, in *Lemma minor* plants exposed to two drugs, one of which was AC.

Among all ROS, hydroxyl radical ($OH^{\cdot}$), formed by the Haber-Weiss reaction, is the most dangerous oxygen-derived radical, inducing lipid peroxidation and substantial damages in several biomolecules (Gill and Tuteja, 2010). Additionally, it is directly associated to programed cell death (PCD) (Demidchik, 2015), once plant cells do not have any specific enzymatic reaction to eliminate this ROS. Thus, since both $O_2^{\cdot-}$ and H_2O_2 are part of the Haber-Weiss reaction, with a 1:1 stoichiometry, the ratio between

these two ROS can gives us information about the potential production of $OH^{\cdot}$ (Bowler et al., 1991). Accordingly, our results clearly showed that the exposure of barley to increased nano-NiO and AC concentrations resulted in a significant increase of this proportion throughout all treatments. Besides that, the lowest concentration (87.8 mg kg^{-1}) of each chemical induced a great boost in this ratio, suggesting that oxidative stress conditions are occurring even at the lowest concentrations tested.

As a result of ROS overproduction, LP of biological membranes, at both cellular and organelle levels can occur. Consequently, high rates of lipid peroxides can, in turn, aggravate the cellular redox imbalance, being able to directly react with proteins and DNA (Sharma et al., 2012). The present work revealed, once again, that the soil application of sequential doses of AC and nano-NiO induced the occurrence of oxidative stress conditions, since LP remained always higher than CTL situation. These results are in accordance with different studies, conducted with several plant species exposed to diverse types of abiotic stress, which point out that the enhancement of LP is a common response of oxidative stress (see reviews by Gill and Tuteja, 2010; Sharma et al., 2012). Although in general, AC-treated plants showed a dose-independent increase of LP, we were very surprised that, for the first three applied concentrations, a gradual decrease of MDA content was noticed. Thus, we hypothesize that the exposure of barley to 87.8 mg kg^{-1} AC led to a cellular redox imbalance (higher $O_2^{\cdot -}$, MDA and cell death levels), but was not enough to elicit a response from the AOX system, thus enhancing LP; in turn, the application of 131.7 and 197.5 mg kg^{-1} resulted in a slightly decrease of MDA – though always higher than the CTL – which could be related to an efficient AOX system response. From this point on, MDA levels were increased again, possibly indicating that above 197.5 mg kg^{-1}, AC negatively affects the plant AOX system performance. Moreover, as seen in the standard procedures, AC was more toxic at high concentrations, particularly above 400 mg kg^{-1}. In accordance to the $O_2^{\cdot -}$ and MDA contents, our study also revealed that nano-NiO and AC affected barley's cell viability, even in the lowest tested concentration. Moreover, a dose-dependent response was observed for the two contaminants, with higher cell death values at the highest applied doses (666.6 and 1000 mg kg^{-1}). It is widely accepted that cell viability, as well as cell death, can be affected by oxidative stress, since ROS are involved in different signaling pathways of programmed cell death (PCD) (Gupta et al., 2015; You and Chan, 2015). In fact, paired with our observations, Faisal et al. (2013) reported that the exposure of tomato to different concentrations of nano-NiO led to a higher percentage of apoptosis; also, using silver (Ag) nanomaterial, a rise in cell death was detected in roots of *Alium cepa* (Panda et al., 2011) and the same response was observed in barley exposed to increased concentrations of aluminum (Al) (Achary et al., 2012).

In opposite to the levels of photosynthetic pigments, the evaluation of different oxidative stress markers generally led to a higher sensitive analysis of the effects of nano-NiO and AC, relatively to the standard procedures. Actually, when comparing the standard methodologies and the biochemical determinations, it is clear that the latter have led to lower LOEC values, allowing a more secure risk evaluation, especially for AC, but also for nano-NiO. Indeed, for AC, all oxidative stress markers were more sensitive than the standard procedures, given the obtained LOEC and NOEC values, possibly indicating that AC is already interfering with the cellular oxidative status in the lowest applied doses. Regarding nano-NiO, though the standard procedures were also very sensitive, it was possible to perceive that the adverse effects of this nano-material on the first tested concentration (87.8 mg kg^{-1}) were more notorious in the biochemical determinations, than in the biometric ones. In agreement with our findings, Gavina et al. (2013) also suggested that the inclusion of different physiological endpoints could improve the accuracy of ecotoxicological studies with plant species.

4.2. Effects of nano-SiO_2 on the tolerance of barley under nano-NiO and AC stress

One of the main goals of this study was to assess if the application of nano-SiO_2 could positively affect barley's tolerance to nano-NiO and AC, since this element is an essential nutrient (Taiz et al., 2015), directly involved in plant responses to stress. Thus, after unraveling the ecotoxicological and physiological effects of increased concentrations of nano-NiO and AC to barley, plants were once again exposed to both contaminants in the presence of nano-SiO_2.

Aiming to achieve a global approach, after the growth period, different biometric and physiological methodologies were applied in order to concretely understand the biochemical and molecular basis of nano-NiO- and AC-mediated stress, as well as the effects of nano-SiO_2 co-application.

Biometric and growth-related parameters

As reported, the evaluation of different growth endpoints is a common tool to estimate the phytotoxic effects of different stress factors, including the presence of metals and xenobiotics. Our results clearly showed that the application of the sub-lethal dose of nano-NiO (120 mg kg^{-1}) and AC (400 mg kg^{-1}) negatively affected the normal growth of *H. vulgare*, inducing a decrease in root length along with a reduction in both fresh and dry weights of leaves and roots. Based on the previous ecotoxicological results and the available bibliographic data (An et al., 2009; Chen et al., 2009; Yusuf et al., 2011;

Hussain et al., 2013), these results were not a surprise and unequivocally indicate that both contaminants are interfering with the normal development of different organs of barley plants. Furthermore, and corroborating our previous data, nano-NiO seemed to have a more negative effect than AC, inducing a more marked decrease in growth-related parameters, at a lowest concentration. It is well established that metal effects are primarily manifested by the inhibition of plant growth (Hussain et al., 2013). Actually, although Ni is an essential nutrient for plants, it easily becomes phytotoxic even in low amounts, affecting the growth and development of plants at multiple levels (Gomes-Junior et al., 2006; Hussain et al., 2013).

Over the recent decades, substantial efforts have been reinforced to develop new and eco-friendly tools to increase plant tolerance to stress, improving their growth traits and performance under adverse conditions. Here, the co-application of nano-SiO_2 to the OECD soil did not statistically alter the negative effect of both nano-NiO and AC on barley's growth performance. However, when analyzing the data of root length and biomass production of leaves and roots, a tendency for plants co-treated with nano-NiO and nano-SiO_2 to exhibit higher values than those grown only in the presence of nano-NiO was observed. In accordance with this observation, different studies have reported the beneficial effects of Si on improving the growth and yield of different plant species, especially those under metal stress (Ali et al., 2013; Bharwana et al., 2013; Farooq et al., 2013; Adrees et al., 2015b). Particularly focusing on Si nanomaterial, although there are only a few available records, it is suggested that nano-Si is also able to counteract the deleterious effects of abiotic stress, when used on its bulk form. Indeed, based on the findings of Tripathi et al. (2015), the exogenous application of nano-Si resulted in a higher tolerance of *Pisum sativum* to chromium (Cr) (IV) stress, improving plant biomass production; in addition, Wang et al. (2015) have also found that Si nanomaterial efficiently ameliorated Cd phytotoxicity in rice, increasing different growth-related parameters, such leaves' and roots' fresh weight. Given these findings, it was expected that nano-SiO_2 co-application would result in a higher improvement of barley's growth when exposed to nano-NiO. However, it should be stressed out that there are no studies regarding the effects of nano-SiO_2 application on plants exposed to other metallic nanomaterials, thus no extrapolations are possible without more studies.

In what concerns AC-treated plants, to the best of our knowledge, there are no reports regarding the possible role of Si on mitigating AC-associated toxicity, neither other xenobiotic and/or organic pollutant. Nevertheless, we cannot exclude the hypothesis that nano-SiO_2 is also able to mitigate the toxicity caused by AC excess only based on biometric parameters.

Ni accumulation pattern

In parallel to the evaluation of several biometric parameters, the accumulation pattern of nano-NiO inside plant tissues was also investigated after 14 days of growth. As expected, the concentrations of Ni were higher in roots than in leaves. In agreement with this result, diverse studies with different plant species, including monocots, like *Triticum aestivum* and *Eichhornia crassipes*, and dicots, like *Solanum nigrum* L. and *Lactuca sativa* L., have already reported that Ni is preferentially accumulated into the radicular system (Gajewska et al., 2006; Gajewska and Skłodowska, 2008; Singh and Pandey, 2011; González et al., 2015; Soares et al., 2016). It is possible that roots may serve as a barrier against Ni translocation to the aerial parts of the plant, possibly representing an efficient tolerance mechanism to avoid metal toxicity (Singh and Pandey, 2011).

As reviewed by Liang et al. (2007), Si-mediated alleviation of metal toxicity can be related to its complexation, compartmentation or co-precipitation of metal ions and/or its ability to reduce metal's uptake from roots. Here, our results clearly showed that the co-exposure of barley to nano-NiO and nano-SiO_2 resulted in a higher content of Ni in roots than in the roots of plants grown only in the presence of nano-NiO. Although several reports state that Si is able to reduce metal absorption as a tolerance mechanism, we suggest that nano-SiO_2 is promoting Ni compartmentation and accumulation in roots, as a defense mechanism to prevent its translocation to leaves, instead of reducing Ni uptake by roots. Also, knowing that nanomaterials may have different uptake and transport mechanisms, it is possible that, in this particular study, nano-SiO_2-mediated protection is related to an improvement of different metabolic adjustments and intracellular processes, instead of only limiting nano-NiO uptake and absorption. In agreement with this hypothesis, Ni concentrations in leaves were lower in plants co-treated with both nanomaterials, though generally these plants accumulated more Ni. Overall, when combining the results of biometric parameters and Ni content, it can be suggested that nano-SiO_2 somehow reverted some phytotoxic effects of nano-NiO, despite the high accumulation of Ni by roots of barley plants.

So far, only a few works explored the patterns of accumulation and distribution of organic pollutants in plant tissues. However, based on what has being described, it is acknowledged that plants are able to absorb xenobiotics, triggering several mechanisms for their translocation or retention in distinct organs, depending on the nature of the pollutant (Kumar et al., 2005; Herklotz et al., 2010; Eggen et al., 2011). More specifically to the case of AC, the first study that has addressed this issue was published by Huber et al. (2009), who tried to understand the mechanisms behind AC metabolism in plants. According to their results, root cells of horseradish (*Armoracia rusticana*) were able to

absorb the drug after a 3 h exposure; another more recent work, carried out with *B. juncea* plants, also came to the same conclusion, detecting AC in both roots and leaves of this species (Bartha et al., 2010). Due to time limitations and technical issues, it was not possible to determine the AC content in barley's leaves and roots exposed to AC alone and in the presence of nano-SiO_2. However, aiming to better understand the relationship between nano-SiO_2 and AC absorption patterns, the estimation of its content in barley's leaves and roots will be further performed.

Photosynthetic activity

Symptoms associated with the toxicity of different classes of pollutants, including nanomaterials and xenobiotics, can occur at different levels, affecting, among other essential processes, photosynthesis and all the photosynthetic machinery. Thus, aiming to determine the possible deleterious effects of nano-NiO and AC, as well as nano-SiO_2-mediated protection, the photosynthetic pigments were quantified, along with the chlorophyll fluorescence analysis. This technique is regarded as a non-invasive procedure, that allows the collection of data regarding the state of PSII and is becoming a very useful tool to understand the photosynthetic mechanisms of plants grown under diverse types of stress conditions (Murchie and Lawson, 2013).

According to some bibliographic data, it is known that metals are able to negatively affect the photosynthesis, frequently inducing a reduction in the levels of photosynthetic pigments. Our results clearly showed that nano-NiO excess culminated in a decrease of total chlorophylls content, corroborating previous results for different plant species grown in the presence of Ni, such as *S. nigrum* and *T. aestivum* (Gajewska and Skłodowska, 2007; Soares et al., 2016). Although there are no studies reporting the effects of nano-NiO on photosynthetic machinery, the exposure of plants to other classes of metal-based nanomaterials suggest that their effects are much identical to their bulk materials. In this way, as discussed earlier, it is assumed that the detrimental effect of nano-NiO in photosynthetic pigments is essentially due to its action on the structure of thylakoid's membranes and the grana, as well as the replacement of Mg ion by Ni (Yusuf et al., 2011).

Based on the results of chlorophyll fluorescence analysis, the presence of 120 mg kg^{-1} nano-NiO caused, once again, phytotoxic effects, since it was registered a reduction of the F_v/F_m, a parameter that quantified the maximum quantum yield of PSII activity (Murchie and Lawson, 2013). Indeed, according to Björkman and Demmig (1987), the value of F_v/F_m for unstressed plants should be around 0.83 and corresponds to the highest photosynthetic activity. Moreover, as a consequence of diverse stresses, F_v/F_m can decrease, indicating the occurrence of photoinhibition. Thus, this value is commonly

used to measure the magnitude of stress in photosynthesis and different studies have already state it as a robust indicator of stress for different plant species (Murchie and Lawson, 2013). Curiously, the evaluation of two other complementary parameters (ETR and ΦPSII) led to ambiguous and contrasting results and two hypothesis can be set forward: 1) despite nano-NiO led to a decrease of photosynthetic pigments and lowered the values of F_v/F_m, barley plants could have developed a defense response to ensure the photosynthetic efficiency and, therefore, the ETR, as well as the photosynthetic efficiency, are superior to the control; 2) the exposure of control plants to dark conditions affected their fitness and, by this reason, ETR and ΦPSII are diminished. In fact, in order to perform this assay, plants were kept in dark conditions for a significant period of time. Thus, knowing that the previous exposure to a certain type of stress can confer protection against other adverse conditions, it can be suggested that nano-NiO-treated plants responded better than control plants to this variation in their growth conditions, somehow camouflaging the obtained results. From the two advanced hypothesis, it is expected that the second is more plausible, given the results obtained for the photosynthetic pigments and F_v/F_m, as well as the various phytotoxic symptoms, such as chlorosis and necrosis, observed in the leaves of plants treated with nano-NiO. Paired with this supposition, it is widely accepted that Ni is able to inhibit the ETR and one of the initial targets of Ni excess is the PSII (Chen et al., 2009; Yusuf et al., 2011).

As has been observed, the co-application of nano-SiO_2 reverted, at least in part, the phytotoxic effects of nano-NiO, since no statistical differences were found among photosynthetic pigments and F_v/F_m. These results are, once again, in accordance to what is reported in bibliography, which support the idea that Si, both in bulk and nano forms, is able to ameliorate the negative effects of many types of abiotic stress on the photosynthetic machinery (Ali et al., 2013; Siddiqui and Al-Whaibi, 2014; Rizwan et al., 2015; Tripathi et al., 2015; Wang et al., 2015).

Contrary to what was observed for the nano-NiO, no variations were find in the contents of photosynthetic pigments of plants exposed to high doses of AC. Regarding this matter, although some studies reported a negative effect of AC on photosynthetic pigments content (An et al., 2009; Hajkova and Kummerová, 2014; Kummerová et al., 2016), Nunes et al. (2014) did not detected any change in the total chlorophylls of two aquatic plant species. Paired with these results, no changes were also recorded in F_v/F_m, neither in ETR and ΦPSII, suggesting that excess of AC did not induce harmful consequences in the photosynthetic activity of barley plants, regardless of being or not co-treated with nano-SiO_2. Similar findings were also reported by Hajkova and

Kummerova (2014), in which no significant changes were observed either in terms of F_v/F_m and ΦPSII in *L. minor* exposed to this chemical.

N nutrition

Given the negative effects that both nano-NiO and AC caused in the development of barley plants, and knowing that N is the major essential macronutrient for plant growth, two of the main enzymes involved in N assimilation pathway were studied: nitrate reductase, the enzyme that catalyzes the reduction of nitrate to nitrite, and glutamine synthetase, the enzyme that converts the ammonium generated from nitrate assimilation or photorespiration into amino acids. However, if it is known that several metals are able to interfere with the absorption and intracellular distribution of several essential nutrients (Marschner, 2011), little is acknowledged about the effects of xenobiotics in these processes. In fact, although recent publications have been suggesting the existence of a relationship between levels of N and P with the availability of various organic pollutants (Allison et al., 2013; Gomes et al., 2016), as herbicides and pesticides, the influence of paracetamol in N nutrition is poorly understood and remains unknown.

The results obtained in this work showed that both enzymes revealed a differential behavior, depending on the organ and experimental condition. Generally, the exposure of plants to nano-NiO induced a positive response in NR and GS activity in leaves. Also, although no significant changes were recorded in roots for GS, a tendency for NR to reduce its activity values was noticed. However, in contrast to our findings, several publications reported that excess of the metallic ion Ni is able to inhibit the activity of NR, as well as other enzymes involved in N assimilation (see review by Hussain et al., 2013). Furthermore, Gajewska et al. (2009), observed that the treatment of wheat plants with 100 µM Ni resulted in a decline of NR and GS activities, confirming the harmful effects of this metal on N metabolism. Despite this disparity, it is correct to point out that the increased activity of the GS is probably related to the elevated levels of Pro observed in barley leaves treated with nano-NiO. In fact, it is known that the accumulation of Pro is closely related to the N cycle in plants, since this amino acid is mostly produced from glutamate, especially under stress conditions (Cheng et al., 2013). In addition, knowing that NR is the first key-enzyme in nitrate assimilation, it is possible to suggest that nano-NiO interfered with the normal uptake of this anion, since reduced activity values of this enzyme were found in roots in relation to the control. Upon nano-SiO_2 co-exposure, roots of barley plants exhibited increased activities of the two studied enzymes relatively to the ones treated with nano-NiO alone, indicating that the application of Si nanomaterial positively affected N nutrition, mainly through the catalytic activity of GS, by the conversion of glutamate to glutamine. In leaves, as reported for nano-NiO single

exposure, NR showed a great increase and, once again, the levels of GS activity are in accordance to the Pro content. Indeed, this positive effect of Si in N nutrition is well documented and reinforces the argument that this nutrient has the ability to positively regulate the uptake and absorption of some macronutrients, like Ca, K and N (Guntzer et al., 2012).

The treatment of barley plants with paracetamol led to a rise in GS activity in leaves and resulted in a decrease of NR in roots. In line to what was described for nano-NiO, the increased activity of GS is likely intrinsically related to the higher levels of proline. On the other hand, the decreased activity of NR in roots can indicate that AC is interfering with the normal uptake of nitrate, compromising the normal development of plants and justifying the observed decrease in biomass. In this case, although not so evident, the exogenous application of nano-SiO_2 also seemed to ameliorate the damaging consequences of AC. Interestingly, in the only situation in which a decrease of NR was observed in response to AC, the co-exposure with nano-SiO_2 reestablished NR activity to the values found in control plants.

Oxidative stress and AOX defense mechanisms

Nowadays it is widely acknowledged that, under different types of adverse conditions to plant growth, pro-oxidative conditions can take place, due to an exacerbated increase of ROS and/or a depletion in AOX system performance (Gill and Tuteja, 2010; Sharma et al., 2012; Gupta et al., 2015). In this way, over the past few years, an increased number of studies has been exploring the physiological implications of oxidative stress in plants, since this process is able to affect the normal cell homeostasis and, ultimately, can culminate in cell death. In the present study, the production of ROS was monitored by the measurement of $O_2^{\cdot-}$ and H_2O_2 and the occurrence of oxidative stress assessed by analysis of LP and levels of total and protein-bond thiols.

As can be noticed, the cultivation of barley in the presence of nano-NiO induced a very pronounced increase in the levels of $O_2^{\cdot-}$ in both leaves and roots. On the other hand, the H_2O_2 content remained unchanged, since no differences were registered in relation to control. Indeed, due to the substantial upsurge of studies concerning the effects of nanoparticles on plants, recent evidences suggested that exposure to high levels of these materials can significantly trigger ROS production (see review by Arrudaet al., 2015). In addition, the influence of various metals, including Ni, in the increased content of ROS is well described in literature (Hossain et al., 1984; Chen et al., 2009; Yusuf et al., 2011). Actually, as discussed in the previous section, although Ni is not considered as a catalyst for the Haber-Weiss reaction, the relationship between its excess and the induction of oxidative damage is progressively more recognized.

According to the studies of Gajewska and Sklodowska (2007), the exposure of wheat plants to high doses of Ni led to increased foliar levels of ROS. Identical results have already been reported for another plant species, including rice and rapeseed (*Brassica napus* L.) (Maheshwari and Dubey, 2009b; Kazemi et al., 2010), and in other experimental models, such as in hairy root culture of *Alyssum bertolonii* (Nedelkoska and Doran, 2001). As a result of the marked increase of ROS, several harmful effects in the cellular metabolism can occur, usually inducing lipid peroxidation and loss of membrane stability (Gill and Tuteja, 2010). In fact, it has been proposed that the peroxidation of lipids is a common metabolic event resulting from plant's exposure to metal excess, including in their nano-sized form, such as Cu and Zn (Dimkpa et al., 2012; Shaw et al., 2014). In the present study we have observed that LP levels in nano-NiO-treated plants were tissue-dependent: MDA content was increased in leaves, but remained unchanged in roots. Actually, the available records about the effect of Ni on LP are not completely consistent, with a great variability between plant species. For example, *S. nigrum* exposure to high levels of Ni did not result in increased LP (Soares et al., 2016); conversely, the same pattern was not observed for pigeon pea, maize and indian mustard, where the content of MDA arose quite increased in response to the metal treatment (Madhava Rao and Sresty, 2000; Baccouch et al., 2001; Ali et al., 2008).

Paired with LP, thiol levels are gradually becoming a common tool to evaluate pro-oxidative conditions and reductions in their content can be correlated with the induction of oxidative stress. It is largely accepted that the thiol-based redox network is involved in plant responses against all types of stress, including soil degradation. Interestingly, a recent review unraveled the multiple biological functions of thiol-containing molecules, unequivocally establishing their importance in plant metabolism. This class of molecules include both protein and non-protein organic compounds, such as the highly recognized thioredoxins and glutaredoxins, and GSH and phytochelatins, respectively (Zagorchev et al., 2013).

In opposition to LP, the content in thiols (both total and protein-bond) was diminished in barley leaves treated with nano-NiO, but a significant increase in roots was noticed. In this way, based on recent evidences which state that thiol groups, among other S-containing molecules, are key elements to the enhancement of plant abiotic stress tolerance (Zagorchev et al., 2013), it can be suggested that the observed rise of this parameter in root cells probably explains the absence of LP in this organ. Thus, it is probable that, under the phytotoxic activity of nano-NiO, root cells stimulated the complex network of thiols as a defense mechanism to counteract the effects of the high content of Ni found in this organ. Besides this, it can be hypothesized that, in leaves, the observed decrease in total thiols is much like related to the reduction of protein-bond

thiols, indicating that some molecules, such as thioredoxins, could be decreased in response to nano-NiO. Indeed, this hypothesis was also supported by the data obtained for photosynthetic pigments, since it is known that thioredoxins play an essential role in photosynthesis (Meyer et al., 2008).

Although the toxic effects of nano-NiO have revealed quite pronounced in barley plants, our results pointed out that co-treatment with nano-SiO_2 has partially contributed to alleviate the stress imposed by the metal. Like other compounds, including phytohormones, such as brassinosteroids and salicylic acid, the occurrence of Si in plant tissues and its ability to reduce oxidative damage is well described in the literature (Guntzer et al., 2012). Actually, even though apparently it was not observed a consistent response among all studied parameters, it was possible to observe that in leaves, where nano-NiO induced a rise in LP levels, the co-treatment of barley with SiO_2 nanomaterial resulted in a decrease of MDA content, accompanied by a reduction in H_2O_2 levels. Moreover, in roots, although no changes were detected in MDA and H_2O_2 contents, the levels of superoxide anion were sharply reduced, strongly supporting the positive effects of this nanomaterial. Furthermore, the benefits of nano-SiO_2 addition were also notorious in increasing the thiol levels, allowing the reestablishment of its content in leaves and in roots. Indeed, these results are paired to what has been proposed for several plant species treated with Si. For instance, recent studies with rice plants reported that the foliar application of nano-SiO_2 allowed the mitigation of Cd-induced phytotoxicity by reducing oxidative damage, namely through inhibiting LP; additionally, according to Tripathi et al. (2015), the contents of $O_2^{\cdot-}$, H_2O_2 and MDA were decreased in plants co-treated with both nano-SiO_2 and Cr (IV). Overall, it can be assumed that the exposure of barley plants to 120 mg kg^{-1} soil nano-NiO induced oxidative damage that were partially counteracted by the application of 0.05 mM nano-SiO_2.

Similar to what is described for metals, a growing number of publications has been suggesting that the presence of xenobiotics can adversely affect plant growth, also favoring the occurrence of oxidative conditions and compromising the redox homeostasis of the cell (Moldes et al., 2008; Teixeira et al., 2011; de Sousa et al., 2013; Kummerová et al., 2016). Although the literature data is scare, there are some works exploring the effects of different drugs, such as AC and diclofenac, on the development of pro-oxidative conditions. Based on the findings of Kummerová et al. (2016), the application of high doses of these two chemicals to *Lemma minor* induced a boost in LP, as in ROS content. Also, increased levels of MDA were reported in alfafa (*Medicago sativa* L.) plants exposed to AC and another study with *Lemma minor* revealed that paracetamol in excess negatively affected the redox balance of the cell (Nunes et al., 2014; Christou et al., 2016). Our results showed that the exposure of barley plants to

400 mg kg^{-1} soil AC did not induce a severe oxidative stress condition, since no changes were found in LP nor thiol groups. Accordingly, the treatment of soybean plants with another xenobiotic did not change the LP levels (Moldes et al., 2008). However, the observed levels of $O_2^{\cdot-}$ and H_2O_2 suggest that AC excess somehow affected the normal redox homeostasis of barley plants. Identical results have already been reported for this species, when plants were simultaneously submitted to two different stress conditions, drought and AC (Khalvati et al., 2010). In general, the assessment of different markers of oxidative stress defined that the treatment of barley plants with AC did not result in a pronounced oxidative damage. Thus, knowing that AC-mediated toxicity is closely related to the production of its sub-product NAPQI, it can be assumed that this compound is not being produced at sufficient high doses to induce harmful effects and/or an efficient detoxification process by GSH action is occurring, limiting its toxicity (Bartha et al., 2010).

Even that, apparently, the toxic effects of paracetamol did not induce a pronounced oxidative stress condition, the co-treatment of plants with nano-SiO_2 somehow ameliorated the performance of barley under AC excess. Indeed, barley plants were benefited by the presence of Si, since reduced levels of LP were found in roots. Furthermore, a great boost in total and protein-bond thiols was detected in this group of plants, revealing that one of the ways Si can enhance plant tolerance to abiotic stress can be related to the synthesis and/or maintenance of -SH groups. Curiously, despite our best efforts, there are not studies regarding the possible beneficial effect of Si against xenobiotic-mediated phytotoxicity. However, overall, the results of the present work indicate that Si application may have a positive role in mitigating this type of stress, although the biochemical and molecular basis of this protection are poorly understood.

In order to cope with oxidative stress, throughout the evolution processes, plants have developed a complex and tiny regulated antioxidant system, comprising both non-enzymatic and enzymatic mechanisms. Aiming to explore the involvement of the non-enzymatic AOX system, the accumulation of soluble proline and the content of ascorbate were analyzed in both leaves and roots. In the last years, many experimental evidences support the idea that the accumulation of Pro is a common response of plants to a large range of stress factors, like soil pollution (Hayat et al., 2012). Besides its functions as an efficient osmoprotectant, the ability of this proteinogenic amino acid to scavenge ROS and to stabilize biological membranes is becoming quickly recognized and its involvement in signaling processes is also already suggested (Szabados and Savoure, 2010). *H. vulgare* responded to high levels of nano-NiO by increasing the levels of proline in leaves very markedly. In fact, corroborating these results, a previous study of our group also detected that Pro accumulation was a typical response of plants to Ni excess (Soares et al., 2016). Besides this, based on the review of Cia et al. (2012), Pro can

assume a protective effect, generally when is accompanied by protein content increase, or act as a sensitive molecule in cases where protein degradation takes place. Here, total protein content was increased after nano-NiO exposure, reason why it can be assumed that Pro had a pivotal role in preventing nano-NiO-induced toxicity, especially in leaves, where its content was greatly increased.

Upon co-exposure with nano-SiO_2, foliar levels of Pro were decreased when compared to plants grown only in the presence of nano-NiO. These results are in accordance with different studies, indicating that the Si-mediated benefits are not related to the accumulation of this soluble osmolyte. Indeed, data from a study with *Spinacia oleracea* revealed that the application of Si to boron-stressed plants did not result in a higher content of Pro and equivalent results were also reported in salt-stressed maize (Moussa, 2006; Gunes et al., 2007).

Regarding AC-treated plants, levels of Pro were also increased in both organs, although statistical differences were only found in leaves. Accordingly, Song et al. (2007) reported that soluble Pro was increased in wheat leaves under chlorotoluron stress, but roots were not so sensitive. Actually, despite the modulation of the AOX system by different types of pharmaceutical compounds have not been properly explored, it is suggested that the exposure of plants to xenobiotics, such herbicides and fungicides, results in a differential response of the AOX system. Indeed, recent data propose that Pro accumulation is also a common response to organic pollutants-mediated stress. According to Teixeira et al. (2011), *S. nigrum* plants grown in the presence of high levels of metalaxyl showed increase Pro levels in roots, possibly as a defense mechanism. Also a previous report from our group showed that metalaxyl induced the accumulation of this amino acid in a cell suspension culture of *S. nigrum* (de Sousa et al., 2013). Under nano-SiO_2 co-exposure, the foliar levels of Pro did not change and a significant reduction was found in roots. In this way, these results corroborate our previous hypothesis, that nano-SiO_2 beneficial effects are not related to the accumulation of this amino acid.

Along with Pro, AsA is also regarded as one of the most powerful antioxidants, being able to prevent and control the damage caused by ROS in plants (Gill and Tuteja, 2010). Under normal physiological conditions, AsA mostly exists in its reduced state. However, under pro-oxidative conditions and/or as a consequence of the activity of certain enzymes, AsA can be converted into DHA, losing its AOX properties. Our results showed that the content of AsA and DHA were always higher in leaves than in roots, behavior that is likely related to the fact that leaves are the main source of AsA biosynthesis (Gill and Tuteja, 2010). As reviewed by Bielen et al. (2013), there is a very strong relation between metal excess and the availability and redox homeostasis of ascorbate. Here, the exposure of barley to 120 mg kg^{-1} soil nano-NiO led to some changes in the content

of total ascorbate in leaves, as well as the relative proportion of both AsA and DHA. Thus, it appears than excess of nano-NiO induced a negative response in ascorbate levels, decreasing its total content and increasing the proportion of DHA. The results are in accordance to what is already described for other plant species under Ni stress, but contradict another works, which pointed out that Ni is able to induce the increase of AsA content, as well as the ratio between AsA and DHA (Bielen et al., 2013 and references therein). This kind of disparity between results is also reported for other metals, like Cd and Zn, and, therefore, it appears that the modulation of ascorbate by Ni is highly dependent on the plant species and the experimental conditions, such as Ni concentration and the exposure time. Moreover, the observed decrease of AsA in nano-NiO-treated leaves helps to understand the harmful effects of this nanomaterial in the photosynthetic apparatus, since ascorbate is essential to different processes in photosynthesis (Bielen et al., 2013).

Once again, the addition of nano-SiO_2 seemed to overcome the negative effects of nano-NiO, stimulating the regeneration and/or biosynthesis of ascorbate, since increased contents of total and AsA proportion were found in leaves of barley plants. In fact, based on the results of both Pro and ascorbate, it can be suggested that the beneficial effects of nano-SiO_2 on the LP levels, as well as H_2O_2, are much likely related to ascorbate accumulation than Pro. In fact, it is kwon that AsA can directly remove the excess of different types of ROS, such as H_2O_2 and $O_2^{\cdot-}$ and, being also able to regenerate α-tocopherol and act as the reducing agent for APX activity (Gill and Tuteja, 2010; Sharma et al., 2012). Overall, results suggest that the non-enzymatic AOX system is being activated by the excess of nano-NiO and that the co-application of nano-SiO_2 improved its mechanisms, namely by modulating the levels of ascorbate in leaves.

In contrast, barley plants grown in the presence of paracetamol did not change its levels of ascorbate in leaves, but a significant reduction in roots was observed, regardless of the plants being or not co-treated with nano-SiO_2. Also, although not statistically relevant, a tendency for both AC and AC + nano-SiO_2 plants to exhibited increased values of DHA was noticed. Given the previous obtained results, it was possible to observe that co-treatment with nano-SiO_2 resulted in a reduction of LP levels in roots, accompanied by a decrease of both Pro and ascorbate. Thus, it can be hypothesized that the higher relative content of DHA in relation to AsA is related to a higher APX activity, which uses AsA as reducing power, oxidizing it into DHA (Gill and Tuteja, 2010; Sharma et al., 2012). Globally, though neither Pro nor ascorbate seemed to have a prominent role in modulating the AOX defense of barley under AC-mediated stress, it cannot be completely excluded that other important metabolites, such as flavonoids and GSH, may be involved. Actually, it is widely accepted that AsA-GSH cycle

plays an important role in the detoxification of xenobiotics and that, as in animals, AC can be conjugated to glutathione (Bartha et al., 2010). By this reason, the quantification of GSH and GSSG contents would be a point of interest in the future, in order to better understand the involvement of the non-enzymatic AOX system under AC stress and the possible effects of nano-SiO_2 on their responses.

Aiming to gain a better insight into the performance of the AOX system under nano-NiO and AC stress, it was evaluated the transcript accumulation and total activity of three key enzymes of plants' antioxidant system: SOD, which catalyzes the dismutation of $O_2^{\cdot-}$ to H_2O_2 and molecular oxygen, CAT and APX, that are both related to H_2O_2 detoxification. Indeed, it is widely accepted that the balance between the performance of these three enzymes is a key element in the management of the redox homeostasis in plant cells (Mittler, 2002).

Overall, there was no strong correlation between mRNA transcript levels and total activity, since the increase in transcript levels was not always followed by an increase in activity and vice-versa. Thus, it is suggested that enzyme stability and activity is being regulated by post-transcriptional and –translational modifications. In accordance to this finding, several studies have also reported a similar pattern between enzyme mRNA accumulation and total activity. For instance, Soares et al. (2016) found that there was no parallel between transcript levels and total enzyme activity in *S. nigrum* plants exposed to Ni and equivalent results were also observed in tobacco and in pea plants subjected to high levels of Cu and Cd, respectively (Kurepa et al., 1997; Romero-Puertas et al., 2007).

Our results clearly showed that the AOX enzymes revealed differential responses under nano-NiO and AC stress and, also, as a response to nano-SiO_2 co-application. SOD is usually considered as the first enzymatic defense line, since it catalyzes the detoxification process of $O_2^{\cdot-}$, which is the first ROS to be produced (Gill and Tuteja, 2010). By this reason, the involvement of SOD in limiting the occurrence of oxidative stress is well described (Gupta et al., 2015). Accordingly, the exposure of barley to nano-NiO positively affected SOD total activity in both analyzed organs, suggesting that this enzyme is being activated as a defense mechanism against high doses of nano-NiO. However, despite SOD increased its activity in both leaves and roots, the levels of $O_2^{\cdot-}$ remained higher in plants exposed to nano-NiO, suggesting that SOD is not sufficient to fully eliminate or control the excessive production of this ROS. As a result of SOD activity, or due to other metabolic processes, H_2O_2 can be generated and its levels need to be tightly coordinated in order to prevent oxidative damage (Sharma et al., 2012). In cells, the maintenance of H_2O_2 levels is mainly achieved by the action of several classes of enzymes, such as catalase and innumerous peroxidases, like APX. Generally, it can be

admitted that nano-NiO excess induced a differential response in CAT and APX activity depending on the analyzed organ. Given the different metabolism of roots and leaves, this fact is not surprising and it is supported by several studies reporting distinct activity patterns of AOX enzymes in different plant tissues (Fidalgo et al., 2011; Fidalgo et al., 2013; Soares et al., 2016). Under nano-NiO excess, CAT activity was positively affected in leaves, indicating that this enzyme might have an important role in H_2O_2 detoxification. In accordance with this result, Farooq et al. (2013) realized that the exposure of cotton plants to Cd induced a boost in CAT activity. On the opposite, in roots, no CAT activity was detected, fact that was quite unexpected, once in a previous recent study from our group the excess of Ni led to higher CAT activities in roots of *S. nigrum* plants (Soares et al., 2016). Nevertheless, the tendency detected in our work was already reported for other metals, such as Cd. Indeed, rice plants exhibited extremely low CAT activity values after 14 days of Cd exposure (Wang et al., 2013). With effect, though CAT is classified as one of the major important AOX enzymes, several authors suggest that its role in H_2O_2 elimination is reduced, except that derived from peroxisome metabolism (Foyer and Noctor, 2005; Halliwell, 2006). On the other hand, the evaluation of APX total activity revealed that this enzyme was unaffected by nano-NiO treatment in leaves, but a significant increase in its activity was detected in roots, most likely to offset the loss of activity recorded on CAT. In fact, even that APX activity is usually higher in photosynthetic tissues, given the increased availability of ascorbate, different studies also suggest that this enzyme can play an important role in heterotrophic organs and its activity can even reach more pronounced values in roots than in shoots of several plant species (Gajewska and Skłodowska, 2008; Maheshwari and Dubey, 2009a; Farooq et al., 2013; Soares et al., 2016). Thus, it appears that CAT comes out as a pivotal element for H_2O_2 detoxification in leaves, while in roots this role is majorly performed by APX.

One of the ways in which Si is able to reduce oxidative damage is related to the stimulation of the activity of different AOX enzymes (Rizwan et al., 2015; Tripathi et al., 2015; Wang et al., 2015; Khaliq et al., 2016). In general, the co-application of SiO_2 nanomaterial resulted in a positive response of the enzymatic AOX system in both leaves and roots of barley plants exposed to high levels of nano-NiO. Remarkably, the only situation in which nano-SiO_2 did not rise SOD activity values matches with increased $O_2^{\cdot-}$ levels. Nevertheless, in this case, the non-enzymatic component and/or the activity of other AOX enzymes seem to have mitigated the deleterious effects of $O_2^{\cdot-}$ excess, since PL was decreased, along with H_2O_2 content. Paired with this hypothesis, the two enzymes involved in H_2O_2 detoxification showed to be increased in leaves, favoring the elimination of H_2O_2 excess and limiting the occurrence of oxidative injury. Equivalent results have already been reported in cotton, where the co-exposure of plants to Cd and

nano-SiO_2 positively affected the performance of AOX enzymes, followed by a reduction in the levels of different oxidative stress markers (Farooq et al., 2013). In roots, the application of nano-SiO_2 led to a rise in total SOD activity, which is consistent with the observed decrease in $O_2^{\cdot-}$ levels. Once again, this data is strongly supported by a recent study of Tripathi et al. (2015), which uncovered that SOD activity was increased in roots of bean simultaneously treated with Cr and nano-SiO_2. Alongside with SOD, a great boost in APX activity was also observed, corroborating the beneficial effects of nano-SiO_2 addition against nano-NiO-induced phytotoxicity. Despite this positive response of the enzymatic AOX system, no signal of CAT activity was detected in roots. Therefore, and bearing in mind that most of Ni content was found in roots, it can be suggested that the excess of this metal was able to irretrievably affect this enzyme, blocking its activity.

Overall, our results support the hypothesis that excess nano-NiO induced a positive response of the AOX system, stimulating the activities of SOD, CAT and APX. However, upon nano-SiO_2 co-exposure, the activation of the AOX system was more pro-active, ameliorating and counteracting the phytotoxic effects of nano-NiO, namely by reducing MDA and H_2O_2 content in leaves and $O_2^{\cdot-}$ levels in roots. Furthermore, based on these findings, it can be hypothesized that a longer exposure time to nano-NiO was necessary to clearly observe the benefits of nano-SiO2 on barley's growth and yield.

Even though xenobiotics display a particular detoxification pathway in plants, it is postulated that these compounds are also able to affect the AOX system, leading to changes in enzyme activity. As an example, a recent report with tomato plants revealed that the foliar exposure to several pesticides triggered a rise in AOX enzymes' performance (Yildiztekin et al., 2015). On the other hand, prometryne-induced oxidative stress culminated in a reduction of CAT, but stimulated the activities of SOD and APX (Jiang and Yang, 2009). Thus, given the disparity between the available data, it appears that xenobiotics' effects on AOX enzymes performance are highly dependent on several factors, such as plant species and stress characteristics, like the nature of the pollutant, the magnitude of the stress and the exposure time. In the present work, SOD activity in response to AC excess was changed according to the levels of $O_2^{\cdot-}$; in roots, the maintenance of SOD activity is probably related to the unchanged levels of this ROS; in leaves, AC induced a great boost of $O_2^{\cdot-}$production, accompanied by a rise in SOD activity. However, given the data obtained for $O_2^{\cdot-}$ quantification, it seems that the enhancement of SOD activity was not enough to overcome the increased generation of this ROS. On the other hand, the complete depletion of CAT activity found in roots of AC-treated plants, along with the maintenance of APX activity values, explains the higher levels of H_2O_2 found in this group of plants. In parallel to our findings, Bartha et al. (2010)

detected that AC greatly inhibited CAT activity in both roots and leaves of *B. juncea*, but did not reported major changes in APX activity.

As previously stated, there is an evident gap in studies focusing on the possible ameliorating effect of Si against xenobiotic-induced stress. Our results allowed to infer that the co-treatment with nano-SiO_2 did not majorly affected the performance of the enzymatic AOX system, since no significant changes were, generally, found in relation to the plants only exposed to AC. Still, the application of this nanomaterial enhanced APX activity in roots and, although the content of H_2O_2 remained higher, it was possible to observe a substantial reduction in LP levels.

Overall, one can conclude that the exposure of barley to 400 mg kg^{-1} soil AC did not trigger a harsh oxidative stress condition and, maybe due to this reason, the protective role of nano-SiO_2, along with its influence on the AOX system, were not so evident. Indeed, it is suggested that, similar to what is reported for BRs (Schnabl et al., 2001), the beneficial effects of Si are much more pronounced in plants grown under stressful conditions.

5. CONCLUSIONS

5.1. Ecotoxicity of nano-NiO and AC to barley plants

- The exposure of barley to increased concentrations of nano-NiO and AC impaired its normal growth and physiological performance;
- Given the obtained EC and LOECs values, nano-NiO was more toxic than AC, inducing a more negative response in barley's metabolism, which also reflected in a much more decreased productivity, however this pattern can be related to the degradation of AC by the microbial community;
- Comparing standard methods and physiological endpoints, we can suggest that the addition of oxidative stress markers helped to detect phytotoxicity signs at lower concentrations than the standard OECD-based methodologies, especially for AC.

5.2. Effects of nano-SiO_2 on the tolerance of barley under nano-NiO and AC stress

- The co-application of nano-SiO_2 to barley plants exposed to nano-NiO and AC did not significantly overcome the negative effect of both contaminants on biometric parameters; however a strong tendency for plants treated simultaneously with nano-NiO and nano-SiO_2 to show increased productivity was observed;
- Data from photosynthetic activity revealed that only nano-NiO induced a negative response in photosynthesis and that, under nano-SiO_2 co-exposure, this negative effect was efficiently counteracted;
- Generally, N nutrition was not negatively affected by neither nano-NiO or AC, yet the co-treatment with nano-SiO_2 improved the response of the two studied enzymes, especially in roots;
- The exposure of barley plants to nano-NiO induced the occurrence of oxidative stress, namely by the overproduction of ROS, but the co-treatment with Si nanomaterial reverted this tendency, generally lowering and/or maintaining the levels of LP and stimulating the thiol redox network; on the other hand, AC-induced toxicity did not culminate in a severe oxidative damage and, by this reason, the positive effects of nano-SiO_2 were not so evident;

- Excess of nano-NiO stimulated the non-enzymatic AOX system and the co-application of nano-SiO_2 improved its mechanisms, by positively modulating the levels of ascorbate in leaves; AC-mediated stress resulted in an increased accumulation of Pro, regardless of the co-treatment with nano-SiO_2;

- The involvement of the enzymatic component of the AOX system showed differential responses between organs and treatments and there was not a positive correlation between q-PCR analysis and total activity data;

- Under nano-NiO-mediated stress, SOD activity was not enough to eliminate the excess of $O_2^{\cdot -}$. Also, CAT and APX seemed to have a pivotal role in H_2O_2 detoxification in leaves and roots, respectively. Upon nano-SiO_2 co-exposure, in general, there was a more proactive response of the AOX system, through a much more pronounced increase of enzyme's activity. AC induced some changes in the AOX system, promoting SOD activity in leaves, whilst inhibiting CAT performance. In this case, the co-exposure with nano-SiO_2 did not substantially alter this pattern;

- Overall, it can be assumed that nano-NiO was more toxic than AC, triggering the occurrence of oxidative stress and the activation of the plant AOX system; however, upon nano-SiO_2 co-exposure, some phytotoxic symptoms were ameliorated, possibly due to the Si-mediated protection against oxidative stress. Nevertheless, AC also induced some phytotoxicity, especially on growth-related parameters, but did not cause serious oxidative damage. Maybe by this reason, the benefits of nano-SiO_2 were not so evident in plants exposed to this contaminant.

6. FUTURE PERSPECTIVES

With this work, it was achieved a clear and elucidative perspective of the toxicity associated with nano-NiO and AC for barley plants and, simultaneously, it was possible to conclude that the application of nano-SiO_2 reverted some phytotoxic effects of both contaminants. However, in the future, interest and attention will be focused on:

- Quantifying the levels of AC in both leaves and roots of barley plants grown in the presence and absence of nano-SiO_2;
- Evaluating the responses of other AOX metabolites, specifically GSH, flavonoids and phenols, as well as other AOX enzymes, such as GSTs GR, MDHAR and DHAR, and other classes of peroxidases;
- Further exploring the uptake pattern of nano-NiO and nano-SiO_2 and their translocation mechanisms;
- Comparing the influence of SiO_2 and nano-SiO_2 in mitigating the adverse symptoms of different stress agents.

7. BIBLIOGRAPHY

Achary, V.M.M., Patnaik, A.R., Panda, B.B., 2012. Oxidative biomarkers in leaf tissue of barley seedlings in response to aluminum stress. Ecotoxicology and environmental safety 75, 16-26.

Adrees, M., Ali, S., Rizwan, M., Ibrahim, M., Abbas, F., Farid, M., Zia-ur-Rehman, M., Irshad, M.K., Bharwana, S.A., 2015a. The effect of excess copper on growth and physiology of important food crops: a review. Environmental Science and Pollution Research 22, 8148-8162.

Adrees, M., Ali, S., Rizwan, M., Zia-ur-Rehman, M., Ibrahim, M., Abbas, F., Farid, M., Qayyum, M.F., Irshad, M.K., 2015b. Mechanisms of silicon-mediated alleviation of heavy metal toxicity in plants: a review. Ecotoxicology and environmental safety 119, 186-197.

Aebi, H., 1984. [13] Catalase in vitro. Methods in enzymology 105, 121-126.

Agency, U.S.E.P., 2007. Final Nanotechnology White Paper. EPA 100/B-07/001. Office of the Science Advisor, Washington.

Ahmad, M.S.A., Ashraf, M., Hussain, M., 2011. Phytotoxic effects of nickel on yield and concentration of macro-and micro-nutrients in sunflower (*Helianthus annuus* L.) achenes. Journal of hazardous materials 185, 1295-1303.

Ahmad, P., Sarwat, M., Sharma, S., 2008. Reactive oxygen species, antioxidants and signaling in plants. Journal of Plant Biology 51, 167-173.

Akinci, I.E., Akinci, S., 2010. Effect of chromium toxicity on germination and early seedling growth in melon (*Cucumis melo* L.). African Journal of Biotechnology 9, 4589-4594.

Albanese, A., Sykes, E.A., Chan, W.C., 2010. Rough around the edges: the inflammatory response of microglial cells to spiky nanoparticles. ACS nano 4, 2490-2493.

Ali, B., Hayat, S., Fariduddin, Q., Ahmad, A., 2008. 24-Epibrassinolide protects against the stress generated by salinity and nickel in Brassica juncea. Chemosphere 72, 1387-1392.

Ali, S., Farooq, M.A., Yasmeen, T., Hussain, S., Arif, M.S., Abbas, F., Bharwana, S.A., Zhang, G., 2013. The influence of silicon on barley growth, photosynthesis and ultra-structure under chromium stress. Ecotoxicology and environmental safety 89, 66-72.

Alkilany, A.M., Murphy, C.J., 2010. Toxicity and cellular uptake of gold nanoparticles: what we have learned so far? Journal of nanoparticle research 12, 2313-2333.

Allison, J.E., Boutin, C., Carpenter, D., 2013. Influence of soil organic matter on the sensitivity of selected wild and crop species to common herbicides. Ecotoxicology 22, 1289-1302.

Alscher, R.G., Erturk, N., Heath, L.S., 2002. Role of superoxide dismutases (SODs) in controlling oxidative stress in plants. Journal of experimental botany 53, 1331-1341.

An, J., Zhou, Q., Sun, F., Zhang, L., 2009. Ecotoxicological effects of paracetamol on seed germination and seedling development of wheat (*Triticum aestivum* L.). Journal of hazardous materials 169, 751-757.

Arruda, S.C.C., Silva, A.L.D., Galazzi, R.M., Azevedo, R.A., Arruda, M.A.Z., 2015. Nanoparticles applied to plant science: A review. Talanta 131, 693-705.

Asada, K., Foyer, C., Mullineaux, P., 1994. Production and action of active oxygen species in photosynthetic tissues. Causes of photooxidative stress and amelioration of defense systems in plants., 77-104.

Baccouch, S., Chaoui, A., El Ferjani, E., 2001. Nickel toxicity induces oxidative damage in *Zea mays* roots. Journal of Plant Nutrition 24, 1085-1097.

Barrena, R., Casals, E., Colón, J., Font, X., Sánchez, A., Puntes, V., 2009. Evaluation of the ecotoxicity of model nanoparticles. Chemosphere 75, 850-857.

Bartelt-Hunt, S.L., Snow, D.D., Damon, T., Shockley, J., Hoagland, K., 2009. The occurrence of illicit and therapeutic pharmaceuticals in wastewater effluent and surface waters in Nebraska. Environmental Pollution 157, 786-791.

Bartha, B., 2012. Uptake and metabolism of human pharmaceuticals in plants - Identification of metabolites and specification of the defense enzyme systems under pharmaceutical exposure. Technische Universität München.

Bartha, B., Huber, C., Harpaintner, R., Schröder, P., 2010. Effects of acetaminophen in *Brassica juncea* L. Czern.: investigation of uptake, translocation, detoxification, and the induced defense pathways. Environmental Science and Pollution Research 17, 1553-1562.

Basantani, M., Srivastava, A., 2007. Plant glutathione transferases-a decade falls short. Botany 85, 443-456.

Bates, L.S., Waldren, R.P., Teare, I.D., 1973. Rapid determination of free proline for water-stress studies. Plant and Soil 39, 205-207.

Batley, G.E., Kirby, J.K., McLaughlin, M.J., 2012. Fate and risks of nanomaterials in aquatic and terrestrial environments. Accounts of chemical research 46, 854-862.

Bharwana, S., Ali, S., Farooq, M., Iqbal, N., Abbas, F., Ahmad, M., 2013. Alleviation of lead toxicity by silicon is related to elevated photosynthesis, antioxidant enzymes suppressed lead uptake and oxidative stress in cotton. Journal of Bioremediation and Biodegradation 4, 187.

Bhatt, I., Tripathi, B.N., 2011. Interaction of engineered nanoparticles with various components of the environment and possible strategies for their risk assessment. Chemosphere 82, 308-317.

Bhattacharjee, S., 2005. Reactive oxygen species and oxidative burst: roles in stress, senescence and signal. Current Science 89, 1113-1121.

Bielen, A., Remans, T., Vangronsveld, J., Cuypers, A., 2013. The influence of metal stress on the availability and redox state of ascorbate, and possible interference with its cellular functions. International journal of molecular sciences 14, 6382-6413.

Biswas, P., Wu, C.Y., 2005. Nanoparticles and the environment. Journal of the Air and Waste Management Association 55, 708-746.

Björkman, O., Demmig, B., 1987. Photon yield of O2 evolution and chlorophyll fluorescence characteristics at 77 K among vascular plants of diverse origins. Planta 170, 489-504.

Boddu, S.R., Gutti, V.R., Ghosh, T.K., Tompson, R.V., Loyalka, S.K., 2011. Gold, silver, and palladium nanoparticle/nano-agglomerate generation, collection, and characterization. Journal of Nanoparticle Research 13, 6591-6601.

Bouguerra, S., Gavina, A., Ksibi, M., da Graça Rasteiro, M., Rocha-Santos, T., Pereira, R., 2016. Ecotoxicity of titanium silicon oxide (TiSiO4) nanomaterial for terrestrial plants and soil invertebrate species. Ecotoxicology and Environmental Safety 129, 291-301.

Bour, A., Mouchet, F., Silvestre, J., Gauthier, L., Pinelli, E., 2015. Environmentally relevant approaches to assess nanoparticles ecotoxicity: A review. Journal of hazardous materials 283, 764-777.

Bowler, C., Montagu, M.V., Inze, D., 1992. Superoxide dismutase and stress tolerance. Annual review of plant biology 43, 83-116.

Bowler, C., Slooten, L., Vandenbranden, S., De Rycke, R., Botterman, J., Sybesma, C., Van Montagu, M., Inzé, D., 1991. Manganese superoxide dismutase can reduce cellular damage mediated by oxygen radicals in transgenic plants. The EMBO journal 10, 1723-1732.

Bradford, M.M., 1976. Rapid and sensitive method for quantitation of microgram quantities of protein utilizing principle of protein-dye binding. Analytical Biochemistry 72, 248-254.

Brodie, B.B., Axelrod, J., 1948. The fate of acetanilide in man. Journal of Pharmacology and Experimental Therapeutics 94, 29-38.

Brown, P.H., Welch, R.M., Cary, E.E., 1987. Nickel: A micronutrient essential for higher plants. Plant Physiology 85, 801-803.

Chapman, P.M., 2007. Determining when contamination is pollution — Weight of evidence determinations for sediments and effluents. Environment International 33, 492-501.

Chen, C., Huang, D., Liu, J., 2009. Functions and toxicity of nickel in plants: recent advances and future prospects. Clean–soil, air, water 37, 304-313.

Chen, F., Wang, F., Wu, F., Mao, W., Zhang, G., Zhou, M., 2010. Modulation of exogenous glutathione in antioxidant defense system against Cd stress in the two barley genotypes differing in Cd tolerance. Plant Physiology and Biochemistry 48, 663-672.

Cheng, T.S., Hung, M.J., Cheng, Y.I., Cheng, L.J., 2013. Calcium-induced proline accumulation contributes to amelioration of NaCl injury and expression of glutamine synthetase in greater duckweed (*Spirodela polyrhiza* L.). Aquatic Toxicology 144–145, 265-274.

Christou, A., Antoniou, C., Christodoulou, C., Hapeshi, E., Stavrou, I., Michael, C., Fatta-Kassinos, D., Fotopoulos, V., 2016. Stress-related phenomena and detoxification mechanisms induced by common pharmaceuticals in alfalfa (*Medicago sativa* L.) plants. Science of The Total Environment 557, 652-664.

Cia, M., Guimarães, A., Medici, L., Chabregas, S., Azevedo, R., 2012. Antioxidant responses to water deficit by drought-tolerant and-sensitive sugarcane varieties. Annals of Applied Biology 161, 313-324.

Coleman, J., Blake-Kalff, M., Davies, E., 1997. Detoxification of xenobiotics by plants: chemical modification and vacuolar compartmentation. Trends in plant science 2, 144-151.

Consortium, I.B.G.S., 2012. A physical, genetic and functional sequence assembly of the barley genome. Nature 491, 711-716.

Crane, M., Watts, C., Boucard, T., 2006. Chronic aquatic environmental risks from exposure to human pharmaceuticals. Science of the Total Environment 367, 23-41.

Daughton, C.G., Ternes, T.A., 1999. Pharmaceuticals and personal care products in the environment: agents of subtle change? Environmental health perspectives 107, 907-938.

Davidonis, G.H., Hamilton, R.H., Mumma, R.O., 1978. Metabolism of 2, 4-dichlorophenoxyacetic acid in soybean root callus and differentiated soybean root cultures as a function of concentration and tissue age. Plant physiology 62, 80-83.

de Sousa, A., Teixeira, J., Regueiras, M.T., Azenha, M., Silva, F., Fidalgo, F., 2013. Metalaxyl-induced changes in the antioxidant metabolism of *Solanum nigrum* L. suspension cells. Pesticide Biochemistry and Physiology 107, 235-243.

Demidchik, V., 2015. Mechanisms of oxidative stress in plants: From classical chemistry to cell biology. Environmental and Experimental Botany 109, 212-228.

Dimkpa, C.O., McLean, J.E., Latta, D.E., Manangón, E., Britt, D.W., Johnson, W.P., Boyanov, M.I., Anderson, A.J., 2012. CuO and ZnO nanoparticles: phytotoxicity, metal speciation, and induction of oxidative stress in sand-grown wheat. Journal of Nanoparticle Research 14, 1-15.

Dionysiou, D.D., 2004. Environmental applications and implications of nanotechnology and nanomaterials. Journal of Environmental Engineering 130, 723-724.

Dixon, D.P., Skipsey, M., Edwards, R., 2010. Roles for glutathione transferases in plant secondary metabolism. Phytochemistry 71, 338-350.

Donahue, J.L., Okpodu, C.M., Cramer, C.L., Grabau, E.A., Alscher, R.G., 1997. Responses of antioxidants to paraquat in pea leaves (relationships to resistance). Plant physiology 113, 249-257.

Doran, J.W., Zeiss, M.R., 2000. Soil health and sustainability: managing the biotic component of soil quality. Applied Soil Ecology 15, 3-11.

Dourado, M., Franco, M., Peters, L., Martins, P., Souza, L., Piotto, F., Azevedo, R., 2015. Antioxidant enzymes activities of Burkholderia spp. strains—oxidative responses to Ni toxicity. Environmental Science and Pollution Research 22, 19922-19932.

Dubey, D., Pandey, A., 2011. Effect of Nickel (Ni) on chlorophyll, lipid peroxidation and antioxidant enzymes activities in black gram (*Vigna mungo*) leaves. International Journal of Science and Nature 2, 395-401.

Edwards, R., Dixon, D.P., 2005. Plant glutathione transferases. Methods in enzymology 401, 169-186.

Eggen, T., Asp, T.N., Grave, K., Hormazabal, V., 2011. Uptake and translocation of metformin, ciprofloxacin and narasin in forage-and crop plants. Chemosphere 85, 26-33.

Epstein, E., 1999. Silicon. Annual Review of Plant Physiology and Plant Molecular Biology 50, 641-664.

Epstein, E., 2009. Silicon: its manifold roles in plants. Annals of Applied Biology 155, 155-160.

Ermler, U., Grabarse, W., Shima, S., Goubeaud, M., Thauer, R.K., 1998. Active sites of transition-metal enzymes with a focus on nickel. Current opinion in structural biology 8, 749-758.

Eskew, D.L., Welch, R.M., Cary, E.E., 1983. Nickel: an essential micronutrient for legumes and possibly all higher plants. Science 222, 621-623.

Eullaffroy, P., 2013. Phytotoxicology: Contaminant Effects on Markers of Photosynthesis. in: Férard, J.F., Blaise, C. (Eds.). Encyclopedia of Aquatic Ecotoxicology. Springer Netherlands, Dordrecht, pp. 855-864.

European Parliament and the Council, E., 2006. Regulation (EC) No 1907/2006 of the European Parliament and of the Council concerning the Registration, Evaluation, Authorisation and Restriction of Chemicals (REACH), establishing a European Chemicals Agency, amending Directive 1999/45/EC of the European Parliament and of the Council and repealing Council Regulation (EEC) No 793/93 and Commission Regulation (EC) No 1488/94, as well as Council Directive 76/769/EEC and Commission Directives 91/155/EEC, 93/67/EEC, 93/105/EC and 2000/21/EC". Jornal Oficial das Comunidades Europeias L396, 1-526.

Faisal, M., Saquib, Q., Alatar, A.A., Al-Khedhairy, A.A., Hegazy, A.K., Musarrat, J., 2013. Phytotoxic hazards of NiO-nanoparticles in tomato: a study on mechanism of cell death. Journal of hazardous materials 250, 318-332.

FAOSTAT, 2013. Food and Agriculture Organization of the United Nations.

Farooq, M.A., Ali, S., Hameed, A., Ishaque, W., Mahmood, K., Iqbal, Z., 2013. Alleviation of cadmium toxicity by silicon is related to elevated photosynthesis, antioxidant enzymes; suppressed cadmium uptake and oxidative stress in cotton. Ecotoxicology and environmental safety 96, 242-249.

Fent, K., Weston, A.A., Caminada, D., 2006. Ecotoxicology of human pharmaceuticals. Aquatic toxicology 76, 122-159.

Fidalgo, F., Azenha, M., Silva, A.F., de Sousa, A., Santiago, A., Ferraz, P., Teixeira, J., 2013. Copper-induced stress in *Solanum nigrum* L. and antioxidant defense system responses. Food and Energy Security 2, 70-80.

Fidalgo, F., Freitas, R., Ferreira, R., Pessoa, A.M., Teixeira, J., 2011. *Solanum nigrum* L. antioxidant defence system isozymes are regulated transcriptionally and posttranslationally in Cd-induced stress. Environmental and Experimental Botany 72, 312-319.

Foyer, C.H., Noctor, G., 2000. Tansley Review No. 112. Oxygen processing in photosynthesis: regulation and signalling. New phytologist 146, 359-388.

Foyer, C.H., Noctor, G., 2005. Oxidant and antioxidant signalling in plants: a re-evaluation of the concept of oxidative stress in a physiological context. Plant, Cell and Environment 28, 1056-1071.

Frear, D., Swanson, H., 1970. Biosynthesis of S-(4-ethylamino-6-isopropylamino-2-s-triazino) glutathione: Partial purification and properties of a glutathione S-transferase from corn. Phytochemistry 9, 2123-2132.

Furtado, C., Oliveira, R., 2011. Infarmed: Análise da Evolução do Mercado Total de Medicamentos entre 2003-2010.

Gajewska, E., Skłodowska, M., 2007. Effect of nickel on ROS content and antioxidative enzyme activitiesin wheat leaves. BioMetals 20, 27-36.

Gajewska, E., Skłodowska, M., 2008. Differential biochemical responses of wheat shoots and roots to nickel stress: antioxidative reactions and proline accumulation. Plant Growth Regulation 54, 179-188.

Gajewska, E., Słaba, M., Andrzejewska, R., Skłodowska, M., 2006. Nickel-induced inhibition of wheat root growth is related to H_2O_2 production, but not to lipid peroxidation. Plant Growth Regulation 49, 95-103.

Gajewska, E., Wielanek, M., Bergier, K., Skłodowska, M., 2009. Nickel-induced depression of nitrogen assimilation in wheat roots. Acta physiologiae plantarum 31, 1291-1300.

Gavina, A., Antunes, S.C., Pinto, G., Claro, M.T., Santos, C., Gonçalves, F., Pereira, R., 2013. Can physiological endpoints improve the sensitivity of assays with plants in the risk assessment of contaminated soils? PloS one 8, e59748.

Gill, S.S., Khan, N.A., Anjum, N.A., Tuteja, N., 2011. Amelioration of cadmium stress in crop plants by nutrients management: morphological, physiological and biochemical aspects. Plant Stress 5, 1-23.

Gill, S.S., Tuteja, N., 2010. Reactive oxygen species and antioxidant machinery in abiotic stress tolerance in crop plants. Plant Physiology and Biochemistry 48, 909-930.

Gillespie, K.M., Ainsworth, E.A., 2007. Measurement of reduced, oxidized and total ascorbate content in plants. Nature Protocols 2, 871-874.

Glassmeyer, S.T., Hinchey, E.K., Boehme, S.E., Daughton, C.G., Ruhoy, I.S., Conerly, O., Daniels, R.L., Lauer, L., McCarthy, M., Nettesheim, T.G., 2009. Disposal practices for unwanted residential medications in the United States. Environment international 35, 566-572.

Godfrey, L., Bailey, I., Toms, N.J., Clarke, G.D., Kitchen, I., Hourani, S.M., 2007. Paracetamol inhibits nitric oxide synthesis in murine spinal cord slices. European journal of pharmacology 562, 68-71.

Gomes-Junior, R., Moldes, C., Delite, F., Gratão, P., Mazzafera, P., Lea, P., Azevedo, R., 2006. Nickel elicits a fast antioxidant response in *Coffea arabica* cells. Plant Physiology and Biochemistry 44, 420-429.

Gomes, M.P., Le Manac'h, S.G., Moingt, M., Smedbol, E., Paquet, S., Labrecque, M., Lucotte, M., Juneau, P., 2016. Impact of phosphate on glyphosate uptake and toxicity in willow. Journal of hazardous materials 304, 269-279.

Gómez-Sagasti, M.T., Epelde, L., Alkorta, I., Garbisu, C., 2016. Reflections on soil contamination research from a biologists point of view. Applied Soil Ecology 105, 207-210.

Gong, N., Shao, K., Feng, W., Lin, Z., Liang, C., Sun, Y., 2011. Biotoxicity of nickel oxide nanoparticles and bio-remediation by microalgae *Chlorella vulgaris*. Chemosphere 83, 510-516.

González, C.I., Maine, M.A., Cazenave, J., Hadad, H.R., Benavides, M.P., 2015. Ni accumulation and its effects on physiological and biochemical parameters of *Eichhornia crassipes*. Environmental and Experimental Botany 117, 20-27.

Gottschalk, F., Nowack, B., 2011. The release of engineered nanomaterials to the environment. Journal of Environmental Monitoring 13, 1145-1155.

Graham, G.G., Scott, K.F., 2005. Mechanism of Action of Paracetamol. American Journal of Therapeutics 12, 46-55.

Gubbins, E.J., Batty, L.C., Lead, J.R., 2011. Phytotoxicity of silver nanoparticles to *Lemna minor* L. Environmental Pollution 159, 1551-1559.

Gunes, A., Inal, A., Bagci, E., Coban, S., Pilbeam, D., 2007. Silicon mediates changes to some physiological and enzymatic parameters symptomatic for oxidative stress in spinach (*Spinacia oleracea* L.) grown under B toxicity. Scientia Horticulturae 113, 113-119.

Guntzer, F., Keller, C., Meunier, J.-D., 2012. Benefits of plant silicon for crops: a review. Agronomy for Sustainable Development 32, 201-213.

Gupta, D.K., Palma, J.M., Corpas, F.J., 2015. Reactive Oxygen Species and Oxidative Damage in Plants Under Stress. Springer.

Haghighi, M., Pessarakli, M., 2013. Influence of silicon and nano-silicon on salinity tolerance of cherry tomatoes (*Solanum lycopersicum* L.) at early growth stage. Scientia Horticulturae 161, 111-117.

Hajkova, M., Kummerová, M., 2014. Growth response of *Lemna minor* L. to paracetamol. MendelNet, 457-462.

Halliwell, B., 2006. Reactive species and antioxidants. Redox biology is a fundamental theme of aerobic life. Plant physiology 141, 312-322.

Hamid, Z.A., Budin, S.B., Jie, N.W., Hamid, A., Husain, K., Mohamed, J., 2012. Nephroprotective effects of Zingiber zerumbet Smith ethyl acetate extract against paracetamol-induced nephrotoxicity and oxidative stress in rats. Journal of Zhejiang University Science B 13, 176-185.

Handy, R.D., Owen, R., Valsami-Jones, E., 2008. The ecotoxicology of nanoparticles and nanomaterials: current status, knowledge gaps, challenges, and future needs. Ecotoxicology 17, 315-325.

Hansen, S.F., Michelson, E.S., Kamper, A., Borling, P., Stuer-Lauridsen, F., Baun, A., 2008. Categorization framework to aid exposure assessment of nanomaterials in consumer products. Ecotoxicology 17, 438-447.

Hao, L., Chen, L., 2012. Oxidative stress responses in different organs of carp (*Cyprinus carpio*) with exposure to ZnO nanoparticles. Ecotoxicology and Environmental Safety 80, 103-110.

Harasim, P., Filipek, T., 2015. Nickel in the environment. Journal of Elementology 20, 525-534.

Hayat, S., Hayat, Q., Alyemeni, M.N., Wani, A.S., Pichtel, J., Ahmad, A., 2012. Role of proline under changing environments: a review. Plant signaling and behavior 7, 1456-1466.

Heath, R.L., Packer, L., 1968. Photoperoxidation in isolated chloroplasts. I. Kinetics and stoichiometry of fatty acid peroxidation. Archives of biochemistry and biophysics 125, 189-198.

Helland, A., Wick, P., Koehler, A., Schmid, K., Som, C., 2008. Reviewing the environmental and human health knowledge base of carbon nanotubes. Ciência and Saúde Coletiva 13, 441-452.

Herklotz, P.A., Gurung, P., Heuvel, B.V., Kinney, C.A., 2010. Uptake of human pharmaceuticals by plants grown under hydroponic conditions. Chemosphere 78, 1416-1421.

Hirai, M., Kawai-hirai, R., Hirai, T., Ueki, T., 1993. Structural change of jack bean urease induced by addition surfactants studied with synchrotron-radiation small-angle X-ray scattering. European journal of biochemistry 215, 55-61.

Horie, M., Fukui, H., Nishio, K., Endoh, S., Kato, H., Fujita, K., Miyauchi, A., Nakamura, A., Shichiri, M., Ishida, N., 2011. Evaluation of acute oxidative stress induced by NiO nanoparticles in vivo and in vitro. Journal of occupational health 53, 64-74.

Hossain, M.A., Nakano, Y., Asada, K., 1984. Monodehydroascorbate reductase in spinach chloroplasts and its participation in regeneration of ascorbate for scavenging hydrogen peroxide. Plant and Cell Physiology 25, 385-395.

Huber, C., Bartha, B., Harpaintner, R., Schröder, P., 2009. Metabolism of acetaminophen (paracetamol) in plants—two independent pathways result in the formation of a glutathione and a glucose conjugate. Environmental Science and Pollution Research 16, 206-213.

Hussain, M.B., Ali, S., Azam, A., Hina, S., Ahsan, M., Farooq, B.A., Bharwana, S.A., Gill, M.B., 2013. Morphological, physiological and biochemical responses of plants to nickel stress: a review. African Journal of Agricultural Research 8(17), 1596-1602.

Hutter, E., Boridy, S., Labrecque, S., Lalancette-Hébert, M., Kriz, J., Winnik, F.M., Maysinger, D., 2010. Microglial response to gold nanoparticles. ACS nano 4, 2595-2606.

ISO, 2005. Soil quality — Determination of pH. ISO—The International Organization for Standardization, Geneva, Switzerland. ISO 10390:2005.

ISO, 2012. ISO Guideline 11269-2: Soil Quality - Determination of the Effects of Pollutants on Soil Flora - Part 2: Effects of Contaminated Soil on the Emergence and Early Growth of Higher Plants. International Organization for Standardization, Geneve, Switzerland.

Ispas, C., Andreescu, D., Patel, A., Goia, D.V., Andreescu, S., Wallace, K.N., 2009. Toxicity and developmental defects of different sizes and shape nickel nanoparticles in zebrafish. Environmental science and technology 43, 6349-6356.

Jana, S., Choudhuri, M.A., 1982. Glycolate metabolism of three submersed aquatic angiosperms during ageing. Aquatic Botany 12, 345-354.

Jiang, L., Yang, H., 2009. Prometryne-induced oxidative stress and impact on antioxidant enzymes in wheat. Ecotoxicology and environmental safety 72, 1687-1693.

Jiménez, A., Hernández, J.A., Pastori, G., del Río, L.A., Sevilla, F., 1998. Role of the ascorbate-glutathione cycle of mitochondria and peroxisomes in the senescence of pea leaves. Plant physiology 118, 1327-1335.

Kaiser, W.M., Brendle-Behnisch, E., 1991. Rapid modulation of spinach leaf nitrate reductase activity by photosynthesis I. Modulation in vivo by CO_2 availability. Plant Physiology 96, 363-367.

Kanematsu, S., Asada, K., 1989. CuZn-superoxide dismutases in rice: occurrence of an active, monomeric enzyme and two types of isozyme in leaf and non-photosynthetic tissues. Plant and cell physiology 30, 381-391.

Kang, G.S., Gillespie, P.A., Gunnison, A., Moreira, A.L., Tchou-Wong, K.M., Chen, L.C., 2011. Long-term inhalation exposure to nickel nanoparticles exacerbated atherosclerosis in a susceptible mouse model. Environmental health perspectives 119, 176-181.

Kapanen, A., Itävaara, M., 2001. Ecotoxicity tests for compost applications. Ecotoxicology and environmental safety 49, 1-16.

Katerji, N., Van Hoorn, J., Hamdy, A., Mastrorilli, M., Fares, C., Ceccarelli, S., Grando, S., Oweis, T., 2006. Classification and salt tolerance analysis of barley varieties. Agricultural water management 85, 184-192.

Kazemi, N., Khavari-Nejad, R.A., Fahimi, H., Saadatmand, S., Nejad-Sattari, T., 2010. Effects of exogenous salicylic acid and nitric oxide on lipid peroxidation and antioxidant enzyme activities in leaves of Brassica napus L. under nickel stress. Scientia Horticulturae 126, 402-407.

Khaliq, A., Ali, S., Hameed, A., Farooq, M.A., Farid, M., Shakoor, M.B., Mahmood, K., Ishaque, W., Rizwan, M., 2016. Silicon alleviates nickel toxicity in cotton seedlings through

enhancing growth, photosynthesis, and suppressing Ni uptake and oxidative stress. Archives of Agronomy and Soil Science 62, 633-647.

Khalvati, M., Bartha, B., Dupigny, A., Schröder, P., 2010. Arbuscular mycorrhizal association is beneficial for growth and detoxification of xenobiotics of barley under drought stress. Journal of Soils and Sediments 10, 54-64.

Khoshgoftarmanesh, A., Bahmanziari, H., Sanaeiostovar, A., 2014. Responses of cucumber to deficient and toxic amounts of nickel in nutrient solution containing urea as nitrogen source. Biologia plantarum 58, 524-530.

Khot, L.R., Sankaran, S., Maja, J.M., Ehsani, R., Schuster, E.W., 2012. Applications of nanomaterials in agricultural production and crop protection: A review. Crop Protection 35, 64-70.

Kinney, C.A., Furlong, E.T., Zaugg, S.D., Burkhardt, M.R., Werner, S.L., Cahill, J.D., Jorgensen, G.R., 2006. Survey of organic wastewater contaminants in biosolids destined for land application. Environmental science and technology 40, 7207-7215.

Klaine, S.J., Alvarez, P.J., Batley, G.E., Fernandes, T.F., Handy, R.D., Lyon, D.Y., Mahendra, S., McLaughlin, M.J., Lead, J.R., 2008. Nanomaterials in the environment: behavior, fate, bioavailability, and effects. Environmental Toxicology and Chemistry 27, 1825-1851.

Kreuzig, R., Kullmer, C., Matthies, B., Plaga, B., Dieckmann, H., Höltge, S., 2005. Verhalten von in der Umwelt vorkommenden Pharmaka und ihren Metaboliten in Modelltestsystemen" Modellsystem Boden. UBA Texte 11.

Krupenikov, I.A., Boincean, B.P., Dent, D., 2011. The Black Earth: Ecological Principles for Sustainable Agriculture on Chernozem Soils. Springer Netherlands.

Kumar, K., Gupta, S., Baidoo, S., Chander, Y., Rosen, C., 2005. Antibiotic uptake by plants from soil fertilized with animal manure. Journal of Environmental Quality 34, 2082-2085.

Kummerová, M., Zezulka, Š., Babula, P., Tříska, J., 2016. Possible ecological risk of two pharmaceuticals diclofenac and paracetamol demonstrated on a model plant Lemna minor. Journal of hazardous materials 302, 351-361.

Küpper, H., Küpper, F., Spiller, M., 1996. Environmental relevance of heavy metal-substituted chlorophylls using the example of water plants. Journal of Experimental Botany 47, 259-266.

Kurepa, J., Van Montagu, M., Inzé, D., 1997. Expression of sodCp and sodB genes in Nicotiana tabacum: effects of light and copper excess. Journal of experimental botany 48, 2007-2014.

Kurwadkar, S., Pugh, K., Gupta, A., Ingole, S., 2014. Nanoparticles in the Environment: Occurrence, Distribution, and Risks. Journal of Hazardous, Toxic, and Radioactive Waste 19 (3).

Li, J., Ye, Q., Gan, J., 2014. Degradation and transformation products of acetaminophen in soil. Water Research 49, 44-52.

Liang, Y., Sun, W., Zhu, Y.-G., Christie, P., 2007. Mechanisms of silicon-mediated alleviation of abiotic stresses in higher plants: A review. Environmental Pollution 147, 422-428.

Lichtenthaler, H.K., 1987. Chlorophylls and carotenoids - pigments of photosynthetic biomembranes. Methods in Enzymology 148, 350-382.

Lienert, J., Güdel, K., Escher, B.I., 2007. Screening method for ecotoxicological hazard assessment of 42 pharmaceuticals considering human metabolism and excretory routes. Environmental science and technology 41, 4471-4478.

Lin, Y., Kao, C., 2007. Proline accumulation induced by excess nickel in detached rice leaves. Biologia plantarum 51, 351-354.

Liu, J., Cai, H., Mei, C., Wang, M., 2015. Effects of nano-silicon and common silicon on lead uptake and translocation in two rice cultivars. Frontiers of Environmental Science and Engineering 9(5), 1-7.

Liu, J., Zhang, H., Zhang, Y., Chai, T., 2013. Silicon attenuates cadmium toxicity in Solanum nigrum L. by reducing cadmium uptake and oxidative stress. Plant Physiology and Biochemistry 68, 1-7.

Livak, K.J., Schmittgen, T.D., 2001. Analysis of relative gene expression data using real-time quantitative PCR and the $2^{-\Delta\Delta CT}$ method. Methods 25, 402-408.

Ludwig, D.F., Iannuzzi, T.J., 2005. Incremental ecological exposure risks from contaminated sediments in an urban estuarine river. Integrated environmental assessment and management 1, 374-390.

Ma, X., Geiser-Lee, J., Deng, Y., Kolmakov, A., 2010. Interactions between engineered nanoparticles (ENPs) and plants: Phytotoxicity, uptake and accumulation. Science of The Total Environment 408, 3053-3061.

Madhava Rao, K.V., Sresty, T.V.S., 2000. Antioxidative parameters in the seedlings of pigeonpea (*Cajanus cajan* (L.) Millspaugh) in response to Zn and Ni stresses. Plant Science 157, 113-128.

Maheshwari, R., Dubey, R., 2009a. Nickel-induced oxidative stress and the role of antioxidant defence in rice seedlings. Plant Growth Regulation 59, 37-49.

Maheshwari, R., Dubey, R.S., 2009b. Nickel-induced oxidative stress and the role of antioxidant defence in rice seedlings. Plant Growth Regulation 59, 37-49.

Marschner, H., 2011. Marschner's mineral nutrition of higher plants. Academic press.

McGill, M.R., Williams, C.D., Xie, Y., Ramachandran, A., Jaeschke, H., 2012. Acetaminophen-induced liver injury in rats and mice: comparison of protein adducts, mitochondrial dysfunction, and oxidative stress in the mechanism of toxicity. Toxicology and applied pharmacology 264, 387-394.

McGonigle, B., Keeler, S.J., Lau, S.-M.C., Koeppe, M.K., O'Keefe, D.P., 2000. A genomics approach to the comprehensive analysis of the glutathione S-transferase gene family in soybean and maize. Plant Physiology 124, 1105-1120.

Meyer, Y., Siala, W., Bashandy, T., Riondet, C., Vignols, F., Reichheld, J.P., 2008. Glutaredoxins and thioredoxins in plants. Biochimica et Biophysica Acta (BBA)-Molecular Cell Research 1783, 589-600.

Miralles, P., Church, T.L., Harris, A.T., 2012. Toxicity, Uptake, and Translocation of Engineered Nanomaterials in Vascular plants. Environmental Science & Technology 46, 9224-9239.

Mittler, R., 2002. Oxidative stress, antioxidants and stress tolerance. Trends in plant science 7, 405-410.

Mittler, R., Zilinskas, B., 1992. Molecular cloning and characterization of a gene encoding pea cytosolic ascorbate peroxidase. Journal of Biological Chemistry 267, 21802-21807.

Moldes, C.A., Medici, L.O., Abrahao, O.S., Tsai, S.M., Azevedo, R.A., 2008. Biochemical responses of glyphosate resistant and susceptible soybean plants exposed to glyphosate. Acta Physiologiae Plantarum 30, 469-479.

Monica, R.C., Cremonini, R., 2009. Nanoparticles and higher plants. Caryologia 62, 161-165.

Morse, H., 1878. Ueber eine neue Darstellungsmethode der Acetylamidophenole. Berichte der deutschen chemischen Gesellschaft 11, 232-233.

Mousavi, S.R., Rezaei, M., 2011. Nanotechnology in agriculture and food production. Journal of Applied Environmental and Biological Sciences 1, 414-419.

Moussa, H.R., 2006. Influence of exogenous application of silicon on physiological response of salt-stressed maize (*Zea mays* L.). International Journal of Agriculture and Biology 8, 293-297.

Mu, Y., Jia, D., He, Y., Miao, Y., Wu, H.-L., 2011. Nano nickel oxide modified non-enzymatic glucose sensors with enhanced sensitivity through an electrochemical process strategy at high potential. Biosensors and Bioelectronics 26, 2948-2952.

Mueller, N.C., Nowack, B., 2008. Exposure modeling of engineered nanoparticles in the environment. Environmental science and technology 42, 4447-4453.

Murchie, E.H., Lawson, T., 2013. Chlorophyll fluorescence analysis: a guide to good practice and understanding some new applications. Journal of experimental botany 64(13), 3983-3998.

Nakano, Y., Asada, K., 1981. Hydrogen-peroxide is scavenged by ascorbate-specific peroxidase in spinach-chloroplasts. Plant and Cell Physiology 22, 867-880.

Nedelkoska, T.V., Doran, P.M., 2001. Hyperaccumulation of Nickel by Hairy Roots of AlyssumSpecies: Comparison with Whole Regenerated Plants. Biotechnology progress 17, 752-759.

Neumann, P.M., Chamel, A., 1986. Comparative phloem mobility of nickel in nonsenescent plants. Plant physiology 81, 689-691.

Nieboer, E., Nriagu, J.O., 1992. Nickel and human health. International Conference on Nickel Metabolism and Toxicology 1988: Espoo, Finland). Wiley.

Noctor, G., Gomez, L., Vanacker, H., Foyer, C.H., 2002. Interactions between biosynthesis, compartmentation and transport in the control of glutathione homeostasis and signalling. Journal of experimental botany 53, 1283-1304.

Nogueira, V., Lopes, I., Rocha-Santos, T., Rasteiro, M., Abrantes, N., Gonçalves, F., Soares, A., Duarte, A., Pereira, R., 2015. Assessing the ecotoxicity of metal nano-oxides with potential for wastewater treatment. Environmental Science and Pollution Research 22, 1-13.

Nowack, B., Bucheli, T.D., 2007. Occurrence, behavior and effects of nanoparticles in the environment. Environmental pollution 150, 5-22.

Nowack, B., Ranville, J.F., Diamond, S., Gallego-Urrea, J.A., Metcalfe, C., Rose, J., Horne, N., Koelmans, A.A., Klaine, S.J., 2012. Potential scenarios for nanomaterial release and subsequent alteration in the environment. Environmental Toxicology and Chemistry 31, 50-59.

Nunes, B., Carvalho, F., Guilhermino, L., 2006. Effects of widely used pharmaceuticals and a detergent on oxidative stress biomarkers of the crustacean Artemia parthenogenetica. Chemosphere 62, 581-594.

Nunes, B., Gaio, A., Carvalho, F., Guilhermino, L., 2008. Behaviour and biomarkers of oxidative stress in Gambusia holbrooki after acute exposure to widely used pharmaceuticals and a detergent. Ecotoxicology and environmental safety 71, 341-354.

Nunes, B., Pinto, G., Martins, L., Gonçalves, F., Antunes, S.C., 2014. Biochemical and standard toxic effects of acetaminophen on the macrophyte species Lemna minor and Lemna gibba. Environmental Science and Pollution Research 21, 10815-10822.

OECD, 2006. Test No. 208: Terrestrial Plant Test: Seedling Emergence and Seedling Growth Test. OECD Publishing.

Olaniran, A.O., Balgobind, A., Pillay, B., 2013. Bioavailability of heavy metals in soil: impact on microbial biodegradation of organic compounds and possible improvement strategies. International journal of molecular sciences 14, 10197-10228.

Panagos, P., Van Liedekerke, M., Yigini, Y., Montanarella, L., 2013. Contaminated Sites in Europe: Review of the Current Situation Based on Data Collected through a European Network. Journal of Environmental and Public Health 158764.

Panda, K.K., Achary, V.M.M., Krishnaveni, R., Padhi, B.K., Sarangi, S.N., Sahu, S.N., Panda, B.B., 2011. In vitro biosynthesis and genotoxicity bioassay of silver nanoparticles using plants. Toxicology *in Vitro* 25, 1097-1105.

Pandolfini, C., Bonati, M., 2005. A literature review on off-label drug use in children. European journal of pediatrics 164, 552-558.

Parween, T., Jan, S., Fatma, T., 2011. Alteration in nitrogen metabolism and plant growth during different developmental stages of green gram (*Vigna radiata* L.) in response to chlorpyrifos. Acta Physiologiae Plantarum 33, 2321-2328.

Patlolla, A.K., Hackett, D., Tchounwou, P.B., 2014. Silver nanoparticle-induced oxidative stress-dependent toxicity in Sprague-Dawley rats. Molecular and Cellular Biochemistry 399, 257-268.

Polacco, J.C., Mazzafera, P., Tezotto, T., 2013. Opinion–Nickel and urease in plants: still many knowledge gaps. Plant science 199, 79-90.

Queirós, F., 2012. Tolerância à salinidade em linha celular de *Solanum tuberosum* L. – estudo bioquímico, proteómico e ultraestrutural. University of Porto, Porto.

Rani, J.D.V., Kamatchi, S., Dhathathreyan, A., 2010. Nanoparticles of nickel oxide and nickel hydroxide using lyophilisomes of fibrinogen as template. Journal of colloid and interface science 341, 48-52.

Raskin, I., Ensley, B.D., 2000. Phytoremediation of toxic metals. John Wiley and Sons.

Rauscher, H., Roebben, G., Amenta, V., Boix, S., Calzolai, L., Emons, H., Gaillard, C., Gibson, P., Linsinger, T., Mech, A., 2014. Towards a review of the EC Recommendation for a definition of the term “nanomaterial”. Eur Union. doi 10, 36237.

Rauser, W.E., 1999. Structure and function of metal chelators produced by plants. Cell biochemistry and biophysics 31, 19-48.

Reeves, R., 1992. The hyperaccumulation of nickel by serpentine plants. The vegetation of ultramafic (serpentine) soils, 253-277.

Reeves, R.D., Baker, A.J., 2000. Metal-accumulating plants. Phytoremediation of toxic metals: using plants to clean up the environment. Wiley, New York, 193-229.

Rizwan, M., Ali, S., Ibrahim, M., Farid, M., Adrees, M., Bharwana, S.A., Zia-ur-Rehman, M., Qayyum, M.F., Abbas, F., 2015. Mechanisms of silicon-mediated alleviation of drought and salt stress in plants: a review. Environmental Science and Pollution Research 22, 15416-15431.

Roco, M.C., 2003. Nanotechnology: convergence with modern biology and medicine. Current opinion in biotechnology 14, 337-346.

Romero-Puertas, M.C., Corpas, F.J., Rodríguez-Serrano, M., Gómez, M., del Río, L.A., Sandalio, L.M., 2007. Differential expression and regulation of antioxidative enzymes by cadmium in pea plants. Journal of Plant Physiology 164, 1346-1357.

Romero-Puertas, M.C., Rodríguez-Serrano, M., Corpas, F.J., Gómez, M., Del Río, L.A., Sandalio, L.M., 2004. Cadmium-induced subcellular accumulation of $O_2^{\cdot-}$ and H_2O_2 in pea leaves. Plant, Cell and Environment 27, 1122-1134.

Salt, D.E., Smith, R., Raskin, I., 1998. Phytoremediation. Annual review of plant biology 49, 643-668.

Sandermann, H., 1992. Plant metabolism of xenobiotics. Trends in biochemical sciences 17, 82-84.

Sandermann Jr, H., 1994. Higher plant metabolism of xenobiotics: the'green liver'concept. Pharmacogenetics and Genomics 4, 225-241.

Scandalios, J.G., 1993. Oxygen stress and superoxide dismutases. Plant physiology 101, 7-12.

Scandalios, J.G., 1997. Oxidative stress and the molecular biology of antioxidant defenses. Cold Spring Harbor Laboratory Press.

Schnabl, H., Roth, U., Friebe, A., 2001. Brassinosteroid-induced stress tolerances of plants. Recent research developments in phytochemistry 5, 169-183.

Schuler, M.A., Werck-Reichhart, D., 2003. Functional genomics of P450s. Annual Review of Plant Biology 54, 629-667.

Seregin, I., Kozhevnikova, A., 2005. Distribution of cadmium, lead, nickel, and strontium in imbibing maize caryopses. Russian Journal of Plant Physiology 52, 565-569.

Seregin, I., Kozhevnikova, A., 2006. Physiological role of nickel and its toxic effects on higher plants. Russian Journal of Plant Physiology 53, 257-277.

Shagimardanova, E.I., Gusev, O.A., Sychev, V.N., Levinskikh, M.A., Sharipova, M.R., Il'inskaya, O.N., Bingham, G., Sugimoto, M., 2010. Expression of stress response genes in barley *Hordeum vulgare* in a spaceflight environment. Molecular Biology 44, 734-740.

Shapiro, B.M., Stadtman, E., 1970. [130] Glutamine synthetase (*Escherichia coli*). Methods in enzymology 17, 910-922.

Sharma, P., Jha, A.B., Dubey, R.S., Pessarakli, M., 2012. Reactive Oxygen Species, Oxidative Damage, and Antioxidative Defense Mechanism in Plants under Stressful Conditions. Journal of Botany, 26 pages.

Shaw, A.K., Ghosh, S., Kalaji, H.M., Bosa, K., Brestic, M., Zivcak, M., Hossain, Z., 2014. Nano-CuO stress induced modulation of antioxidative defense and photosynthetic performance

of Syrian barley (*Hordeum vulgare* L.). Environmental and Experimental Botany 102, 37-47.

Shimabukuro, R., 1976. Glutathione conjugation of herbicides in plants and animals and its role in herbicide selectivity. The Asian-Pacific Weed Science Society, 183-186.

Siddiqui, M.H., Al-Whaibi, M.H., 2014. Role of nano-SiO 2 in germination of tomato (*Lycopersicum esculentum* seeds Mill.). Saudi journal of biological sciences 21, 13-17.

Singh, K., Pandey, S.N., 2011. Effect of nickel-stresses on uptake, pigments and antioxidative responses of water lettuce, *Pistia stratiotes* L. Journal of Environmental Biology 32, 391-394.

Smirnoff, N., 2008. Antioxidants and reactive oxygen species in plants. John Wiley and Sons.

Soares, C., de Sousa, A., Pinto, A., Azenha, M., Teixeira, J., Azevedo, R.A., Fidalgo, F., 2016. Effect of 24-epibrassinolide on ROS content, antioxidant system, lipid peroxidation and Ni uptake in *Solanum nigrum* L. under Ni stress. Environmental and Experimental Botany 122, 115-125.

Song, N.H., Yin, X.L., Chen, G.F., Yang, H., 2007. Biological responses of wheat (*Triticum aestivum*) plants to the herbicide chlorotoluron in soils. Chemosphere 68, 1779-1787.

Sun, T.Y., Gottschalk, F., Hungerbühler, K., Nowack, B., 2014. Comprehensive probabilistic modelling of environmental emissions of engineered nanomaterials. Environmental Pollution 185, 69-76.

Sunderman, F., Oskarsson, H., 1991. Nickel. Metals and their compounds in the environment. Merian ed. VCH Weinheim.

Szabados, L., Savoure, A., 2010. Proline: a multifunctional amino acid. Trends in plant science 15, 89-97.

Taiz, L., Zeiger, E., Moller, I.M., Murphy, A., 2015. Plant Physiology and Development, Sixth ed. Sinauer Associates, Inc., Sunderland, U.S.A.

Teixeira, J., de Sousa, A., Azenha, M., Moreira, J.T., Fidalgo, F., Silva, A.F., Faria, J.L., Silva, A.M., 2011. *Solanum nigrum* L. weed plants as a remediation tool for metalaxyl-polluted effluents and soils. Chemosphere 85, 744-750.

Temple, M.D., Perrone, G.G., Dawes, I.W., 2005. Complex cellular responses to reactive oxygen species. Trends in cell biology 15, 319-326.

Thomé, A., Reddy, K.R., Reginatto, C., Cecchin, I., 2015. Review of Nanotechnology for Soil and Groundwater Remediation: Brazilian Perspectives. Water, Air, and Soil Pollution 226, 1-20.

Tiyagi, S.A., Ajaz, S., Azam, M., 2004. Effect of some pesticides on plant growth, root nodulation and chlorophyll content of chickpea. Archives of Agronomy and Soil Science 50, 529-533.

Tratnyek, P.G., Johnson, R.L., 2006. Nanotechnologies for environmental cleanup. Nano today 1, 44-48.

Tripathi, D.K., Singh, V.P., Prasad, S.M., Chauhan, D.K., Dubey, N.K., 2015. Silicon nanoparticles (SiNp) alleviate chromium (VI) phytotoxicity in *Pisum sativum* (L.) seedlings. Plant Physiology and Biochemistry 96, 189-198.

Ushimaru, T., Maki, Y., Sano, S., Koshiba, K., Asada, K., Tsuji, H., 1997. Induction of enzymes involved in the ascorbate-dependent antioxidative system, namely, ascorbate

peroxidase, monodehydroascorbate reductase and dehydroascorbate reductase, after exposure to air of rice (*Oryza sativa*) seedlings germinated under water. Plant and Cell Physiology 38, 541-549.

Ushimaru, T., Nakagawa, T., Fujioka, Y., Daicho, K., Naito, M., Yamauchi, Y., Nonaka, H., Amako, K., Yamawaki, K., Murata, N., 2006. Transgenic Arabidopsis plants expressing the rice dehydroascorbate reductase gene are resistant to salt stress. Journal of plant physiology 163, 1179-1184.

van der Perk, M., 2013. Soil and Water Contamination, 2nd Edition. Taylor and Francis.

Venkateswara Rao, K., Sunandana, C., 2008. Effect of fuel to oxidizer ratio on the structure, micro structure and EPR of combustion synthesized NiO nanoparticles. Journal of nanoscience and nanotechnology 8, 4247-4253.

Von Mering, J., 1893. Beitrage zur Kenntniss der antipyretica. Ther Monatsch 7, 577-587.

Wang, S., Wang, F., Gao, S., 2015. Foliar application with nano-silicon alleviates Cd toxicity in rice seedlings. Environmental Science and Pollution Research 22, 2837-2845.

Whatmore, R.W., 2006. Nanotechnology—what is it? Should we be worried? Occupational Medicine 56, 295-299.

Wiesner, M.R., Lowry, G.V., Alvarez, P., Dionysiou, D., Biswas, P., 2006. Assessing the risks of manufactured nanomaterials. Environmental science and technology 40, 4336-4345.

Wu, S., Zhang, L., Chen, J., 2012. Paracetamol in the environment and its degradation by microorganisms. Applied microbiology and biotechnology 96, 875-884.

Xie, Y., McGill, M.R., Dorko, K., Kumer, S.C., Schmitt, T.M., Forster, J., Jaeschke, H., 2014. Mechanisms of acetaminophen-induced cell death in primary human hepatocytes. Toxicology and applied pharmacology 279, 266-274.

Yildiztekin, M., Kaya, C., Tuna, A.L., Ashraf, M., 2015. Oxidative stress and antioxidative mechanisms in tomato (*Solanum lycopersicum* L.) plants sprayed with different pesticides. Pakistan Journal of Botany 42, 717-721.

You, J., Chan, Z., 2015. ROS Regulation During Abiotic Stress Responses in Crop Plants. Frontiers in Plant Science 6.

Yusuf, M., Fariduddin, Q., Hayat, S., Ahmad, A., 2011. Nickel: an overview of uptake, essentiality and toxicity in plants. Bulletin of environmental contamination and toxicology 86, 1-17.

Zagorchev, L., Seal, C.E., Kranner, I., Odjakova, M., 2013. A central role for thiols in plant tolerance to abiotic stress. International journal of molecular sciences 14, 7405-7432.

Zhang, H., Lian, C., Shen, Z., 2009. Proteomic identification of small, copper-responsive proteins in germinating embryos of *Oryza sativa*. Annals of botany 103, 923-930.

Zhar, J., 1996. Biostatistical analysis. 3rd Edition. Prentice-Hall International Inc., New Jersey.

Zhu, H., Han, J., Xiao, J.Q., Jin, Y., 2008. Uptake, translocation, and accumulation of manufactured iron oxide nanoparticles by pumpkin plants. Journal of Environmental Monitoring 10, 713-717.

8. ANNEX

Annex I

I. Ecotoxicity of Nano-NiO and AC to barley plants

Table 1. *Summary of ANOVA statistical data obtained for barley plants exposed to increased concentrations of nano-NiO and AC.*

	Parameter	nano-NiO	AC
Root lenght	**Seed germination**	F (7, 16) = 1.524; *p*> 0.05	F (7, 16 = 0.2845; *p*> 0.05
	Petri Plate	F (7, 131) = 58.38; *p*< 0.001	F (7, 147) = 76.14; *p*< 0.001
	OECD soil	F (7, 23) = 82.4; *p*< 0.001	F (7, 23) = 7.518; *p*< 0.001
	Roots fresh weight	F (7, 24) = 34.33; *p*< 0.001	F (7, 19) = 12.08; *p*< 0.001
	Roots dry weight	F (7, 20) = 7.958; *p*< 0.001	F (7, 21) = 6.341; *p*< 0.001
	Leaves fresh weight	F (7, 24) = 59.44; *p*< 0.001	F (7, 24) = 18.13; *p*< 0.001
	Leaves dry weight	F (7, 24) = 44.94; *p*< 0.001	F (7, 22) = 14.32; *p*< 0.001
	Chlorophylls	F (7, 20) = 13.55; *p*< 0.001	F (7, 18) = 2.268; *p*> 0.05
	Carotenoids	F (7, 19) = 15.58; *p*< 0.001	F (7, 19) = 3.646; *p*> 0.05
	LP	F (7, 18) = 7.576; *p*< 0.001	F (7, 20) = 17.16; *p*< 0.001
	O2.-	F (7, 20) = 58.64; *p*< 0.001	F (7, 26) = 8.898; *p*< 0.001
	H2O2	F (7, 23) = 3.337; *p*< 0.001	F (7, 21) = 2.029; *p*> 0.05
	O2.-/H2O2	F (7, 16) = 42.00; *p*< 0.001	F (7, 20) = 8.041; *p*< 0.001
	Cell death	F (7, 24) = 7.016; *p*< 0.001	F (7, 19) = 16.28; *p*< 0.001

II. Effects of nano-SiO_2 on the tolerance of barley under nano-NiO and AC stress

Table 2. *Summary of ANOVA statistical data obtained for barley plants cultivated for 14 days in OECD soil in the presence and absence of four concentrations of nano-SiO2 under single or co-exposure with 120 mg kg^{-1} nano-NiO and 400 mg kg^{-1} AC.*

Parameter	nano-SiO_2	nano-NiO	AC
Root lenght	F (4, 14) = 0.4674; *p*> 0.05	F (5, 19) = 3.908; *p*< 0.05	F (5,20) = 0.8075; *p*> 0.05
Roots fresh weight	F (4, 16) = 2.335; *p*> 0.05	F (5, 19) = 8.224; *p*< 0.001	F (5, 19) = 7.697; *p*< 0.001
Roots dry weight	F (4, 17) = 1.302; *p*> 0.05	F (5, 21) = 7.163; *p*< 0.001	F (5,21) = 4.337; *p*< 0.05
Leaves fresh weight	F (4, 16) = 7.212; *p*< 0.05	F (5,20) = 24.58; *p*< 0.001	F (4, 18) = 9.976; *p*< 0.001
Leaves dry weight	F (4, 17) = 0.4868; *p*> 0.05	F (5,22) = 7.873; *p*< 0.001	F (5,20) = 4.099 *p*< 0.05

Table 3. *Summary of ANOVA statistical data obtained for leaves of barley plants cultivated for 14 days in OECD soil.*

Parameter	nano-NiO	AC
Fresh weight	F (3, 14) = 37,37; $p < 0.001$	F (3, 13) = 20,56; $p < 0.001$
Dry weight	F (3, 16) = 9,309; $p < 0.001$	F (3, 16) = 6,142; $p < 0.05$
Ni content	F (2, 6) = 152,6; $p < 0.001$	-
Chlorophylls	F (3, 12) = 6,778; $p < 0.05$	F (3, 12) = 1,336; $p > 0.05$
Carotenoids	F (3, 11) = 0,2746; $p > 0.05$	F (3, 12) = 0,7637; $p > 0.05$
F_v/F_m	F (3, 34) = 9,921; $p < 0.001$	F (3, 33) = 1,949; $p > 0.05$
ETR	F (3, 17) = 12,74; $p < 0.001$	F (3, 19) = 4,004; $p > 0.05$
Φ PSII	F (3, 17) = 13,66; $p < 0.001$	F (3, 17) = 11,62; $p < 0.001$
GS	F (3, 28) = 15,29; $p < 0.001$	F (3, 28) = 59,59; $p < 0.001$
NR	F (3, 9) = 83,97; $p < 0.001$	F (3, 9) = 7,232; $p < 0.05$
LP	F (3, 10) = 7,271; $p < 0.05$	F (3, 11) = 0,9030; $p > 0.05$
Total thiols	F (3, 8) = 16,04; $p < 0.05$	F (3, 8) = 4,871; $p < 0.05$
protein thiols	F (3, 8) = 12,89; $p < 0.05$	F (3, 8) = 4,177; $p > 0.05$
$O_2^{\cdot-}$	F (3, 12) = 55,24; $p < 0.001$	F (3, 11) = 40,35; $p < 0.001$
H_2O_2	F (3, 11) = 6,008; $p < 0.05$	F (3, 11) = 0,6797; $p > 0.05$
Pro	F (3, 11) = 23,98; $p < 0.001$	F (3, 10) = 6,615; $p < 0.05$
Total ascorbate	F (3, 16) = 2,446; $p > 0.05$	F (3, 16) = 4,043; $p < 0.05$
AsA/Total ascorbate	F (3, 18) = 1,761; $p > 0.05$	F (3, 19) = 2,063; $p > 0.05$
DHA/Total ascorbate	F (3, 12) = 20,52; $p < 0.001$	F (3, 12) = 4,328; $p < 0.05$
Total protein	F (3, 23) = 14,77; $p < 0.001$	F (3, 11) = 17,57; $p < 0.001$
SOD	F (3, 8) = 5,221; $p < 0.05$	F (3, 8) = 29,60; $p < 0.001$
CAT	F (3, 10) = 24,00; $p < 0.001$	F (3, 8) = 13,83; $p < 0.05$
APX	F (3, 8) = 6,579; $p < 0.05$	F (3, 8) = 1,279; $p > 0.05$

Table 4. *Summary of ANOVA statistical data obtained for roots of barley plants cultivated for 14 days in OECD soil.*

Parameter	nano-NiO	AC
Root lenght	F (3, 12) = 1.872; $p > 0.05$	F (3, 13) = 0.2370; $p > 0.05$
Fresh weight	F (3, 12) = 13.91; $p < 0.001$	F (3, 13) = 7,477; $p < 0.001$
Dry weight	F (3, 13) = 21,48; $p < 0.001$	F (3, 13) = 14,96; $p < 0.001$
Ni content	F (2, 6) = 8534; $p < 0.001$	-
GS	F (3, 39) = 55,62; $p < 0.001$	F (3, 38) = 2,577; $p > 0.05$
NR	F (3, 9) = 31,74; $p < 0.001$	F (3, 8) = 111,4; $p < 0.001$
LP	F (3, 10) = 1,192; $p > 0.05$	F (3, 9) = 5,732; $p > 0.05$
Total thiols	F (3, 9) = 33,36; $p < 0.001$	F (3, 9) = 13,91; $p < 0.05$
Protein thiols	F (3, 8) = 15,97; $p < 0.05$	F (3, 7) = 9,651; $p < 0.05$
$O_2^{\cdot-}$	F (3, 13) = 5,906; $p < 0.05$	F (3, 9) = 2,184; $p > 0.05$
H_2O_2	F (3, 12) = 0,9866; $p > 0.05$	F (3, 10) = 5,765; $p < 0.05$
Pro	F (3, 37) = 7,253; $p < 0.001$	F (3, 44) = 9,553; $p < 0.001$
Total ascorbate	F (3, 8) = 9,060; $p < 0.05$	F (3, 8) = 17,35; $p < 0.001$
AsA/Total ascorbate	F (3, 8) = 0,4799; $p > 0.05$	F (3, 8) = 4,231; $p < 0.05$
DHA/Total ascorbate	F (3, 8) = 0,4799; $p > 0.05$	F (3, 8) = 4,231; $p < 0.05$
Total protein	F (3, 17) = 9,898; $p < 0.001$	F (3, 11) = 29,89; $p < 0.001$
SOD	F (3, 8) = 14,93; $p < 0.05$	F (3, 8) = 2,733; $p > 0.05$
CAT	-	-
APX	F (3, 8) = 51,48; $p < 0.001$	F (3, 8) = 10,22; $p < 0.05$

Annex II

Soares, C., Branco-Neves, S., de Sousa, A., Pereira, R., Fidalgo, F., 2016. Ecotoxicological relevance of nano-NiO and acetaminophen to *Hordeum vulgare* L.: combining standardized procedures and physiological endpoints. Chemosphere 165, 442-452 (DOI: 10.1016/j.chemosphere.2016.09.053).

Chemosphere 165 (2016) 442–452

Contents lists available at ScienceDirect

Chemosphere

journal homepage: www.elsevier.com/locate/chemosphere

Ecotoxicological relevance of nano-NiO and acetaminophen to *Hordeum vulgare* L.: Combining standardized procedures and physiological endpoints

Cristiano Soares [a, *], Simão Branco-Neves [a], Alexandra de Sousa [a], Ruth Pereira [b, c], Fernanda Fidalgo [a]

[a] Department of Biology, BioISI - Biosystems & Integrative Sciences Institute, Faculty of Sciences, University of Porto, Rua do Campo Alegre, s/n, 4169-007 Porto, Portugal
[b] Department of Biology & Green-UP/CITAB-UP, Faculty of Sciences, University of Porto, Rua do Campo Alegre, s/n, 4169-007 Porto, Portugal
[c] CIIMAR - Interdisciplinary Centre of Marine & Environmental Research, Rua dos Bragas, n. 289, 4050-123 Porto, Portugal

HIGHLIGHTS

- Acetaminophen and nano-NiO impaired the growth and physiological performance of barley.
- Nano-NiO induced a more negative response in the metabolism of barley than acetaminophen.
- Biochemical determinations can represent an advantage in ecotoxicology studies.
- Oxidative stress markers detected toxicity at lower doses than the standard methods.
- Combination of diverse methods allows a more robust risk assessment of contaminants.

ARTICLE INFO

Article history:
Received 13 July 2016
Received in revised form
24 August 2016
Accepted 14 September 2016
Available online 30 September 2016

Handling Editor: Caroline Gaus

Keywords:
Ecotoxicology
Barley plants
Emerging contaminants
Growth parameters
Oxidative stress markers
Reactive oxygen species

ABSTRACT

The present work aimed to assess the ecotoxicological relevance of acetaminophen (AC) and nickel oxide nanomaterial (nano-NiO) to barley plants. Combining standard procedures and several biochemical determinations, a global approach regarding the biological effects of these two contaminants was performed. After 14 days of growth, the exposure of barley to increased concentrations (0, 87.8, 131.3, 197.5, 296.5, 444.4, 666.6, and 1000 mg kg^{-1}) of each contaminant resulted in a marked decrease in biomass production and biometric parameters. Photosynthetic pigments and markers of oxidative stress were analyzed to assess if any of the treatments interfered with the physiological performance and with the cellular redox state. Our observations revealed that only nano-NiO induced a negative response in total chlorophylls and carotenoids, confirming the macroscopic phytotoxicity symptoms (chlorosis). However, both contaminants led to a significant increase in lipid peroxidation (LP), superoxide anion ($O_2^{\cdot -}$), and cell death for all the tested concentrations, suggesting that AC and nano-NiO cause oxidative stress in barley, even at the lowest applied dose (87.8 mg kg^{-1}). Comparing the two studied approaches (parameters included in standard protocols and several biochemical determinations), it is concluded that the inclusion of several biochemical endpoints, especially those related to oxidative stress, resulted in a more sensitive analysis and thus, a more sensitive risk evaluation of these two contaminants for barley plants.

1. Introduction

In the recent years, increased industrialization is the leading cause of contamination of several environmental matrices, including soil, with different kinds of chemicals that differ in their nature, characteristics, and potential toxic effects (Ruffini and Cremonini, 2009; Li et al., 2014). Likewise, because of diverse anthropogenic activities, drugs, nanomaterials (NMs), and other emerging compounds have become important worldwide contaminants, representing a possible threat to ecosystem dynamics (Langford and Thomas, 2009; Arruda et al., 2015). Indeed, different types of synthetic products such as pesticides, cosmetics, and

* Corresponding author.
E-mail address: up201003798@fc.up.pt (C. Soares).

http://dx.doi.org/10.1016/j.chemosphere.2016.09.053
0045-6535/

Abbreviations

EPs	emerging pollutants
ROS	reactive oxygen species
NiO	nickel oxide
$O_2^{\cdot-}$	superoxide anion
H_2O_2	hydrogen peroxide
MDA	malondialdehyde
nano-NiO	nickel oxide nanomaterial
AC	acetaminophen
HS	Hoagland solution
PAR	photosynthetically active radiation
OECD	Organization for Economic Cooperation and Development
WHC_{max}	maximum water holding capacity
LP	lipid peroxidation
TBARSs	thiobarbituric acid-reactive substances
SDS	sodium dodecyl sulfate
STDEV	standard error of the mean
ECx	effective concentration causing x% of effect
LOEC	lowest-observed-effect concentration
NOEC	no-observed-effect concentration
Ni	nickel
$OH^{\cdot}$	hydroxyl radical
PCD	programmed cell death
Ag	silver
Al	aluminum

pharmaceuticals are already known not only as contaminants but also as emerging pollutants (EPs; Gavrilescu et al., 2015). According to EURO-STAT, more than half of the total production of chemical products can cause harmful effects in the environment (EURO-STAT, 2013).

Because of all these reasons, it is extremely important to define strategies to understand the mode-of-action of these EPs as well as their accumulation and fate throughout food chains in order to underline principles to minimize their negative consequences to the ecosystems and human health. Ecotoxicology, which, according to Newman and Zhao (2008), is "the science dealing with contaminants in the biosphere," tries to address the effects of pollution at different biological levels (Dave, 2013), occupying a central role in the evaluation of the risk associated with a certain stress factor, including EPs. Frequently, the ecotoxicological studies are based on bioassays according to standardized procedures, which evaluate and analyze the response of organisms exposed to contaminants (van Straalen, 2002).

Although the effects of different EPs on many animal species are relatively well described (Crane et al., 2006; Hao and Chen, 2012; McGill et al., 2012; Patlolla et al., 2014; Nogueira et al., 2015), their toxicological relevance for plants is poorly studied and remains unclear. Plants are the main producers of ecosystems, occupying a central role in biosphere dynamics, and are the basis of human and animal feeding. Being sessile organisms, plants are unable to move and have to directly deal with different types of adverse circumstances such as soil degradation and contamination. Therefore, the assessment of the potential risks of emerging contaminants on different plant species, including food crops, should be adequately addressed. Currently, the available standard methods for estimating the phytotoxicity of EPs are based only on growth-related parameters such as biometric determinations (e.g., root length and shoot length) and biomass production or on the macroscopic analysis of specific phytotoxic signs such as chlorosis and necrosis (OECD, 2006). Indeed, although the studies focused in obtaining phytotoxicity data are increasing, the standard methodologies do not always represent the real plant physiology status and might mask the real toxic effects of the stress agents on plant metabolism and homeostasis at environmentally relevant concentrations.

One of the common characteristics of the exposure of plants to abiotic stress is the induction of oxidative stress due to the overproduction of reactive oxygen species (ROS), which can be used as exposure biomarkers for the precautionary detection of harmful contaminants. ROS are subproducts of normal plant metabolism, whose production can be enhanced under adverse conditions such as exposure to degraded soils (Gill and Tuteja, 2010; Sharma et al., 2012). Because ROS play a dual role in plant physiology, being involved in cellular signaling at low concentrations and also acting as potent oxidative agents, when at above the threshold level, these oxygen-derived molecules can cause great damage to cells, inducing many cellular abnormalities such as the peroxidation of lipids, the oxidation of proteins, and the degradation of photosynthetic pigments (Demidchik, 2015; Gupta et al., 2015). If the exacerbated ROS production persists, DNA damage can also occur, ultimately, leading to cell apoptosis (Gill and Tuteja, 2010; Ahmad, 2014; You and Chan, 2015). Thus, in order to cope with oxidative stress, higher plants need to develop an efficient antioxidant system that can induce and control several defense mechanisms mediated by both antioxidant enzymes and metabolites (Sharma et al., 2012; You and Chan, 2015).

Thus, given the higher sensitivity and discriminatory power of different biochemical indicators, the inclusion of physiological status markers and oxidative stress markers could represent a potential tool to improve phytotoxicity assays. Although there are only a few records regarding this question, the inclusion of physiological endpoints can help to detect false-negative results and better understand the mode-of-action of the tested stress agents. In fact, in a study conducted on maize plants, the authors found that the analysis of many biochemical markers led to a greater sensitivity and a more reliable evaluation of the ecotoxicological relevance of contaminated soils (Gavina et al., 2016). Nevertheless, more studies are needed to reinforce this idea, as plant responses are heavily dependent on species and development stages.

Considering this information, and the lack of scientific reports of plants' responses to EPs, this work aims to understand the toxicological effects of two different emerging contaminants – nickel oxide nanomaterial (nano-NiO; nano-based product, applied in a wide range of technologies (e.g., catalyst, battery electrode, and gas sensor)) and acetaminophen (AC), known as paracetamol (a widely used antipyretic and anti-inflammatory drug) – on the growth and physiological responses of barley (*Hordeum vulgare* L.). To answer these questions, different methodologies were combined, comprising both parameters evaluated on standard protocols and the analysis of different physiological endpoints. Thus, in addition to the evaluation of the fresh and dry weight of plant material, the quantification of total chlorophylls and carotenoids was addressed. Furthermore, the occurrence of oxidative stress was evaluated by the quantification of the two most common ROS – superoxide anion ($O_2^{\cdot-}$) and hydrogen peroxide (H_2O_2), as well as the malondialdehyde (MDA) content, a subproduct of lipid peroxidation (LP), and cell death, estimated by Evans Blue staining.

2. Materials and methods

2.1. Plant material and growth conditions

Seeds of *H. vulgare* L. were used as biological material and were purchased from a local supplier. Before germination, the seeds were individually observed to discard the damaged ones and then surface sterilized with 70% (v/v) ethanol for 15 min and 20% (v/v) commercial bleach (3.5% of active chlorine) for 10 min, followed by three series of washing with sterilized deionized water.

2.2. Chemicals and treatments

Nano-NiO (nearly spherical with a particle size of 100 nm, surface area of 6 $m^2\ g^{-1}$, and 99% purity) and AC were purchased from Nanostructured & Amorphous Materials Inc. (Houston, TX, USA) and Sigma-Aldrich® (Sigma-Aldrich, Germany), respectively. A series of sequential doses of each contaminant was applied to all the experiments, ranging from 0 to 1000 mg kg^{-1} of soil, with a dilution factor of 1.5, resulting in the following concentrations: 87.8, 131.7, 197.5, 296.5, 444.4, 666.7, and 1000 mg kg^{-1} of soil. For the Petri dishes assay, the same procedure was followed, but the concentrations were expressed in mg L^{-1}. The maximum concentration was based on ISO instructions, which suggest that 1000 mg kg^{-1} should be the maximum concentration tested in ecotoxicological studies (ISO, 2012). Above this level, chemical substances should be considered as nontoxic.

2.3. Characterization of nano-NiO powder

The characterization of nano-NiO to obtain its size and shape was evaluated by transmission electron microscopy (TEM) using Hitachi H8100 with a LaB6 filament operated at an acceleration voltage of 200 kV. The images were acquired with an Olympus KeenView digital camera by using iTEM software. The powder sample was suspended in ethanol, and a drop was then allowed to dry on a Cu grid coated with a formvar film.

2.4. Petri dish assays

H. vulgare seeds were placed in Petri dishes with a filter paper embedded in 0.25 × modified Hoagland solution (HS; Taiz et al., 2015), with different concentrations of each contaminant (please see section 2.2). Simultaneously, a control, without AC and without nano-NiO, was included. In the first 48 h, the seeds were kept in dark conditions at 21 °C. Subsequently, during the next 72 h, Petri dishes were transferred to a growth chamber, with controlled conditions of photoperiod (16 h − light/8 h − dark), temperature (21 °C), and a photosynthetically active radiation (PAR) of 60 μmol $m^{-2}\ s^{-1}$. At the end of the 5-day assay period, seed germination and elongation as well as macroscopic symptoms of toxicity were recorded. For each concentration tested, three biological replicates were considered with 10 seeds each.

2.5. Ecotoxicological assays in soil pots

The ecotoxicological assays were performed following the OECD guidelines (OECD, 2006). Pots with 200 g of artificial OECD soil (5% organic matter, pH 5.5) mixed with each tested concentration of each contaminant were used. The maximum water holding capacity (WHC_{max}), determined as previously recommended (ISO, 2005), was previously adjusted to 40%, and the exact volume of distilled water needed for this adjustment was used as a carrier to prepare each contaminant suspension or solution to obtain the range of concentrations described above. To guarantee the maintenance of soil moisture, a cup filled with distilled water was placed under each test pot. The communication between these was achieved by allowing a cotton rope to pass through a hole in the bottom of the test pot. Twenty barley seeds, surface sterilized as stated before, were placed in each pot and carefully covered with the soil. At this moment, to guarantee the availability of nutrients, 120 mL of HS were added to the cup of each pot. For each experimental condition, 8 replicates were prepared, and a negative control was included that was grown in OECD artificial soil without any of the contaminants and thus only moistened with water.

The assay started after 50% of the control seeds germinate and lasted for 14 days. Only the first 5 germinated seeds were left in each pot to avoid intraspecific competition. Plants were maintained in a greenhouse, with controlled conditions of temperature (21 °C), photoperiod (16 h − light/8 h − dark), and PAR (60 μmol $m^{-2}\ s^{-1}$), and the water content of each pot was adjusted when necessary. At the end of the experiment, the plants were collected and separated into roots and shoots. Randomly, part of the plant material was immediately used for the estimation of the standard biomarkers (fresh and dry weights), and the remaining was used for biochemical analysis. Regarding biochemical techniques, the second and third leaves were used from one randomly selected plant per biological replicate.

2.6. Photosynthetic pigment quantification

Samples of fresh leaf material (100 mg) were homogenized at room temperature with a mortar and a pestle by using 80% (v/v) acetone. After centrifugation (for 10 min at 1400 *g*), the supernatant was collected and completed with 80% (v/v) acetone to a known final volume. The levels of chlorophylls and carotenoids were spectrophotometrically determined by recording the absorbance at 470, 647, and 663 nm, and calculated using the formulas of Lichtenthaler (1987).

2.7. LP estimation

LP was evaluated with regard to MDA, a thiobarbituric acid-reactive substance (TBARS), following the method of Heath and Packer (1968). After measuring the absorbance at 532 and 600 nm, the obtained values at 600 nm were subtracted to the ones of 532 nm to minimize unspecific turbidity effects. The content of MDA was estimated using the extinction coefficient of 155 $mM^{-1}\ cm^{-1}$ and expressed as nmol g^{-1} of fresh weight.

2.8. Evaluation of ROS content

In this study, the levels of H_2O_2 and O_2^- were spectrophotometrically quantified by using fresh plant material of approximately 300 mg. The content of H_2O_2 was evaluated by spectrophotometry at 410 nm according to the procedure described by Jana and Choudhuri (1982) and calculated using the extinction coefficient of 0.28 $\mu M^{-1}\ cm^{-1}$. The results are expressed as nmol g^{-1} of fresh weight. Regarding O_2^-, its levels were determined using the protocol of Gajewska and Skłodowska (2007). After a 2-h incubation in dark conditions, the reaction solution was heated at 85 °C for 15 min. Subsequently, the content of O_2^- was obtained by measuring the absorbance at 580 nm, and the results expressed as $Abs_{580\ nm}\ g^{-1}$ of fresh weight.

2.9. Cell death analysis

To detect possible changes in cell viability, the leaves of each experimental condition were incubated in dark conditions for 24 h in 0.25% (w/v) Evans Blue solution (Romero-Puertas et al., 2004).

The leaves were then incubated in boiling 96% (v/v) ethanol to remove the pigments. At this point, cell death stained as blue spots on the leaves was photographically recorded using a digital camera. The leaves were then cut in small and equal pieces and incubated in a solution of 1% (w/v) sodium dodecyl sulfate (SDS) in 50% (v/v) ethanol for 18 h at 50 °C to solubilize the dye agent. Subsequently, the absorbance of each sample was recorded at 600 nm, and the results expressed as $Abs_{600\ nm}\ g^{-1}$ of fresh weight.

2.10. Statistical analysis

All the biochemical measurements were, at least, performed in triplicate for each replica, and the results are expressed as mean ± standard error of the mean (STDEV). To assess the differences between each tested concentration and the control, and after checking the homoscedasticity of variances by using Levene's test, a one-way analysis of variance (ANOVA) was performed, followed by a Dunnett post hoc test, and significant differences were recorded ($p < 0.05$). As one-way ANOVA is regarded as a robust and time-consuming analysis, even when the assumptions of homogeneity were not met, parametric tests were always used instead of nonparametric tests (Zhar, 1996). After ensuring that similar results were obtained with the nonparametric test Kruskal–Wallis, this procedure was followed for the few cases with a $p < 0.05$ in Levene's test. Statistical analysis was performed using GraphPad® Prism 6 software (GraphPad Software Inc., USA). The calculation of ECx (effective concentration causing x% of effect) values and the corresponding 95% confidence limits was performed using the nonlinear least square regression model procedure using Statistica software (version 13).

3. Results

3.1. Characterization of nano-NiO by TEM analysis

As shown in Fig. 1, nano-NiO are nearly spherical with an irregular surface, and despite some smaller nanoparticles were present (<100 nm), overall the NA showed a maximum size of approximately 100 nm in all the dimensions, corroborating the manufacture's information. Furthermore, although this NM has a tendency to agglomerate when suspended in water (Nogueira et al., 2015), the agglomeration observed in the figure was probably due to the preparation of the grids for TEM observations.

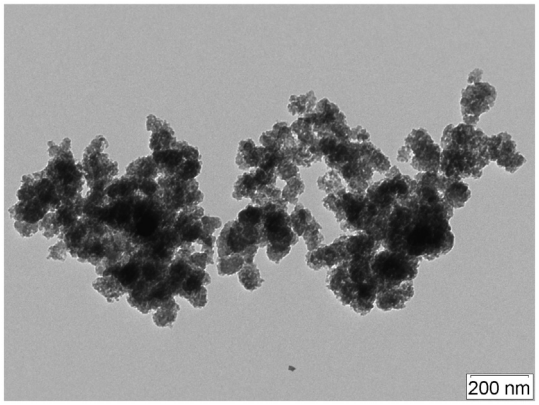

Fig. 1. Transmission electron microscopy (TEM) images of nano-NiO.

3.2. Seed germination

As the exposure of *H. vulgare* to increasing concentrations of AC and nano-NiO did not affect seed germination, no significant differences were found among all tested concentrations and the respective control (Tables 1 and 2).

3.3. Root length – petri plate and OECD soil assay

Plants growing in the presence of different AC concentrations resulted in an inhibition of root elongation in both tested assays (Petri plate assay: $F(7, 147) = 76.14$; $p < 0.0001$; OECD soil assay: $F(7, 23) = 7.518$; $p < 0.0001$; Fig. 2). However, as shown in Table 1, the Petri plate experiment was more sensitive than the OECD soil.

With regard to nano-NiO-mediated stress, a strong inhibition effect of this NM was detected for all concentrations tested (Petri plate assay: $F(7, 131) = 58.38$; $p < 0.0001$; Dunnett: $p < 0.05$; OECD soil assay: $F(7, 23) = 82.40$; $P < 0.0001$; Dunnett: $p < 0.05$; Fig. 2 and Table 2).

3.4. Biomass production – fresh and dry weight

As shown in Figs. 3 and 4, the cultivation of barley plants in OECD soil contaminated with increased concentrations of AC or nano-NiO resulted in a decrease in total productivity of both organs, even though different patterns of effects between AC and nano-NiO on fresh and dry weight of seedlings were observed (Tables 1 and 2).

Regarding AC experiment, significant differences were detected only for higher concentrations in both roots (fresh weight: $F(7, 19) = 12.08$; $p < 0.0001$; Dunnett: $p < 0.05$ for concentrations ≥ 197.5 mg kg^{-1}; dry weight: $F(7, 21) = 6.341$; $p < 0.0001$; Dunnett: $p < 0.05$ for concentrations ≥ 666.7 mg kg^{-1}) and leaves (fresh weight: $F(7, 24) = 18.13$; $p < 0.0001$; Dunnett: $p < 0.05$ for concentrations ≥ 197.5 mg kg^{-1} dry weight: $F(7, 22) = 14.32$; $p < 0.0001$; Dunnett: $p < 0.05$ for concentrations ≥ 296.3 mg kg^{-1}), with roots being the most sensitive organ (Figs. 3 and 4).

Relative to nano-NiO, as Figs. 3 and 4 suggest, a strong adverse effect on biomass production was recorded in roots (fresh weight: $F(7, 24) = 34.33$; $p < 0.0001$; Dunnett: $p < 0.05$; dry weight: $F(7, 20) = 7.958$; $p < 0.0001$; Dunnett: $p < 0.05$ for concentrations ≥ 296.3 mg kg^{-1}) and leaves (fresh weight: $F(7, 24) = 59.44$; $p < 0.0001$; Dunnett: $p < 0.05$; dry weight: $F(7, 24) = 44.94$; $p < 0.0001$; Dunnett: $p < 0.05$ for concentrations ≥ 131.7 mg kg^{-1}), especially for the fresh weight of the leaves (Table 2).

3.5. Photosynthetic pigments

As shown in Fig. 5 and Table 1, the exposure of *H. vulgare* up to 1000 mg kg^{-1} AC did not affect the total chlorophyll content and the carotenoid content ($p > 0.05$).

Conversely, excess nano-NiO induced a clear negative response in photosynthetic pigments, while a significant reduction in both chlorophyll ($F(7, 20) = 13.55$; $p < 0.0001$; Dunnett: $p < 0.05$ for concentrations ≥ 197.5 mg kg^{-1}) and carotenoid ($F(7, 19) = 15.58$; $p < 0.0001$; Dunnett: $p < 0.05$) contents was observed (Fig. 5). When comparing the two photosynthetic pigments, Table 2 suggests that carotenoids represent a more sensitive biomarker than chlorophylls for nano-NiO-mediated stress.

3.6. LP – MDA content

The LP damage was measured in terms of MDA content in the

Table 1
Summary of ecotoxicological data obtained for AC experiment. Concentrations and corresponding 95% confidence intervals are expressed as mg kg^{-1} of soil, except for Petri dish assays, where the values are expressed as mg L^{-1}.

Endpoint		AC					
		NOEC	LOEC	Units of estimated model (p; r)	EC_{10}	EC_{20}	EC_{50}
Germination rate		≥1000	–	–	–	–	–
Root lenght	Petri plate	197.5	296.3	0.87; 0.93	194 (95.5–292.4)	288.2 (182.7–393.7)	566.4 (459.0–674.0)
	OECD soil	444.4	666.6	0.62; 0.79	323.6 (100.7–546.5)	490.9 (75.1–706.5)	999.9 (733.8–1265.9)
Root fresh weight		87.8	131.7	0.76; 0.87	63.2 (−0.8 to 127.2)	124.6 (33.0–216.3)	397.4 (242.4–552.3)
Root dry weight		444.4	666.6	0.70; 0.83	65.6 (−11.7 to 142.9)	131.1 (18.3–243.9)	427.7 (236.9–618.4)
Leaf fresh weight		131.7	197.5	0.79; 0.89	87.7 (15.0–160.3)	180.6 (75.4–285.7)	620 (438.9–801.1)
Leaf dry weight		197.5	296.3	0.77; 0.88	108.5 (16.3–200.6)	207.7 (84.2–331.2)	630.4 (443.9–816.9)
Chlorophylls		≥1000	–	–	–	–	–
Carotenoids		≥1000	–	–	–	–	–
Lipid peroxidation		–	≤87.8	–	–	–	–
O_2^-		–	≤87.8	–	–	–	–
H_2O_2		≥1000	–	–	–	–	–
O_2^-/H_2O_2		–	≤87.8	–	–	–	–
Cell death		–	≤87.8	–	–	–	–

NOEC – Non-observed-effect concentration; *LOEC* – Lowest-observed-effect concentration; *ECx* – effective concentration causing x% of the effect.

Table 2
Summary of ecotoxicological data obtained for nano-NiO experiment. Concentrations and corresponding 95% confidence intervals are expressed as mg kg^{-1} of soil, except for Petri dish assays, where the values are expressed as mg L^{-1}.

Endpoint		nano-NiO					
		NOEC	LOEC	Units of estimated model (p; r)	EC_{10}	EC_{20}	EC_{50}
Germination rate		≥1000	–	–	–	–	–
Root lenght	Petri plate	–	≤87.8	0.85; 0.92	23.9 (0.08–47.72)	54.9 (14.7–95.1)	227.2 (141.0–313.4)
	OECD soil	–	≤87.8	0.90; 0.95	28.6 (10.3–46.9)	58.8 (30.7–86.9)	201.5 (150.1–252.9)
Root fresh weight		–	≤87.8	0.90; 0.95	18.6 (5.1–32.2)	37.2 (17.0–57.4)	121.1 (87.5–154.7)
Root dry weight		197.5	296.3	0.73; 0.86	39.2 (−5.0 to 83.5)	73.5 (10.7–136.3)	214.5 (112.0–317.0)
Leaf fresh weight		–	≤87.8	0.95; 0.97	13.8 (5.9–21.7)	30.9 (17.8–44.1)	122.6 (96.9–148.3)
Leaf dry weight		87.8	131.7	0.86; 0.93	29 (8.1–49.9)	59.2 (27.5–90.9)	200.5 (142.5–258.5)
Chlorophylls		131.7	197.5	0.76; 0.87	45.1 (−10.1 to 100.2)	128.3 (21.5–234.9)	764.2 (438.3–1090.1)
Carotenoids		–	≤87.8	0.74; 0.86	29.2 (−18.8 to 77.3)	143.6 (5.9–281.2)	2175.5 (308.7–4042.3)
Lipid peroxidation		–	≤87.8	–	–	–	–
O_2^-		–	≤87.8	–	–	–	–
H_2O_2		–	–	–	–	–	–
O_2^-/H_2O_2		–	≤87.8	–	–	–	–
Cell death		–	≤87.8	–	–	–	–

NOEC – Non-observed-effect concentration; ***LOEC*** – Lowest-observed-effect concentration; ***ECx*** – effective concentration causing x% of the effect.

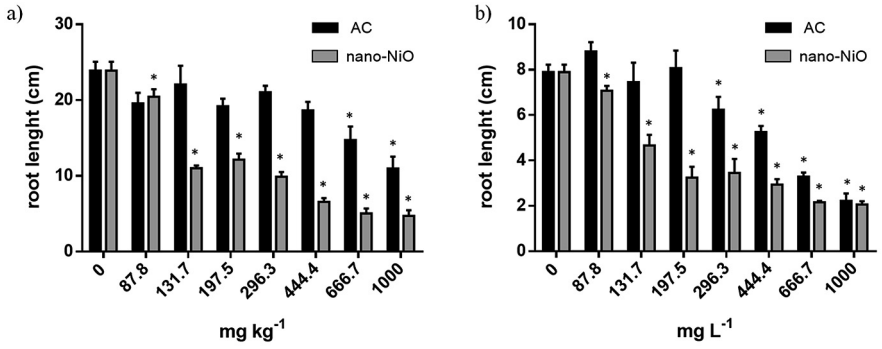

Fig. 2. Effects of increased concentrations of AC and nano-NiO on the root length of barley plants grown for 14 days in OECD soil (a) and for 5 days in Petri plates (b). Data presented are mean ± STDEV (n ≥ 3). * Above bars indicate significant statistical differences from the control at $p \leq 0.05$.

leaves of barley plants growing under increased concentrations of each contaminant.

Plants grown under exposure of increasing doses of AC exhibited higher values of MDA than those of the control ($F(7, 20) = 17.16$; $p < 0.0001$; Dunnett: $p < 0.05$; Fig. 6a and Table 1).

In the nano-NiO-treated plants, significant changes in the control were observed for all tested doses (Table 2; $F(7, 18) = 7.576$; $p < 0.0001$; Dunnett: $p < 0.05$) in a concentration-independent manner (Fig. 6a).

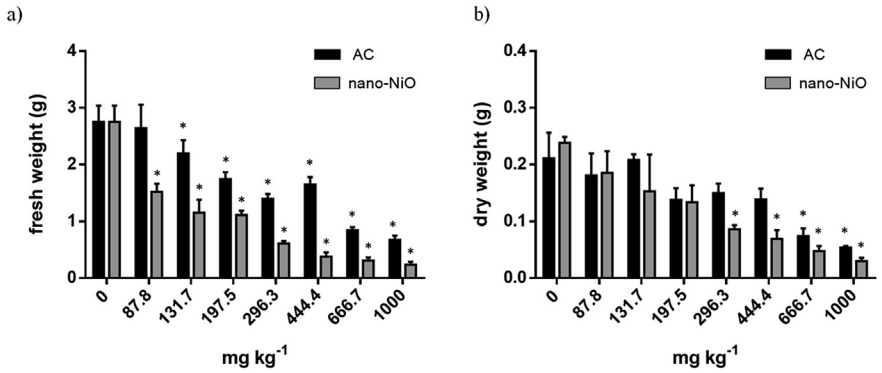

Fig. 3. Effects of increased concentrations of AC and nano-NiO on roots' fresh (a) and dry (b) weights of barley plants grown for 14 days in OECD soil. Data presented are mean ± STDEV (n ≥ 3). * Above bars indicate significant statistical differences from the control at $p \leq 0.05$.

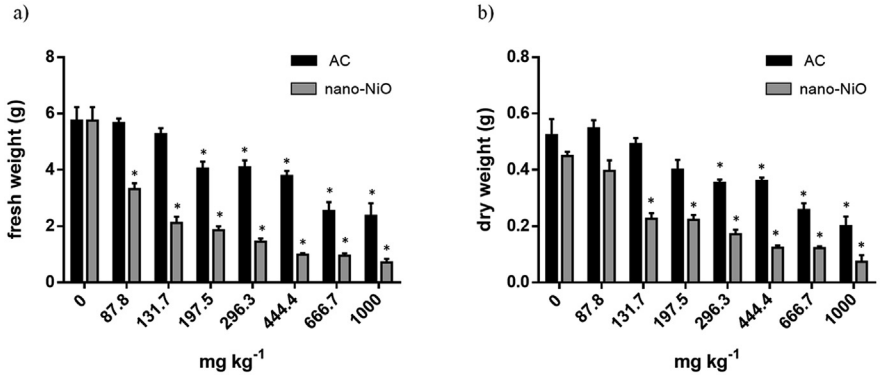

Fig. 4. Effects of increased concentrations of AC and nano-NiO on leaves' fresh (a) and dry (b) weights of barley plants grown for 14 days in OECD soil. Data presented are mean ± STDEV (n ≥ 3). * Above bars indicate significant statistical differences from the control at $p \leq 0.05$.

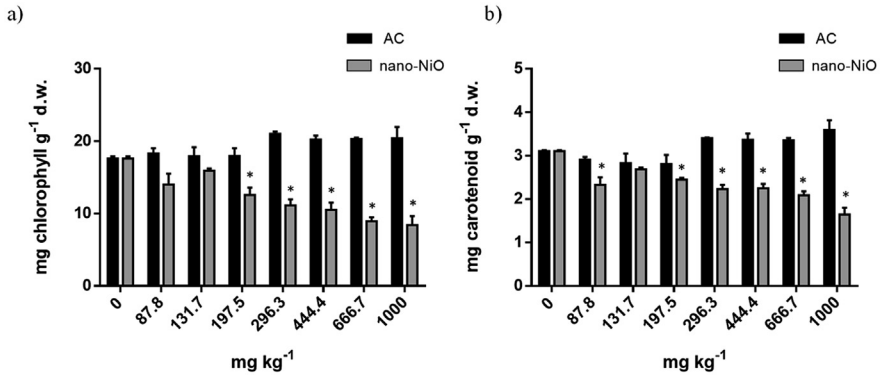

Fig. 5. Effects of increased concentrations of AC and nano-NiO on the photosynthetic pigment content of barley plants grown for 14 days in OECD soil. (a) total chlorophylls; (b) carotenoids. Data presented are mean ± STDEV (n ≥ 3). * Above bars indicate significant statistical differences from the control at $p \leq 0.05$.

3.7. ROS levels – O_2^- and H_2O_2

3.7.1. H_2O_2 content

The exposure of barley to AC did not affect the total content of H_2O_2 ($p > 0.05$), because no significant differences were found between the applied doses and the control (Fig. 6b).

However, nano-NiO affected the production of H_2O_2 ($F(7, 23) = 3.337$; $p < 0.0133$), though it was not observed as a constant response among all treatments (Fig. 6b).

3.7.2. O_2^- content

As shown in Fig. 6c, the levels of superoxide anion were increased in response to AC treatments, even at the lowest applied doses ($F(7, 26) = 8.898$; $p < 0.0001$; Dunnett: $p < 0.05$; Fig. 6c).

In the nano-NiO experiment, higher values of this ROS were detected in all the tested concentrations relative to the control ($F(7, 20) = 58.64$; $p < 0.0001$; Dunnett: $p < 0.05$; Fig. 6c).

3.7.3. O_2^-/H_2O_2 ratio

The ratio of O_2^-/H_2O_2 was changed in response to both AC and nano-NiO treatments. The application of sequential doses of AC to

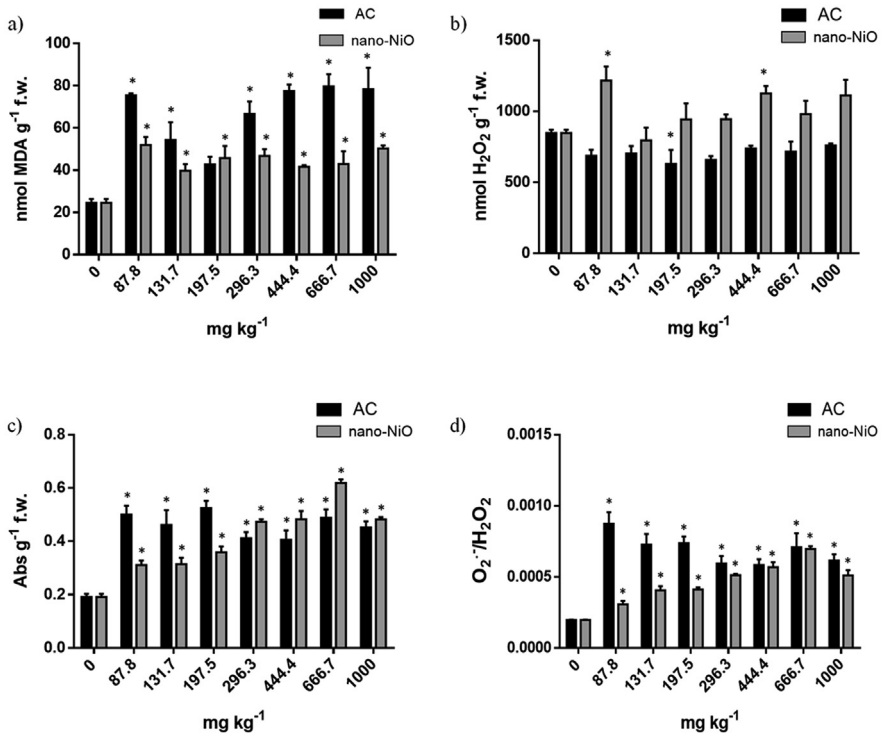

Fig. 6. Effects of increased concentrations of AC and nano-NiO on the oxidative stress markers of barley plants grown for 14 days in OECD soil. (a) MDA; (b) H_2O_2; (c) O_2-; and (d) O_2-/H_2O_2. Data presented are mean ± STDEV (n ≥ 3). * Above bars indicate significant statistical differences from the control at $p \leq 0.05$.

soil-grown barley resulted in an increase in this proportion, in a concentration-independent manner ($F(7, 20) = 8.041$; $p < 0.0001$; Dunnett: $p < 0.05$; Fig. 6d).

Regarding nano-NiO experiment, higher values of O_2^-/H_2O_2 in all the tested concentrations were found relative to the CTL in a dose-dependent manner ($F(7, 16) = 42.00$; $p < 0.0001$; Dunnett: $p < 0.05$; Fig. 6d).

3.8. Cell death – histochemical detection and quantification

An increase in cell death of barley leaves was observed for all the tested concentrations of both AC ($F(7, 19) = 16.28$; $p < 0.0001$; Dunnett: $p < 0.05$) and nano-NiO ($F(7, 24) = 7.016$; $p < 0.0001$; Dunnett: $p < 0.05$) in a concentration-dependent manner (Figs. 7 and 8).

Overall, as Tables 1 and 2 suggest, all studied oxidative stress markers showed a high sensitivity to AC- and nano-NiO-mediated stress, although the levels of H_2O_2 did not follow this tendency. Indeed, for LP, O_2^-, O_2^-/H_2O_2, and cell death, the first applied concentration was always defined as the lowest-observed-effect concentration (LOEC) value for both contaminants.

4. Discussion

Currently, the evaluation of effects of different stress factors on plant's development, growth, and physiology is a matter of major importance. Thus, phytotoxicology is now an essential part of ecotoxicology research (Eullaffroy, 2013).

In the present study, the main focus was on the possible phytotoxicity significance of two different emerging contaminants (nano-NiO and AC) for soil-grown barley at both organismal and cellular levels. In attempts to achieve a deeper and more reliable analysis, different methodologies were combined and comparisons between endpoints evaluated on standard protocols and other physiological parameters were made.

As sessile organisms, plants are constantly and directly exposed to contaminated soils since the early steps of germination throughout their life-cycle stages. Thus, seed germination is often used to estimate pollution effects on plants (Miralles et al., 2012). However, our results clearly showed that the application of both AC and nano-NiO did not affect this parameter, even at the highest tested concentration (1000 mg kg^{-1}). In agreement with these data, several authors also reported the lack of sensitiveness of seed germination on ecotoxicological studies for both inorganic and organic compounds (An et al., 2009; Gavina et al., 2016; Bouguerra et al., 2016). Indeed, the potential risk of metals and other contaminants in the impairment of seed germination is highly dependent on their ability to reach embryogenic tissues, which are strongly protected by seed coats, structures with differential permeability to different types of substances (Seregin and Kozhevnikova, 2005; Akinci and Akinci, 2010).

Together with the evaluation of germination, it is also common to analyze parameters related to growth, because plant's growth measurements are important bioassay endpoints to evaluate the toxicity of a specific compound (Kapanen and Itävaara, 2001; Adrees et al., 2015) and its effects on soil production function. Here, barley plants were grown in OECD soil for 14 days with AC and nano-NiO at different concentrations ranging from 87.8 to 1000 mg kg^{-1}. In addition to the OECD standard assay, a parallel experiment was performed in Petri plates where seeds were allowed to germinate and seedlings' development was evaluated after 5 days. Although these experiences may not reflect the real conditions of plants' exposure to contaminants, because their availability is expected to be higher than in the soil, we observed a good correlation between the results of the assays of the Petri plate and soil for nano-NiO, with very similar $EC_{10, 20, 50}$ values between them. With regard to AC, the same pattern was not observed, and the $EC_{10, 20, 50}$ values were always lower in the Petri plate assay than

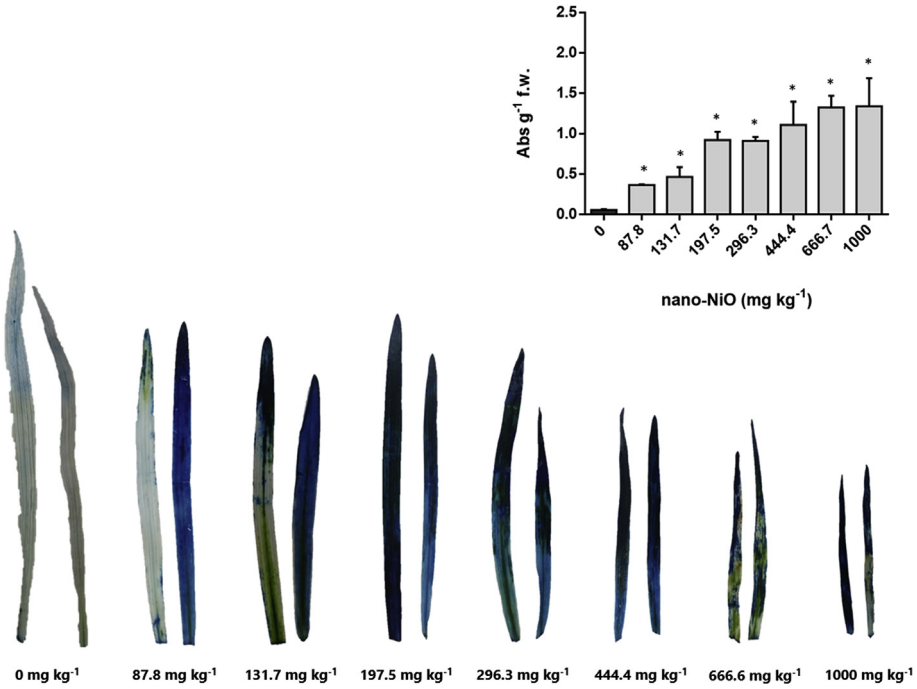

Fig. 7. Effects of increased concentrations of nano-NiO on the leaves, measured by cell death in barley plants grown for 14 days in OECD soil. Data presented are mean ± STDEV ($n \geq 3$). * Above bars indicate significant statistical differences from the control at $p \leq 0.05$.

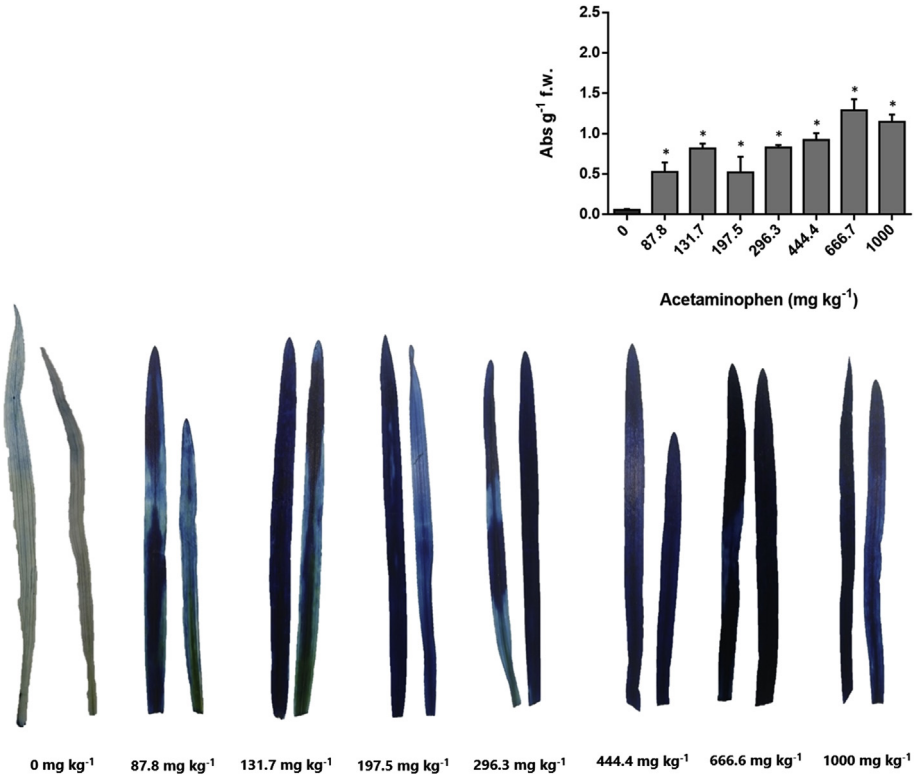

Fig. 8. Effects of increased concentrations of AC on the leaves, measured by cell death in barley plants grown for 14 days in OECD soil. Data presented are mean ± STDEV ($n \geq 3$). * Above bars indicate significant statistical differences from the control at $p \leq 0.05$.

in the soil assay. In fact, even in soil substrate, the bioavailability of certain compounds can be changed with regard to different soil properties. Particularly focusing on metals, it is widely accepted that the soil pH and the presence of other ions such as phosphate can alter metal's bioavailability, thus changing its possible effects on a biota (Olaniran et al., 2013). In addition, recent findings showed that phosphate and nitrogen can affect the availability of several xenobiotics in soil (Allison et al., 2013). Thus, it appears that

these kinds of approaches are highly species, contaminant and substrate dependent and, hence, rather than excluding one or another, combined strategies could represent an advantage to risk assessment; moreover, Petri dish assays could be useful for an initial screening of the toxicity of new contaminants. Our results demonstrated that both tested contaminants, particularly nano-NiO, induced a marked decrease in root length. The reduction of root length is a common response of plants exposed to different types of stresses, including metals such as Ni. Although very few studies are available regarding the effects of nano-NiO on plants, the inhibition of root growth as a consequence of excess Ni was detected in a wide range of plant species (see works reviewed by Hussain et al., 2013). Regarding AC, An et al. (2009) found that the exposure of wheat plants to paracetamol negatively affected root elongation, with an EC_{50} of approximately 670 mg L^{-1}. In accordance, on the basis of the results of the Petri plate assay, an EC_{50} of approximately 550 mg L^{-1} was estimated for AC effects on root length, corroborating the previous results with wheat, which is also a monocotyledonous species such as barley.

Simultaneously with the reduction of root growth, the exposure of barley to AC and nano-NiO induced a significant decrease in the biomass production of roots and leaves, evaluated in terms of both fresh and dry weights. Interestingly, for both contaminants and organs, fresh weight was always more sensitive than dry weight, with lower $EC_{10,\ 20,\ 50}$ values. Moreover, it was clear that nano-NiO caused deleterious effects at lower concentrations than AC. However, we cannot completely assume that nano-NiO is more toxic than AC; indeed, it seems that AC-mediated toxicity is related to its degradation pathways in soil. According to Li et al. (2014), AC is rapidly degraded in the soil, with microorganisms playing a central role in this process. Thus, we cannot exclude the hypothesis that AC may have been metabolized by soil microbial community, and hence, only higher concentrations led to negative effects on barley's growth performance. In fact, considering the different $EC_{10,\ 20,\ 50}$ values of AC in Petri dish and OECD soil assays, it was found that Petri dish assays help in maintaining aseptic conditions and prevented AC degradation, aggravating its toxicity.

When plants are grown on contaminated soils, the first main target of stress is the radicular system; hence, the evaluation of root responses can help us understand the potential hazards of different contaminants. However, in many ecotoxicology studies on plants, the evaluation of root's development and biomass is not considered. Here, we noticed a differential discriminatory power between the roots and the leaves growing in a contaminant-dependent manner, with the biomass of the roots being more sensitive than leaves for AC and less sensitive for nano-NiO. This fact might be related to the different chemical nature of AC and nano-NiO as well as their possible effects on plant physiology. Indeed, although high levels of Ni are phytotoxic, this metal is regarded as an essential micronutrient for plant growth and plants have specific translocation pathways for Ni. Therefore, we can hypothesize that nano-NiO is absorbed by the radicular system and then translocated to the leaves, as a protection mechanism for roots. This idea was also proposed by different authors and publications (see review by Yusuf et al., 2011) and strengthened by the macroscopic phytotoxicity symptoms observed in our study in Ni-treated leaves (data not shown). However, although AC is not found in normal plant metabolism, it is supposed that plants may possess an effective detoxification pathway for different xenobiotics such as AC (Bartha et al., 2010). Because there are no records regarding the toxic effects of this antipyretic drug on plant growth, we suggest that roots are the main targets of AC-mediated stress, although a marked decrease in fresh and dry weight of leaves was also observed for high doses. Paired with this hypothesis, several studies on other organic contaminants such as fungicides and pesticides also reported a decrease in plant biomass, particularly in the roots (Tiyagi et al., 2004; Parween et al., 2011; Teixeira et al., 2011; Yildiztekin et al., 2015).

As previously mentioned, one of the major objectives of this work was to assess if the inclusion of diverse biochemical endpoints could improve the sensitivity of ecotoxicology tests. Therefore, the levels of photosynthetic pigments were quantified to have a better insight about the effects of AC and nano-NiO on the physiological status of barley plants and on their mechanisms of action. Although no significant changes were found regarding AC treatments, a gradual decrease in both chlorophylls and carotenoids was reported in the nano-NiO-exposed plants. Indeed, several references indicate that excess Ni can lead to a lower photosynthetic pigment content (Lin and Kao, 2007; Ahmad et al., 2011; Dubey and Pandey, 2011; Soares et al., 2016), possibly due to a higher activity of chlorophyllase and/or inhibition of chlorophyll production (Ali et al., 2008). Moreover, it is known that Ni can replace the Mg ion in the chlorophyll molecule, leading to a lower photosynthetic activity (Küpper et al., 1996). In general, on the basis of the LOEC and $EC_{10,20,50}$ values obtained, we can assume that the inclusion of photosynthetic pigment analysis did not contribute to a higher discriminatory evaluation of the potential risks of AC and nano-NiO.

One of the main common characteristics of the exposure of plants to different kinds of stress, including soil pollution, is the induction of oxidative stress by an overproduction of ROS (Gill and Tuteja, 2010; Sharma et al., 2012). Although ROS are continuously produced as a consequence of the aerobic and photosynthetic metabolism, an exacerbated increase in their production can trigger great damage to plant cells, eventually leading to cell apoptosis (Gill and Tuteja, 2010). In the present study, particular emphasis was given to different types of oxidative stress indicators, namely the content of O_2^- and H_2O_2 as well as LP and cell death histochemical detection.

Although Ni is not considered as a catalyst of the Haber–Weiss reaction, because it is not a redox-active metal, the relationship between Ni excess and the occurrence of oxidative stress in plants is well described in the literature (Gomes-Junior et al., 2006; Gajewska et al., 2009; Yusuf et al., 2011; Hussain et al., 2013; Dourado et al., 2015; Soares et al., 2016). Here, in general, the contents of both O_2^- and H_2O_2 were increased by nano-NiO treatments, although the quantification of O_2^- led to higher statistical differences. Indeed, even though large amounts of hydrogen peroxide can lead to toxic effects in plant cells, the role of this ROS as a signaling molecule is being progressively recognized; thus, its production can also be related to a hypothetical mechanism of cell signaling (Sharma et al., 2012). Therefore, three hypotheses can be considered to explain the maintenance of H_2O_2 levels between control and stressed plants: this molecule could be used as an intracellular messenger, be efficiently removed by the AOX enzymatic system, and/or react with O_2^- favoring the production of $OH^{\bullet}$. Regarding AC, similar to the nano-NiO situation, O_2^- was a more sensitive marker than H_2O_2. Despite the lack of information about the possible effects of AC on plant oxidative status, we can suggest that excess of this drug triggers the production of O_2^-, which is usually the first ROS to be produced (Gill and Tuteja, 2010; Sharma et al., 2012; Gupta et al., 2015). In accordance with this hypothesis, Kummerová et al. (2016) reported an increase in ROS content, particularly O_2^-, in *Lemna minor* plants exposed to two drugs, one of which was AC.

Among all ROS, hydroxyl radical ($OH^{\bullet}$), formed by the Haber–Weiss reaction, is the most hazardous oxygen-derived radical, inducing LP and substantial damages in other biomolecules (Gill and Tuteja, 2010). In addition, it is directly associated with programmed cell death (PCD; Demidchik, 2015), once plant cells do not

have any specific enzymatic reaction to eliminate this ROS. Thus, as both O_2^- and H_2O_2 are part of the Haber–Weiss reaction, with a 1:1 stoichiometry, the ratio between these two ROS can give us information about the potential production of $OH^•$ (Bowler et al., 1991). Accordingly, our results clearly showed that the exposure of barley to increased nano-NiO and AC concentrations resulted in a significant increase in this proportion throughout all treatments. In addition, the lowest concentration (87.8 mg kg^{-1}) induced a great boost in this ratio, suggesting that oxidative stress conditions are occurring even at the lowest concentrations tested.

Because of ROS overproduction, LP of different biological membranes can occur at both cellular and organelle levels. Consequently, high rates of lipid peroxides can, in turn, aggravate the cellular redox imbalance, being able to directly react with proteins and DNA (Sharma et al., 2012). The present work again revealed that the soil application of sequential doses of AC and nano-NiO induced the occurrence of oxidative stress conditions, as LP remained always higher than the control in all treatments. These results are in accordance with different studies, conducted with several plant species exposed to diverse types of abiotic stress, which indicate that the enhancement of LP is a common response of oxidative stress (see reviews by Gill and Tuteja, 2010; Sharma et al., 2012). Although in general, AC-treated plants showed a dose-independent increase in LP, surprisingly, for the first three applied concentrations, a gradual decrease in MDA content was noticed. Thus, we hypothesize that the exposure of barley to 87.8 mg kg^{-1} of AC led to a cellular redox imbalance (higher O_2^-, MDA, and cell death levels), but was not enough to elicit a response from the AOX system, thus enhancing LP; in turn, the application of 131.7 and 197.5 mg kg^{-1} resulted in a slight decrease in MDA – though always higher than the control – which could be related to an efficient AOX system response. From this point onwards, MDA levels were increased again, possibly indicating that above 197.5 mg kg^{-1}, AC negatively affects the plant AOX system performance. Moreover, as seen in the standard procedures, AC was more toxic at high concentrations, particularly above 400 mg kg^{-1}. In accordance with the O_2^- and MDA content, our study also revealed that AC and nano-NiO affected barley's cell viability, even in the lowest tested concentration. Moreover, a dose-dependent response was observed for the two contaminants, with higher cell death staining in the highest applied doses (666.6 and 1000 mg kg^{-1}). It is widely accepted that cell viability as well as cell death can be affected by oxidative stress, as ROS are involved in different signaling pathways of PCD (Gupta et al., 2015; You and Chan, 2015). In fact, paired with our observations, Faisal et al. (2013) reported that the exposure of tomato to different concentrations of nano-NiO led to a higher percentage of apoptosis; in addition, using silver (Ag) NA, an increase in cell death was detected in the roots of *Allium cepa* (Panda et al., 2011) and the same result was observed in barley exposed to increased concentrations of aluminum (Al; Achary et al., 2012).

Compared to the quantification of photosynthetic pigments, the evaluation of different oxidative stress markers generally led to a higher-sensitive analysis of the effects of AC and nano-NiO, relatively to the standard procedures. In fact, when comparing the standard methodologies and the biochemical determinations, it is clear that the latter have led to lower LOEC values, allowing a more protective risk evaluation for nano-NiO and especially for AC in barley. Indeed, for AC, all oxidative stress markers were more sensitive than the standard procedures, given the obtained LOEC and no-observed-effect concentration (NOEC) values, possibly indicating that AC is already interfering with the cellular oxidative status in the lowest applied doses. Regarding nano-NiO, although the standard procedures were also very sensitive, it was possible to perceive that the adverse effects of this NM on the first tested concentration (87.8 mg kg^{-1}) were more notorious in the biochemical determinations than in the biometric ones. In agreement with our findings, Gavina et al. (2013) also suggested that the inclusion of different physiological endpoints could improve the accuracy of ecotoxicological studies with plant species. Furthermore, in the future, the evaluation of root responses with regard to the occurrence of oxidative stress should be performed to achieve a global vision about the AC- and nano-NiO-mediated phytotoxicity. Indeed, according to Gratão et al. (2015), the exposure of tomato to high levels of Cd induced differential responses in the roots and shoots, suggesting that signaling mechanisms and root-to-shoot translocation processes might occur to minimize the adverse effects of stress.

5. Conclusions

In conclusion, the present work clearly showed that both nano-NiO and AC impaired the normal growth and physiological performance of barley. Given the obtained EC and LOECs values, we can conclude that nano-NiO was more toxic than AC, inducing a more negative response in the metabolism of barley, which also reflected in a much more decreased productivity. Our data also propose that the use of Petri dish assays can represent an advantage to estimate the consequences of EC at the early stages of plant development, while pot experiments can provide a wide perspective about the negative effects of soil contamination at the productivity and organismal levels. Comparing standard and physiological endpoints, we can suggest that the addition of oxidative stress markers helped to detect phytotoxicity signs at lower concentrations than the standard OECD-based methodologies, especially for AC.

Thus, combining an innovative risk evaluation strategy, we demonstrated that the inclusion of biochemical determinations, particularly those related to oxidative stress, can represent an advantage in ecotoxicology studies, with a high discriminatory and fidelity power, especially for low concentrations. Nevertheless, given the differential responses found between nano-NiO and AC, we suggest that risk assessment strategies must be suitable to the different types of pollutants, combining a comprehensive overview, to understand the mode of action of the contaminant and thus avoid underestimation or overestimation of its effects on plant development. With this work, we hope that in the future, efforts could be reinforced to unravel the adverse consequences of soil degradation on plants, especially on food crops.

Acknowledgments

This research was partially supported by the Strategic Funding UID/Multi/04423/2013 (FCT through CIIMAR) through national funds provided by FCT – Foundation for Science and Technology and European Regional Development Fund (ERDF) in the framework of the program PT2020 and PEst-OE/BIA/UI4046/2014 (FCT through BioISI).

References

Achary, V.M.M., Patnaik, A.R., Panda, B.B., 2012. Oxidative biomarkers in leaf tissue of barley seedlings in response to aluminum stress. Ecotoxicol. Environ. Saf. 75, 16–26.

Adrees, M., Ali, S., Rizwan, M., Ibrahim, M., Abbas, F., Farid, M., Zia-ur-Rehman, M., Irshad, M.K., Bharwana, S.A., 2015. The effect of excess copper on growth and physiology of important food crops: a review. Environ. Sci. Pollut. Res. 22, 8148–8162.

Ahmad, M.S.A., Ashraf, M., Hussain, M., 2011. Phytotoxic effects of nickel on yield and concentration of macro-and micro-nutrients in sunflower (*Helianthus annuus* L.) achenes. J. Hazard. Mater. 185, 1295–1303.

Ahmad, P., 2014. Oxidative Damage to Plants: Antioxidant Networks and Signaling. Elsevier Science.

Akinci, I.E., Akinci, S., 2010. Effect of chromium toxicity on germination and early

seedling growth in melon (*Cucumis melo* L.). Afr. J. Biotechnol. 9, 4589–4594.
Ali, B., Hayat, S., Fariduddin, Q., Ahmad, A., 2008. 24-Epibrassinolide protects against the stress generated by salinity and nickel in *Brassica juncea*. Chemosphere 72, 1387–1392.
Allison, J.E., Boutin, C., Carpenter, D., 2013. Influence of soil organic matter on the sensitivity of selected wild and crop species to common herbicides. Ecotoxicology 22, 1289–1302.
An, J., Zhou, Q., Sun, F., Zhang, L., 2009. Ecotoxicological effects of paracetamol on seed germination and seedling development of wheat (*Triticum aestivum* L.). J. Hazard. Mater. 169, 751–757.
Arruda, S.C., Silva, A.L., Galazzi, R.M., Azevedo, R.A., Arruda, M.A., 2015. Nanoparticles applied to plant science: a review. Talanta 131, 693–705.
Bartha, B., Huber, C., Harpaintner, R., Schröder, P., 2010. Effects of acetaminophen in *Brassica juncea* L. Czern.: investigation of uptake, translocation, detoxification, and the induced defense pathways. Environ. Sci. Pollut. Res. 17, 1553–1562.
Bouguerra, S., Gavina, A., Ksibi, M., da Graça Rasteiro, M., Rocha-Santos, T., Pereira, R., 2016. Ecotoxicity of titanium silicon oxide ($TiSiO_4$) nanomaterial for terrestrial plants and soil invertebrate species. Ecotoxicol. Environ. Saf. 129, 291–301.
Bowler, C., Slooten, L., Vandenbranden, S., De Rycke, R., Botterman, J., Sybesma, C., Van Montagu, M., Inzé, D., 1991. Manganese superoxide dismutase can reduce cellular damage mediated by oxygen radicals in transgenic plants. EMBO J. 10, 1723–1732.
Crane, M., Watts, C., Boucard, T., 2006. Chronic aquatic environmental risks from exposure to human pharmaceuticals. Sci. Total Environ. 367, 23–41.
Dave, G., 2013. Ecotoxicological risk assessment and management of tire wear particles. In: Férard, J.-F., Blaise, C. (Eds.), Encyclopedia of Aquatic Ecotoxicology. Springer, Netherlands.
Demidchik, V., 2015. Mechanisms of oxidative stress in plants: from classical chemistry to cell biology. Environ. Exp. Bot. 109, 212–228.
Dourado, M., Franco, M., Peters, L., Martins, P., Souza, L., Piotto, F., Azevedo, R., 2015. Antioxidant enzymes activities of Burkholderia spp. strains—oxidative responses to Ni toxicity. Environ. Sci. Pollut. Res. 22, 19922–19932.
Dubey, D., Pandey, A., 2011. Effect of Nickel (Ni) on chlorophyll, lipid peroxidation and antioxidant enzymes activities in black gram (*Vigna mungo*) leaves. Int. J. Sci. Nat. 2, 395–401.
Eullaffroy, P., 2013. Phytotoxicology: contaminant effects on markers of photosynthesis. In: Férard, J.F., Blaise, C. (Eds.), Encyclopedia of Aquatic Ecotoxicology. Springer Netherlands, Dordrecht, pp. 855–864.
EURO-STAT, 2013. Statistical Office of the European Communities.
Faisal, M., Saquib, Q., Alatar, A.A., Al-Khedhairy, A.A., Hegazy, A.K., Musarrat, J., 2013. Phytotoxic hazards of NiO-nanoparticles in tomato: a study on mechanism of cell death. J. Hazard. Mater. 250, 318–332.
Gajewska, E., Skłodowska, M., 2007. Effect of nickel on ROS content and antioxidative enzyme activities in wheat leaves. BioMetals 20, 27–36.
Gajewska, E., Wielanek, M., Bergier, K., Skłodowska, M., 2009. Nickel-induced depression of nitrogen assimilation in wheat roots. Acta Physiol. Plant. 31, 1291–1300.
Gavina, A., Antunes, S.C., Pinto, G., Claro, M.T., Santos, C., Gonçalves, F., Pereira, R., 2013. Can physiological endpoints improve the sensitivity of assays with plants in the risk assessment of contaminated soils? PLoS One 8, e59748.
Gavina, A., Bouguerra, S., Lopes, I., Marques, C.R., Rasteiro, M.G., Antunes, F., Rocha-Santos, T., Pereira, R., 2016. Impact of organic nano-vesicles in soil: the case of sodium dodecyl sulphate/didodecyl dimethylammonium bromide. Sci. Total Environ. 547, 413–421.
Gavrilescu, M., Demnerova, K., Aamand, J., Agathos, S., Fava, F., 2015. Emerging pollutants in the environment: present and future challenges in biomonitoring, ecological risks and bioremediation. New Biotechnol. 32, 147–156.
Gill, S.S., Tuteja, N., 2010. Reactive oxygen species and antioxidant machinery in abiotic stress tolerance in crop plants. Plant Physiol. Biochem. 48, 909–930.
Gomes-Junior, R., Moldes, C., Delite, F., Gratão, P., Mazzafera, P., Lea, P., Azevedo, R., 2006. Nickel elicits a fast antioxidant response in *Coffea arabica* cells. Plant Physiol. Biochem. 44, 420–429.
Gratão, P.L., Monteiro, C.C., Tezotto, T., Carvalho, R.F., Alves, L.R., Peters, L.P., Azevedo, R.A., 2015. Cadmium stress antioxidant responses and root-to-shoot communication in grafted tomato plants. Biometals 28, 803–816.
Gupta, D.K., Palma, J.M., Corpas, F.J., 2015. Reactive Oxygen Species and Oxidative Damage in Plants under Stress. Springer.
Hao, L., Chen, L., 2012. Oxidative stress responses in different organs of carp (*Cyprinus carpio*) with exposure to ZnO nanoparticles. Ecotoxicol. Environ. Saf. 80, 103–110.
Heath, R.L., Packer, L., 1968. Photoperoxidation in isolated chloroplasts. I. Kinetics and stoichiometry of fatty acid peroxidation. Arch. Biochem. Biophys. 125, 189–198.
Hussain, M.B., Ali, S., Azam, A., Hina, S., Ahsan, M., Farooq, B.A., Bharwana, S.A., Gill, M.B., 2013. Morphological, physiological and biochemical responses of plants to nickel stress: a review. Afr. J. Agric. Res. 8 (17), 1596–1602.
ISO, 2005. Soil quality — Determination of pH. ISO—The International Organization for Standardization, Geneva, Switzerland. ISO 10390:2005.
ISO, 2012. ISO Guideline 11269–2: Soil Quality - Determination of the Effects of Pollutants on Soil Flora - Part 2: Effects of Contaminated Soil on the Emergence and Early Growth of Higher Plants. International Organization for Standardization, Geneve, Switzerland.
Jana, S., Choudhuri, M.A., 1982. Glycolate metabolism of three submersed aquatic angiosperms during ageing. Aquat. Bot. 12, 345–354.
Kapanen, A., Itävaara, M., 2001. Ecotoxicity tests for compost applications. Ecotoxicol. Environ. Saf. 49, 1–16.
Kummerová, M., Zezulka, Š., Babula, P., Tříska, J., 2016. Possible ecological risk of two pharmaceuticals diclofenac and paracetamol demonstrated on a model plant *Lemna minor*. J. Hazard. Mater. 302, 351–361.
Küpper, H., Küpper, F., Spiller, M., 1996. Environmental relevance of heavy metal-substituted chlorophylls using the example of water plants. J. Exp. Bot. 47, 259–266.
Langford, K.H., Thomas, K.V., 2009. Determination of pharmaceutical compounds in hospital effluents and their contribution to wastewater treatment works. Environ. Int. 35, 766–770.
Li, J., Ye, Q., Gan, J., 2014. Degradation and transformation products of acetaminophen in soil. Water Res. 49, 44–52.
Lichtenthaler, H.K., 1987. Chlorophylls and carotenoids - pigments of photosynthetic biomembranes. Methods Enzym. 148, 350–382.
Lin, Y., Kao, C., 2007. Proline accumulation induced by excess nickel in detached rice leaves. Biol. Plant. 51, 351–354.
McGill, M.R., Williams, C.D., Xie, Y., Ramachandran, A., Jaeschke, H., 2012. Acetaminophen-induced liver injury in rats and mice: comparison of protein adducts, mitochondrial dysfunction, and oxidative stress in the mechanism of toxicity. Toxicol. Appl. Pharmacol. 264, 387–394.
Miralles, P., Church, T.L., Harris, A.T., 2012. Toxicity, uptake, and translocation of engineered nanomaterials in vascular plants. Environ. Sci. Technol. 46, 9224–9239.
Newman, M., Zhao, Y., 2008. Ecotoxicology nomenclature: LC, LD, LOC, LOEC, MAC. In: Jorgensen SE, F.B. (Ed.), Encyclopedia of Ecology. Elsevier, Amsterdam, pp. 1187–1193.
Nogueira, V., Lopes, I., Rocha-Santos, T., Rasteiro, M., Abrantes, N., Gonçalves, F., Soares, A., Duarte, A., Pereira, R., 2015. Assessing the ecotoxicity of metal nanooxides with potential for wastewater treatment. Environ. Sci. Pollut. Res. 22, 13212–13224.
OECD, 2006. Test No. 208: Terrestrial Plant Test: Seedling Emergence and Seedling Growth Test. OECD Publishing.
Olaniran, A.O., Balgobind, A., Pillay, B., 2013. Bioavailability of heavy metals in soil: impact on microbial biodegradation of organic compounds and possible improvement strategies. Int. J. Mol. Sci. 14, 10197–10228.
Panda, K.K., Achary, V.M.M., Krishnaveni, R., Padhi, B.K., Sarangi, S.N., Sahu, S.N., Panda, B.B., 2011. *In vitro* biosynthesis and genotoxicity bioassay of silver nanoparticles using plants. Toxicol. Vitro 25, 1097–1105.
Parween, T., Jan, S., Fatma, T., 2011. Alteration in nitrogen metabolism and plant growth during different developmental stages of green gram (*Vigna radiata* L.) in response to chlorpyrifos. Acta Physiol. Plant. 33, 2321–2328.
Patlolla, A.K., Hackett, D., Tchounwou, P.B., 2014. Silver nanoparticle-induced oxidative stress-dependent toxicity in Sprague-Dawley rats. Mol. Cell. Biochem. 399, 257–268.
Romero-Puertas, M.C., Rodríguez-Serrano, M., Corpas, F.J., Gómez, M., Del Río, L.A., Sandalio, L.M., 2004. Cadmium-induced subcellular accumulation of $O_2^{\cdot-}$ and H_2O_2 in pea leaves. Plant, Cell Environ. 27, 1122–1134.
Ruffini, M., Cremonini, R., 2009. Nanoparticles and higher plants. Caryologia 62, 161–165.
Seregin, I., Kozhevnikova, A., 2005. Distribution of cadmium, lead, nickel, and strontium in imbibing maize caryopses. Russ. J. Plant Physiol. 52, 565–569.
Sharma, P., Jha, A.B., Dubey, R.S., Pessarakli, M., 2012. Reactive oxygen species, oxidative damage, and antioxidative defense mechanism in plants under stressful conditions. J. Bot. 2012, 26. Article ID 217037.
Soares, C., de Sousa, A., Pinto, A., Azenha, M., Teixeira, J., Azevedo, R.A., Fidalgo, F., 2016. Effect of 24-epibrassinolide on ROS content, antioxidant system, lipid peroxidation and Ni uptake in *Solanum nigrum* L. under Ni stress. Environ. Exp. Bot. 122, 115–125.
Taiz, L., Zeiger, E., Moller, I.M., Murphy, A., 2015. Plant Physiology and Development, sixth ed. Sinauer Associates, Inc., Sunderland, U.S.A.
Teixeira, J., de Sousa, A., Azenha, M., Moreira, J.T., Fidalgo, F., Silva, A.F., Faria, J.L., Silva, A.M., 2011. *Solanum nigrum* L. weed plants as a remediation tool for metalaxyl-polluted effluents and soils. Chemosphere 85, 744–750.
Tiyagi, S.A., Ajaz, S., Azam, M., 2004. Effect of some pesticides on plant growth, root nodulation and chlorophyll content of chickpea. Arch. Agron. Soil Sci. 50, 529–533.
van Straalen, N.M., 2002. Assessment of soil contamination—a functional perspective. Biodegradation 13, 41–52.
Yildiztekin, M., Kaya, C., Tuna, A.L., Ashraf, M., 2015. Oxidative stress and antioxidative mechanisms in tomato (*Solanum lycopersicum* L.) plants sprayed with different pesticides. Pak. J. Bot. 42, 717–721.
You, J., Chan, Z., 2015. ROS regulation during abiotic stress responses in crop plants. Front. Plant Sci. 6, 1092.
Yusuf, M., Fariduddin, Q., Hayat, S., Ahmad, A., 2011. Nickel: an overview of uptake, essentiality and toxicity in plants. Bull. Environ. Contam. Toxicol. 86, 1–17.
Zhar, J., 1996. Biostatistical Analysis, third ed. Prentice-Hall International Inc., New Jersey.